SVENSKA GEOFYSISKA FÖRENINGEN

VOLUME 3, NUMBER 3 **Tellus** AUGUST 1951

A QUARTERLY JOURNAL OF GEOPHYSICS

The Effect of Winds and Tides on the Length of the Day

By YALE MINTZ[1] and WALTER MUNK[2], University of California

Abstract

The seasonal variation in the zonal winds of the atmosphere are reexamined and estimated to account for a January to July change of 0,5 milliseconds in the length of the day. Thus only one third of the change in length of the day reported by the astronomers is explained by angular momentum transfers between the earth and atmosphere. The corresponding effect of the varying equilibrium body tide of the earth caused by changes in the sun's distance and longitude is negligible.

Introduction

Slight seasonal deviations of astronomic time from accurate clock time have been reported by various astronomers, notably Stoyko, Finch and Uhink. If these variations are to be ascribed to seasonal variations in the earth's angular velocity, as has been suggested, then the length of the day varies by two milliseconds between early spring and late summer and by 1.5 ms between mid-January and mid-July. It is not yet quite certain whether this interpretation should account for all of the observed effect.

In a previous paper (MUNK and MILLER, 1950) it was shown that ocean currents and shifts in air and water masses could play only a relatively minor role, whereas the seasonal variations in zonal winds were estimated to account for a variation of 1.6 milliseconds in the length of the day. From new information on zonal winds (HUTCHINGS, 1950; MINTZ and DEAN, 1951) we now estimate this effect to be only one third as large. We have also computed the effect of seasonal variations in the earth's moment of inertia due to earth tides. This effect may account for some of the reported semi-annual component, but only a very small part of the annual component.

Astronomic observations

Measurements by Stoyko, Finch and Uhink give, on the average (STOYKO, 1951),

$$\Delta t = 58 \sin (\odot + 28^\circ) + 8.3 \sin 2 (\odot + 146^\circ),$$

for the difference in milliseconds between mean annual time and astronomic time, as function of the sun's longitude $\odot$. We shall assume this to be due entirely to variations in the earth's angular velocity. Differentiation yields

$$\Delta T_{\text{astr}} = \frac{2\pi}{365} \frac{d(\Delta t)}{d\odot} = 1.00 \cos (\odot + 28^\circ) + 0.29 \cos 2 (\odot + 146^\circ)$$

for the anomaly in milliseconds in the length

[1] U. C. L. A. Department of Meteorology, Papers in Meteorology, No. 12. The research reported in this paper has been sponsored in part by the Geophysical Research Division of the Air Force Cambridge Research Center under Contract No. 19 (122)—48.

[2] Contribution from the Scripps Institution of Oceanography, New Series No. 543, supported under a contract with the office of Naval Research.

of the day.[1] The three observers differ on the average by 5 per cent with regard to the amplitude of the annual term, and by 24 per cent with regard to the semi-annual term. For the longest day, $\triangle T = 0.99$ ms, $\odot = 3°$ (March 24); for the shortest day, $\triangle T = -1.23$ ms, $\odot = 137°$ (Aug. 7).

Earth tides

The fluctuation in the length of the day is due partly to seasonal changes in the semi-diurnal tides. There is a slight additional protuberance, on the average, in the equatorial region at the expense of the polar regions, and a resulting increment in the earth's moment of inertia by

$$\delta I = -k I \frac{M'}{M} \frac{r^3}{r'^3} (2-3 \cos^2 \Theta)$$

over what it would be if the sun were absent. Here $I = (1/3)\, Mr^2$ is the earth's moment of inertia, M its mass and r its radius; M', r' and Θ refer to the mass, the distance and the declination of the sun; $k = 0.27$ is Love's number. The essential effects here are variations $\triangle(\delta I)$ which occur because of seasonal changes in the heliocentric distance, by

$$\triangle r' = -0{,}0168\, r'_0 \sin (\odot + 168°),$$

and because of changes in the sun's longitude according to

$$\Theta = 23.5° \sin \odot$$

due to the obliquity of the ecliptic. The resulting variations in T, the length of the day, in ms, is

$$\triangle T_{\text{tides}} = \frac{\triangle(\delta I)}{I} T = 0.02 \cos (\odot + 73°) + 0.15 \cos 2 \odot.$$

Certain modifications may be required to allow for the difference in the yielding of land and sea to tidal forces.

The obliquity of the ecliptic, which leads to the semi-annual term in the above expression, can account for half the amplitude of the reported semi-annual effect, but not all, even if allowance is made for the large observational error. There is no agreement with regard to phase. Prof. JEFFREYS (1928) drew attention to this possible role of the obliquity on accurate time-keeping before this effect was discovered. A somewhat larger effect on $\triangle T$ must be expected from the variation in lunar tides, but because of the short period of this variation the effect on the cumulative time anomaly $\triangle t$ is relatively small and has not yet been observed.

Subtracting the tidal effect from the observed effect leaves

$$\triangle T_{\text{astr}} - \triangle T_{\text{tides}} = 0.98 \cos (\odot + 27°) + 0.27 \cos 2 (\odot + 131°)$$

to be accounted for by other causes. The difference mid-January minus mid-July equals 1.5 ms.

The effect of zonal winds

Because the total angular momentum of the earth and atmosphere are conserved, it follows that anomalies in the length of the day due to variations in zonal winds (MUNK and MILLER, 1950) are given by

$$\triangle T_{\text{wind}} = \frac{\triangle(I_a \omega_a)}{I \Omega_e} T,$$

where

$$I_a \omega_a = \frac{2\pi r^3}{g} p_0 \int_{-\pi/2}^{\pi/2} \tilde{u} \cos^2 \phi \, \delta\phi$$

is the angular momentum of the atmosphere, $I\Omega_e$ the angular momentum of the planet earth, g gravity, ϕ latitude, and where

$$\tilde{u} = \frac{1}{2\pi} \int_0^{2\pi} \delta\lambda \frac{1}{p_0} \int_{p_0}^{0} u \, \delta p$$

is the zonal wind averaged over all longitudes λ and pressures p.

In fig. 1, $(\tilde{u}_{\text{Jan}} - \tilde{u}_{\text{July}})$ is plotted against $\int_0^{\phi} \cos^2 \phi \, \delta \phi$. The area under the curve is therefore proportional to $(I_a \omega_a)_{\text{Jan}} - (I_a \omega_a)_{\text{July}}$.

[1] Because of a numerical error STOYKO (1951) obtains only 0.17 ms for the amplitude of the semi-annual term.

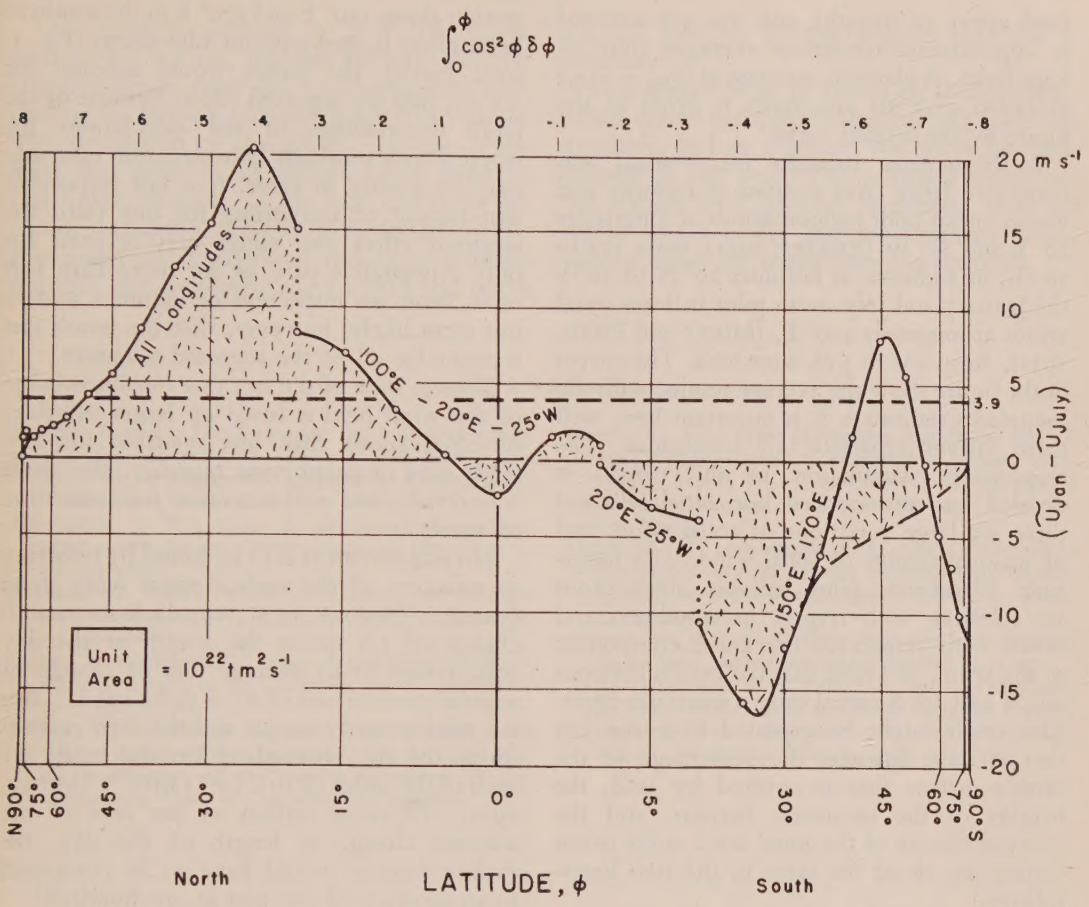

Fig. 1. The seasonal change of zonal wind, as a function of latitude ϕ. The mean zonal wind $\tilde{u}$ is averaged from 101 to 0 cb and over all longitudes. The abscissa has been chosen as a particular function of ϕ for which the area under the curve is proportional to change in angular momentum: unit area equals 10^{22} t m² s^{-1}, corresponding to 0.15 milliseconds in the length of the day. In order to account for a reported change of 1.5 ms, the mean value of the curve should equal 3.9 m s^{-1}, as indicated by the dashed line.

In order to account for a difference of 1.5 ms, the mean value of $(\tilde{u}_{Jan} - \tilde{u}_{July})$ should equal 3.9 m sec^{-1}, as shown.

For the latitude belt 20°—90° North, $(\tilde{u}_{Jan} - \tilde{u}_{July})$ was computed from cross sections of the mean January and July geostrophic zonal winds averaged over *all* longitudes (MINTZ and DEAN, 1951), between pressures 101 and 5 cb (instead of sea level pressure p_0 and 0 cb), with the results shown in fig. 1.

For the latitude belt 20°—75° South, $(\tilde{u}_{Jan} - \tilde{u}_{July})$ was computed from summer and winter cross sections of geostrophic zonal winds in the longitudes of New Zealand (HUTCHINGS, 1950), from 101 to 5 cb; and east coast Australia (LOEWE and RADOK, 1950), from 101 to 15 cb, with the average for the two longitudes shown in the figure by the solid curve. The subtropical part of this curve was assumed to approximate conditions averaged over all longitudes of the southern hemisphere, [although this assumption is not without its uncertainties, as in the northern hemisphere the variation of $(\tilde{u}_{Jan} - \tilde{u}_{July})$ with longitude is as great as $(\tilde{u}_{Jan} - \tilde{u}_{July})$ itself; and in the southern hemisphere, at 30° S, $(\tilde{u}_{Jan} - \tilde{u}_{July})$ is 6 m sec^{-1} greater at 170° E than at 150° E.] The temperate and higher latitude part of the solid curve shows the seasonal change of zonal wind in the region of the Ross Sea low

(and upper air trough), and was not assumed to approximate conditions averaged over all longitudes. A plausible estimate of $(\tilde{u}_{\text{Jan}} - \tilde{u}_{\text{July}})$ averaged over all longitudes is given in the figure by the broken curve.

In the tropical latitudes $(\tilde{u}_{\text{Jan}} - \tilde{u}_{\text{July}})$ was computed from cross sections of summer and winter mean pilot balloon winds at longitudes 20° E and 25° W (EKHART, 1941), from 101 to 30 cb; in addition, at latitudes 20° N to 10° S the January and July mean pilot balloon zonal winds at longitude 100° E, (MINTZ and DEAN, 1951), from 101 to 5 cb were used. The curves in the figure show the average results, with the longitudes indicated. It is uncertain how well these curves represent all longitudes. The tropospheric circulation in the tropics is divided into pronounced horizontal cells and there are large variations of zonal wind, and of seasonal change of zonal wind, with longitude. Moreover, pilot balloon observations are selective with respect to cloudiness and hence with respect to the zonal component of the wind. We note that the curves between 20° N and 20° S reveal only a small net effect. This result might be expected from the fact that at these latitudes the percentage of the earth's surface that is covered by land, the heights of the mountain barriers, and the seasonal change of the zonal wind at the ocean surface are about the same in the two hemispheres.

Table 1. Seasonal change of atmospheric angular momentum and the resulting changes in the length of the day, for stated latitude belts.

	90°N—20° N	20°N—20° S	20° S—90° S	90°N—90° S
$(I_a \omega_a)_{\text{Jan}} - (I_a \omega_a)_{\text{July}}$, in $10^{22} t$ m² s⁻¹	8.0	1.3	— 5.9	3.4
$(\Delta T_{\text{wind}})_{\text{Jan}} - (\Delta T_{\text{wind}})_{\text{July}}$, in millisec	1.2	0.2	— 0.9	0.5

By integration of the shaded area in the figure, the values in Table 1 were computed. According to these figures the winds account for only one third of the reported seasonal variation in the length of the day.[1] If the section along 150° E and 170° E in the southern hemisphere is used without adjustment (Fig. 1, solid curve), the winds would account for 0.8 ms, half the reported effect. Because of the large uncertainties in the calculations for tropical and southern latitudes, our estimates may be greatly in error. It is not impossible that instead of accounting for one third the reported effect the winds may account for only a negligible part, or for more than half of it. From an inspection of Figure 1 it does not seem likely, however, that the winds can account for all of the reported variation.

Thus in spite of the fact that our knowledge of the wind field is based on larger numbers of observations than are available for any other kind of geophysical quantity, the result is uncertain, and will remain so for some time to come.

No improvement is to be found by resorting to estimates of the surface zonal wind stress (VAN DEN DUNGEN, et al., 1950). A six month change of 1.5 ms in the length of the day corresponds to an average rate of change of angular momentum of $0.7 \times 10^{16}\ t$ m² s^{-2}. But the total westerly torque and the total easterly torque of the atmosphere on the earth are each of the order of $10 \times 10^{16}\ t$ m² s^{-2}, (MINTZ, 1951). To come within 25 per cent of the seasonal change in length of the day, the surface torques would have to be computed to an accuracy of one part in one hundred!

Conclusions

Astronomic observations indicate that the mean length of the day in January exceeds that in July by 1.5 milliseconds. It is however possible that this difference might be smaller, due to periodic errors in the right ascension system of the fundamental catalogue of star places. More information on this point will be available within the next few years, when the new Greenwich Photographic Zenith Tube comes into action.[1] We may also expect increased accuracy from the improvement of clocks, possibly the use of atomic clocks.

[1] Previous computations by MUNK and MILLER (1950) gave too high a value principally because in the northern hemisphere they used the published sections along 100 E° and 80° W, where, as it now turns out, the variations in the zonal winds are larger than at all other longitudes.

[1] We are indebted to the Astronomer Royal for information concerning these developments.

Our present estimate is that the winds account for 0.5 ms, but this estimate may be considerably in error due to uncertainties concerning the tropical southern hemisphere winds. The circulation of the ocean, changes in sea level and shifts in air masses might possibly contribute another 0.5 ms, but this is by no means established (MUNK and MILLER, 1950). If in each case we put down the largest possible number, the combined effect might add up to 1.5 ms, but we do not suggest that this is the case.

One might hope to return to this problem when more complete meteorologic data are available, and to compute the effect for each month of the year. The principal needs are for station level pressure variations (not reduced to sea level), and for southern hemisphere upper air winds over the open sea.

REFERENCES

EKHART, E., 1941: Die Strömung der Luft über Afrika und den angrenzenden Gebieten: Ein Beitrag zur Kenntnis der allgemeinen Zirkulation. Reichsamt für Wetterdienst, REIHE A, Nr. 10, Berlin.

HUTCHINGS, J. W., 1950: A meridional atmospheric cross section for an oceanic region. *J. Meteor.*, **7**, 2, pp. 94—100.

JEFFREYS, H., 1928: Possible tidal effects on accurate time-keeping. *M. N. R. A. S., Geophys. Suppl.*, **2**, pp. 56—58.

LOEWE, F., and RADOK, U., 1950: A meridional aerological cross section in the Southwest Pacific. *J. Meteor.*, **7**, 1, pp. 58—65.

MINTZ, Y., and DEAN, G., 1951: The observed mean field of motion of the atmosphere. Part 2, Report No. 7, Investigation of the general circulation of the atmosphere. *Univ. of California*, Los Angeles.

MINTZ, Y., 1951: The geostrophic meridional flux of angular momentum for the month of January 1949. Part 1, Report No. 7, Investigation of the general circulation of the atmosphere. *Univ. of California*, Los Angeles.

MUNK, W. H., and MILLER, R. L., 1950: Variations in the Earth's Angular velocity resulting from fluctuations in atmospheric and oceanic circulation. *Tellus*, **2**, pp. 93—101.

STOYKO, N., 1951: La Variation de la Vitesse de Rotation de la Terre. *Bull. Astronomique*, **15**, fasc. 3, 14 pp.

VAN DEN DUNGEN, F. H., COX, J. F., and VAN MIEGHEM, J., 1950: Variations in the Earth's angular velocity resulting from fluctuations in atmospheric and oceanic circulation. *Tellus*, **2**, 4, pp. 319—320.

Optical Measurement of Particle Distribution in the Sea

By N. G. JERLOV, Oceanographic Institute, Gothenburg

(Manuscript received 2 July 1951)

Abstract

A method has been developed for studying the distribution of suspended particles in the sea. The intensity of the light from a Tyndall beam scattered in the water samples is measured. Essential precautions in the study of clear ocean water are given. The method is illustrated by the particle distribution found off the Nile estuary and in the Strait of Gibraltar. The possibilities offered by the method suggest that it should be more widely employed for characterizing water masses and for studying horizontal and vertical movements in the sea. Other pertinent problems, *re* the settling of suspensoids near land and the flushing of harbours, may also be investigated in this way.

Introduction

During recent years the study of particle distribution in the sea has gained new interest. In particular, attention has been paid to the production of living matter in the sea. The production problem has been closely investigated *i.a.* by RILEY, STOMMEL, and BUMPUS (1949) for the Western North Atlantic and by HARVEY (1950) for the sea off Plymouth.

By filtration of the water samples and determination of dry weight it is possible to obtain a measure of the total amount of suspended particles. ARMSTRONG and ATKINS (1950) have used this procedure, combined with an inorganic analysis of the ignited dry matter. KREY (1949) has developed a simple method of filtering particles according to size, followed by a microscopic analysis. In addition, he measured the content of chlorophyll and albumen in the suspended matter in order to arrive at a qualitative and quantitative control of the decrease or increase of its organic content.

In the upper strata, suspensoids are to a large extent living organisms but organic *detritus* also plays an important rôle. Besides, inorganic matter is present, derived from land or, in shallow water, from the bottom. By currents and horizontal eddies fine material can be transported far away from shore. Air-borne terrigenous dust is also an important contributor to marine suspensoids. While sinking, the dead planton or the *detritus* is gradually decomposed. From the upwelling water west of Africa WATTENBERG (1937) has followed the different stages of this disintegration process.

The biological interest in particle distribution is chiefly directed to the upper, illuminated water strata. From a hydrographical point of view the question has a somewhat different aspect, since the distribution of suspended matter in the whole water column is significant. Particles affect both physical and chemical conditions in the water, in the first place the optical conditions. These effects have been discussed by KALLE (1947).

The marked influence of suspended matter on light suggests the use of optical methods for studying the content of particles. In 1937, KALLE (1939) introduced a method in which the intensity of a Tyndall beam projected into the water sample is determined.

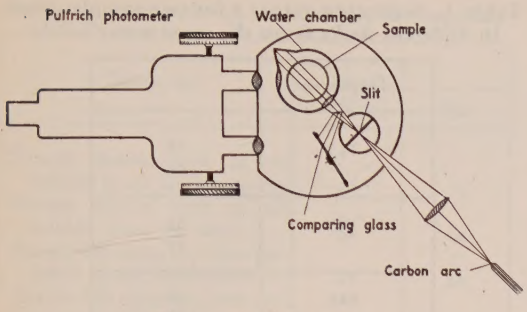

Fig. 1. Tyndall meter.

A similar method was developed and employed during the Swedish Deep Sea Expedition. Measurements of the particle content in the water samples were accordingly included in the routine hydrographical work on board.

Tyndall meter

The device used for measuring the intensity to the Tyndall beam is a Zeiss turbidity meter with some technical modifications. Since the high transparency of the samples requires an intense light source the electrical lamp in the original apparatus is replaced with a slit (width 1 mm) illuminated by a carbon arc (fig. 1). A parallel Tyndall beam is obtained in the sample, which is contained in a small glass flask (60 ml) and submerged in a chamber filled with water. The intensity of the light scattered from the Tyndall beam at an angle of 45° is measured by means of a Pulfrich photometer. A scattering glass, against which some initial light is reflected, serves as a comparison. Low-scattering samples are compared with a slightly etched glass, those of a medium scattering power with a more strongly etched glass, and high-scattering samples with a milkglass. The photometer is provided with a red filter (centre of gravity 615 mμ), a green filter (535 mμ), and a blue filter (470 mμ).

During the expedition the Tyndall meter was placed in the optical darkroom. An asbestos wall shielded the observer from light from the carbon arc. For the clearest samples it was necessary to work with completely adapted eyes. Then, the accuracy realized by the Tyndall reading is the same as that normally obtainable with the Pulfrich photometer (see URBACH, 1937).

Procedure

The method, if it is also to be employed for clear ocean water, demands that great care be taken to avoid contamination during the collection of samples, and that the samples are studied before any change of the particle content occurs.

For collecting samples at subsurface levels Knudsen water-bottles were used. As the nickel-plated interior of the bottle is likely to contaminate the enclosed water it is advisable to coat the inside of the bottles with ceresin which CLARKE and JAMES (1938) used when measuring the absorption of light by sea water. The covering power of ceresin was checked by us in the following way. An iron vessel with fresh rust was lined with ceresin. The transmission of double-distilled water to blue light did not show any measurable change after the water had been shaken in the vessel. Not only the metal parts, including the central spring, but also the rubber packings were lined but without preventing the lids to close properly. Although the central spring is stretched and slackened when the bottle is used its ceresin coating did not show any flaws.

When the water bottle was brought on board a sample was drawn off into a small glass flask with a ground stopper. The flasks were externally cleaned with 50% alcohol and placed in the Tyndall meter where tests were run. During the measurement the flask was kept rotating round its vertical axis, in order to eliminate the influence of small optical irregularities in the glass. The rotation also served to stir up big particles from the bottom. The water chamber was frequently refilled with clear deep-sea water.

The intensity of the Tyndall beam was determined in the blue and in the red, sometimes also in the green, three times for each colour.

Tyndall unit

It is worth while to ascertain whether the intensity of the Tyndall beam in an 45° direction, represented by the Tyndall reading, could be expressed in a known unit such as a scattering coefficient. The extinction of a beam of light by sea water is the sum of absorption and scattering. For the ocean the scattering coeffi-

cient attains only low values, and so, it is proportional to the amount of light lost by scattering. The problem of scattering by particles suspended in water has been treated for instance by BLUMER (1926) and by LE GRAND (1939) under the assumption that the particles are spherical and transparent. However, the ocean contains particles of different kinds, and it is therefore necessary to determine by experiment the ratio of the total scattering coefficient S and the Tyndall reading A.

Table 1. Ratio of total scattering coefficient S to Tyndall reading A for blue light (470 mμ)

Station	S/A
29	0.00046
46	54
108	62
111	51
123	50
338	50
371	53
Mean value	0.00052

Table 1 is prepared to show this ratio S/A for blue light and for different stations. The readings A are as determined with the low-scattering comparison glass. The values of S were derived through comparison between daylight measurements and transparency measurements (JERLOV, 1951).

In view of the accuracy attainable in determinations of S the variations found in S/A are unimportant and may be disregarded; the ratio may be considered as a constant = 0.00052. In the total scattering S, the scattering produced by the water itself (0.003 m^{-1} at 470 mμ) is also included. Hence the scattering caused by particles only, s, conveniently expressed in km^{-1}, is found by the formula:

$$s = 0.52\ A - 3$$

In the ocean the scattering by particles predominates over the absorption by particles and dissolved substance. Thus the Tyndall effect could be given almost as well as an extinction coefficient as KALLE (1939) has done.

The Tyndall effect produced by ocean particles was found to be only slightly dependent on the wave-length of the light. This indicates that the size of the suspended particles in general exceeds 3 μ. Thus, the derived scattering values give an approximate measure of the total particle surface (DALLA VALLE, 1948). The relation between scattering and mass per unit-volume is dependent on particle size. In nutrient-rich water the plankton is on an average of larger size than in less fertile areas. Therefore, for a given scattering the mass is higher in the former than in the latter case.

Table 2. Scattering values s for two samples taken in different flasks from the same water bottle

Depth m	s
145	68 60
185	55 57
344	56 56
440	55 55
538	50 54
728	50 53

Discussion of the method

Some experiments were devised to check the accuracy of the method and to delineate the necessary precautions.

From the same water bottle two samples were taken in different flasks. A comparison between the two s-values for various levels in Table 2 shows the normal uncertainty in the determination of s. Table 3 gives the results obtained from different ways of filling

Table 3. Different ways of filling the flask from the water bottle

Technique used	s
Rubber tube at the tap, the first water of the bottle	33
Rubber tube at the tap, the last water of the bottle	35
Flask close to the tap	31
Some distance between flask and tap	30

Table 4. Influence of air dust on the samples

Treatment	s	
	before	after
Sample shaken with an air bubble from the laboratory	41	54
Sample shaken with an air bubble from the deck.....	41	44
Sample left open for three minuter in the laboratory . . .	27	42
Sample left open for three minutes on the deck.....	24	31

the flasks from the water bottle. In this case the bottle contained water from 2 500 m. In routine work the filling was made with the flask near the tap.

To demonstrate how easily the samples may be contaminated (Table 4), an air bubble was put into the flask which was shaken afterwards. The pure air taken from the deck did not affect the sample in a measurable degree, but the laboratory air, being full of dust, spoiled the sample. Likewise if the flask was left open for three minutes the sample receives enough dust to raise the *s*-value appreciably. The clarity of deep-sea samples is illustrated by the low *s*-value of 20 frequently found, whereas distilled water in the laboratory gave $s = 60$.

The change with time of the particle content in the sample remains to be considered. In some cases a sample was studied immediately and a control sample of the same water was left standing during 12 hours without exposure to light before the measurement. The change in *s* was from 39 to 41 (mean of three samples), *i.e.* negligible. But, if water is left in the water bottle for a day the particle content will decrease considerably because particles settle. A similar decrease occurs in a sample for which tests are run repeatedly. Table 5 based on observations made in the Indonesia seas contains the average decrease with time of different *s*-values. The reduction is only slight for clear water but grows to as much as 50 % for turbid samples. This decrease is caused by particles becoming disintegrated, associating with each other, or adhering to the walls and to the bottom of the flask, so that even a rapid rotation does not bring them into suspension. Apparently the effect in question is accelerated by irradiation.

Table 5. Average decrease with the time of scattering *s* in a sample

Hours	*s*				
0	25	50	75	100	125
2	25	49	73	96	116
4	24	48	69	89	106
6	23	44	63	80	94
8	21	40	56	70	78
10	21	39	52	63	67
12	21	39	51	59	61

As a precaution it is advisable to make measurements as soon as possible after the sample is taken.

A possible objection to the method concerns contaminations from the wire which is in close proximity to the water bottle. There is no reason to believe that the wire could supply the water sampled with an additional amount of particles. Loose particles at the wire, not being washed away when the wire runs through the water with a speed of three meters per second, are not likely to become detached at rest. During the hydrographical work the wire was rusty during long periods but among the numerous samples taken only a few were found to contain red or brown particles indicated by a higher scattering of red than of blue light. However, in these cases it is much more probable that the coloured particles are inherent in the water, *i.e* are plankton or *detritus*.

When the wire had been oiled, scattering values found before and afterwards did not differ appreciably.

Results

As has already been stated the Tyndall measurements reveal a fine-stratification in particle distribution in the interesting layers quite close to the ocean floor (JERLOV, 1950). A cloud of particles was repeatedly observed some tens of meters above the bottom, whereas the water below that level was very transparent. An explanation would be that currents are carrying sediment particles from ridges on adjacent parts of the ocean floor, which implies an influence on sedimentation from local topography.

Also in higher levels, layers rich in suspended matter were frequently encountered

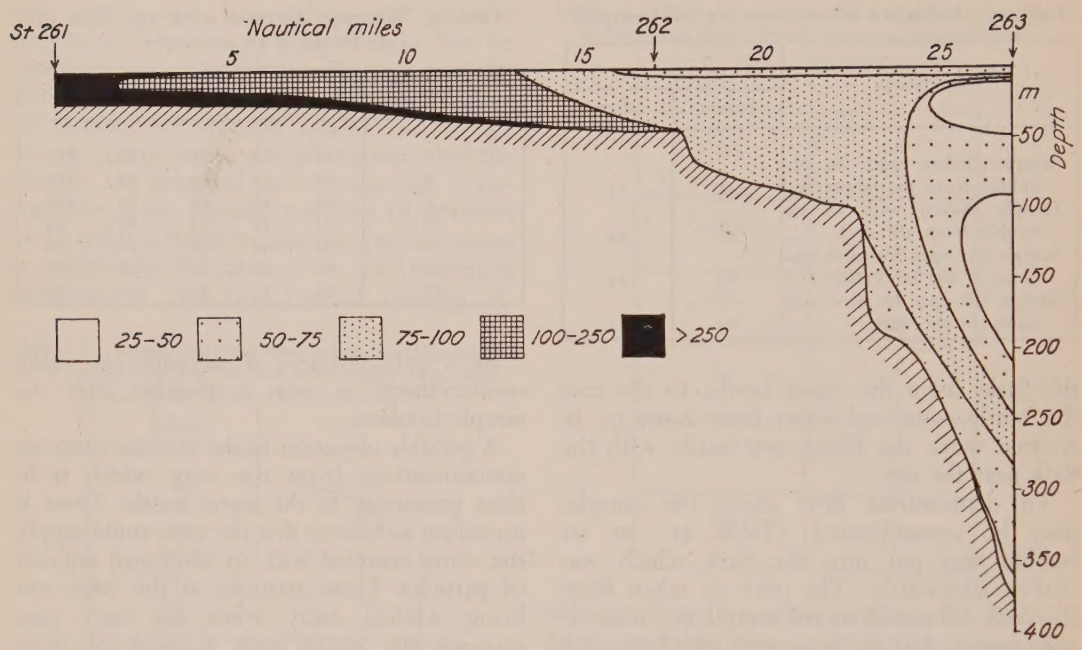

Fig. 2. Particle distribution in a vertical section off the Nile estuary.

(compare KALLE, 1939) for which a similar explanation may be valid. A typical illustration of particles characterizing the water is given for the Romanche Deep in the Atlantic (JERLOV, 1950). Here the inflow of the Antarctic Bottom Water at 4,000 m could be detected by a strong decrease in the content of particles.

It is not the aim of this paper to give a full report of the results from the expedition but only to demonstrate in some cases how the method is employed. The complete paper will appear in Reports of the Swedish Deep Sea Expedition, III.

As an illustration a vertical section of particle distribution off the Nile estuary near Port Said is shown in fig. 2. The positions of the stations are given in Table VI. Only three stations, 261—263, fall within this section but another, more easterly, section (not shown here) supports the main features of distribution in the shallow water.

Judging from observations of temperature and salinity the salt Mediterranean water is mixed with the Nile water, and no stratification is found. The temperature shows a slight decrease with increase of depth. The salinity ($\sim$ 38,9 ‰) also seems to be a little higher at the surface but the deviation is nearly within the limits of accuracy of the observations. On the other hand, conditions at Station 263 are typical for the eastern Meditarranean, the intermediate water exhibiting at 150 m a salinity maximum of 39,13 ‰ (SVERDRUP, JOHNSON and FLEMING, 1946).

From fig. 2 it is seen that the large amount of sediment carried by the Nile flocculates and settles rapidly. Thus, already some tens of miles from the coast the water is practically free from particles from the river. It must, however, be born in mind that sediment is also transported away by the prevailing current which is directed to the east.

Table 6. Stations

Area	Station number	Latitude	Longitude
Nile estuary	261	N 31° 25′	E 32° 25′
	262	31° 41′	32° 30′
	263	31° 51′	32° 34′
Strait of Gibraltar	306	N 36° 02′	W 02° 59′
	307	35° 52′	05° 54′
	308	35° 45′	06° 50′
	309	34° 56′	07° 44′

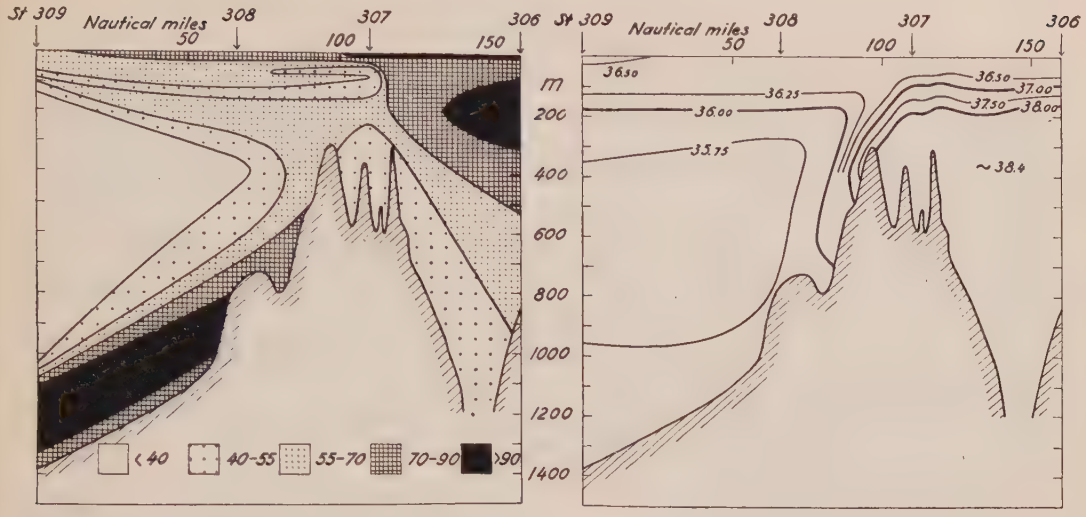

Fig. 3. Distribution of particles and salinity in a vertical section through the Strait of Gibraltar.

The slope of the bottom characterized by ledges becomes very steep towards Station 263. Here the turbid water is free from the bottom and is present as a tongue at 250 m, whereas the water close to the bottom is clear. The content of particles in the surface water is already normal, and the very clear Mediterranean water is found at 25 m and at 100—200 m.

Another section shows the particle distribution in the Strait of Gibraltar (fig. 3). It is based on observations made on 12 June 1948 (Stations 306,307, and 308) and during the morning of the 13th (Station 309). Positions of the stations are given in Table 6.

Isohalines derived for the momentary hydrographical situation are presented in fig. 3. The well-known, main feature in the exchange of water through the Strait is the sinking of the salt Mediterranean water across the ridges and down the shelf and its replacement through inflow of Atlantic water in the upper layers. According to RAMALHO and DENTINHO (1931), the salt water does not, however, spread so far to the south as Station 309. Further details about the water exchange through the Strait have been given by SCHOTT (1928) who states that the average rate of inflow is of medium strength in spring.

The superimposed tidal currents do not play any important rôle at Stations 306 and 308; it may be mentioned that these observations were carried out at low tide. But Station 307 was occupied three hours after low tide and there was in the whole water column a west-moving current which was weak in the upper layers but grew in strength below 200 m. This is consistent with the salinity distribution as isohalines for Station 307 are at higher levels than in the normal situation.

As regards the particle distribution in the Strait, the following features are noticed. The Mediterranean water at Station 306 is characterized by an abundance of particles not only at the surface but also round 200 m. On the Atlantic side the water is fairly poor in particles except the layers near the bottom which contain large amounts. There is no obvious connection of very turbid water between these two large concentrations of particles on each side of the sill; no level at Station 307 attains an *s*-value of 70. Possibly the observations may have missed a cloud of particles at some intermediate depth but the intensive mixing in the Strait evidently favours a more homogenous distribution.

Summing up, it may be said that the exchange mechanism in the Strait of Gibraltar carries particles with the Mediterranean water across the sill to the bottom layers at the Atlantic shelf, in particular when the tidal currents are favourable for a strong depth current being developed. But the trend of the 36 ‰ isohaline indicates that to some degree a downward transport of Atlantic particles also takes place.

REFERENCES

Armstrong, F. A. J., and Atkins, W. R. G., 1950: The suspended matter of sea water. *Jour. Marine Biol. Assoc.*, **29**, 1, p. 139

Blumer, H., 1926: Die Farbenzerstreuung an kleinen Kugeln. *Zeits. f. Physik*, **39**, p. 195.

Clarke, G. L., and James, H. R., 1939: Laboratory analysis of the selective absorption of light by sea water. *Jour. Opt. Soc. Amer.*, **29**, p. 43.

Dalla Valle, J. M., 1948: *Micromeritics*. New York.

Harvey, H. W., 1950: On the production of living matter in the sea off Plymouth. *Jour. Marine Biol. Assoc.*, **29**, 1, p. 97.

Jerlov, N. G., 1951: Optical studies of ocean waters. *Reports of the Swedish Deep-sea Expedition*, **3**, No. 1.

— 1950: Optische Bestimmungen von Schwebestoffen im Meere. *Naturwissenschaften*, **15**, p. 359.

Kalle, K., 1939: Die chemischen Arbeiten auf der "Meteor"-Fahrt Januar bis Mai 1938. *Ann d. Hydr. u. Mar. Met.* Beiheft zum Januarheft, p. 23.

— 1947: *Der Stoffhaushalt des Meeres*. Leipzig.

Krey, J., 1949: Über Art und Menge des Seston im Meere. *Verhandl. d. Deutschen Zoologen in Mainz*, 1949, p. 295.

Le Grand, Y., 1939: La pénétration de la lumière dans la mer. *Annales de l'institut océanographique*, **19**, p. 393.

Ramalho, A., and Dentinho, L., 1931: Contribution à l'étude océanographique du Golfe de Gibraltar. *Conseil Perm. Internat. p. l'Explor. de la Mer, Rapp. et Proc.-Verb.*, **70**, p. 82.

Riley, G. A., Stommel, H., and Bumpus, D. F., 1949: Quantitative ecology of the plankton of the Western North Atlantic. *Bull. Bingham Oceanographic Coll.*, **12**, No. 3.

Schott, G., 1928: Die Wasserbewegungen im Gebiete der Gibraltarstrasse. *Conseil Perm. Internat. p. l'Explor. de la Mer, Jour. du Conseil*, **3**, p. 139.

Sverdrup, H. U., Johnson, M. W., and Fleming, R. H., 1946: *The Oceans*. New York.

Urbach, C., 1937: *Stufen-photometrische Trinkwasseranalyse*. Wien und Leipzig.

Wattenberg, H., 1937: Die chemischen Arbeiten auf der "Meteor"-Fahrt Februar bis Mai 1937. Mit Bemerkungen zur Verteilung und Regeneration der Minimumstoffe. *Ann. d. Hydrogr.*, **65**.

Das Phänomen »Blaue Sonne«

Von WERNER JENNE,
Deutsche Akademie der Wissenschaften zu Berlin, Geodätisches Institut, Potsdam

(Manuscript received 9 March 1951)

Abstract

The phenomenon "Blue Sun" could be observed in Scotland September 26, 1950, in other parts of Europe, for instance in Sweden and Germany, on the following day. An attempt was made approximately to fix the probable geographical limits, inside of which the bluish colour of the sun could be seen. The investigation deals also with the explanation of the phenomenon from the point of view of theoretical physics.

Die tägliche Wetterkarte der Hauptwetterdienststelle Potsdam des Meteorologischen Dienstes der Deutschen Demokratischen Republik brachte am 29. September 1950 die folgende Mitteilung:

»Starke Lufttrübung. — Am Mittwoch[1] wurde im Gebiet der Deutschen Demokratischen Republik und auch im übrigen Deutschland eine starke Trübung des Himmels festgestellt, die örtlich so stark war, dass die Sonne im bläulichen Licht erschien und mit blossem Auge betrachtet werden konnte. In Mecklenburg war die Trübung besonders eindrucksvoll. ... Die Hauptwetterdienststelle Potsdam gibt dazu folgende Erklärung:

Seit mehreren Tagen wüten in Kanada ungeheure Waldbrände, deren dichter gelblicher Qualm etwa seit Sonntag[2] aus dem Ursprungsgebiet mit starken südwestlichen Winden in Richtung Grönland—Island und von dort mit nordwestlicher Strömung über den Nordatlantik auf Mitteleuropa zu geführt wurde. Die mittlere Windgeschwindigkeit auf dem Wege von Kanada über Grönland nach Mitteleuropa betrug während der letzten Tage in 5 000 m Höhe bis zu 100 km/h, am Mittwoch auf dem nördlichen Atlantik und in Schottland in 9 000 m Höhe bis 200 km/h.

Auch in Potsdam konnte am Mittwochnachmittag die Trübung und ein fahles bläuliches Licht der Sonne und während der ersten Nachthälfte auch beim Mond festgestellt werden.»

Zufällig auf der Insel Rügen weilend konnte ich die Erscheinung selbst unter günstigen Bedingungen beobachten. Durch die Seltenheit des Ereignisses beeindruckt, versuchte ich, zur weiteren Aufklärung der mit dem Phänomen zusammenhängenden Umstände einiges beizutragen.

In dem Literaturverzeichnis findet man bereits fünf in deutschen wissenschaftlichen Zeitschriften erschienene Mitteilungen zu dem gleichen Thema angegeben. Da wohl nicht anzunehmen ist, dass diese Zeitschriften allen Lesern der Tellus ohne weiteres zugänglich sind, müssen einige Hauptpunkte der betreffenden Mitteilungen hier kurz erwähnt werden.

[1] = 27. Sept.
[2] = 24. Sept.

I. Die meteorologische Erklärung der ungewöhnlichen Lufttrübung

a) Verschiedene Beobachtungen deutscher Fachleute

Im Interesse derjenigen Leser, die die Erscheinung nicht selbst beobachten konnten, sei aus der Mitteilung von H. Runge (1951) eine der amtlichen Beobachtungen hier im Wortlaut wiedergegeben.

»Wetterdienststelle Schwerin. Beobachtungen der Trübung und Blaufärbung der Sonne am 27.9.1950. — Bei Sonnenaufgang (0607 MEZ) war der Himmel mit Stratus in 250 m bedeckt. Diese Schicht löste sich gegen 8 Uhr auf und es verblieb ein geschlossener Schleier, den man weder als dünnen AS noch als CS ansprechen konnte. Die Höhe war nicht genau zu schätzen, jedoch lag sie wahrscheinlich über 5 000 m. Optische Erscheinungen, wie Halo und Hof, wurden nicht beobachtet. Dieser Schleier bedeckte den Himmel den ganzen Tag über. Ausserdem war noch wechselnde Stratocumulus-Bewölkung in mehreren Höhen vorhanden. Die Sonne, die man durch diesen Schleier erkennen konnte, war stark getrübt und erschien als blaue Scheibe mit schwarzem Rand, ähnlich wie man sie, abgesehen von der Farbe, durch eine sehr dünne Hochnebeldecke beobachtet. Von 8.15 Uhr bis 9,30 war die Blaufärbung am stärksten. Die Sonne hatte während dieser Zeit etwa die Farbe des blauen Himmels. Zeitweise wies auch die nähere Umgebung der Sonne einen schwachen bläulichen bis violetten Schimmer auf. Die Sonnenstrahlen waren stark gedämpft. Sehr schwache Schattenwirkungen konnten nur zeitweilig beobachtet werden. Durch die Sonne bestrahlte Gegenstände bekamen ein hellblaues bis violettes Aussehen. Etwa um 9,30 Uhr, als die Blaufärbung schwächer wurde, konnte man eine deutliche gelbliche Färbung des Schleiers und der darunter liegenden Stratocumulus-Bewölkung in halber Sonnenhöhe erkennen. Nach 9,30 Uhr liess sowohl die Trübung als auch die Blaufärbung der Sonne nach. Sie wurde zeitweise so hell, dass man nicht mehr mit blossem Auge hineinsehen konnte und hatte einen leicht bläulichen Schimmer, wie etwa eine Quarzlampe.

Am Nachmittag verdichtete sich der Schleier. Manchmal konnte man deutlich die an der Sonnenscheibe vorbeiziehende Schicht beobachten. Bei einer Sonnenhöhe von 15° war die Absorption der Lichtstrahlen bereits so stark, dass die Sonne wenig später im Schleier verschwand. Gegen 19,30 Uhr tauchte der Mond in etwa 15° Höhe aus dem Schleier auf. Er war ebenfalls leicht getrübt und hatte einen bläulichen bis violetten Schimmer. Mit zunehmender Mondhöhe ging das bläulichviolette Mondlicht in ein Weissblau über. Der Schleier wurde allmählich dünner und der Mond hatte wieder fast normales Aussehen . . .«

W. Gelbke, Greifswald, konnte von der »Blauen Sonne« einige Farbaufnahmen machen, von denen eine in der Zeitschrift für Meteorologie reproduziert wurde (1951). Diese Aufnahme wurde unter Vorschaltung eines Zeiss-Glases mit einer Kleinbildkamera gemacht.

Im Observatorium Gotha (Thüringen) wurde durch die laufend angestellten Strahlungs- und Polarisationsmessungen mit einem Linke-Feussner-Panzeraktinometer ebenfalls eine anomale Trübung der Atmosphäre festgestellt. Hierüber erschien ein Bericht von G. Dietze (1951).

P. Wellmann (1951) hat auf der Sternwarte Hamburg-Bergedorf das Phänomen spektralphotographisch untersucht. Auf diese und die Gothaer Messungen wird speziell bei den Bemerkungen zur physikalischen Erklärung des Phänomens zurückzukommen sein.

b) Herkunft, Weg und Vebreitung der lufttrübenden Partikel

In der eingangs wiedergegebenen Mitteilung der Hauptwetterdienststelle Potsdam wurden bereits grosse Waldbrände in Kanada zur Erklärung der Erscheinung herangezogen; die erzeugte Rauchdecke hatte nach H. Runge bereits nahe am Entstehungsort eine Breite von rund 300 km. Es schien mir nicht uninteressant, über diese riesigen Waldbrände näheres in Erfahrung zu bringen; zumal da die Londoner Zeitung »The Daily Telegraph« am 28. Sept. 1950 u. a. die Bemerkung brachte: »British meteorologists believe these phenomena may have been caused by particles in the air originating from a volcanic eruption of a forest fire.«

Ein Einblick in kanadische Zeitungen zeigte einen anderen Entstehungsgrund der Waldbrände. Die in Montreal erscheinende Zeitung »The Gazette« gab am 28. Sept. 1950 eine

Korrespondentenmeldung wieder, aus der ich nachstehend einige Sätze citiere:

»Edmonton, Sept. 27. 1950. — (CP) — Snow and drought-ending rain today put the last smothering blanket over a giant chain of forest fires in the Canadian Northwest which had attracted the attention of much of the continent.

Several inches of snow has fallen along the southern end of the Alaska Highway in northeastern British-Columbia and a steady drizzle has dampened tinder-dry northern Alberta in the last 24 hours.

Only a few days ago, these regions were in the grip of some 100 forest fires. They stretched from the Saskatchewan border across northern Alberta and 300 miles north along the Alaska Highway . . .

An 18-day drought ending Monday,[1] during which a fall heat wave sent northern Alberta temperatures soaring into the eighties[2] for 10 days, gave the fire chain its start Sept. 17 . . .

Terrific heat waves generated by these fires tossed airplanes around in the air as if they were toys . . . On one flight . . . a shifting cargo of coffins injured 25 persons aboard an American transport.

But late today all of Alberta was reported clear of forest fire smoke.«

Während ausgedehnte Waldbrände in Kanadas Wäldern im Frühjahr und Frühsommer häufig aufzutreten pflegen, wurde demnach der Ausbruch der riesigen Herbstbrände des Jahres 1950 offenbar durch eine für den September dort ungewöhnliche Dürre- und Hitzeperiode begünstigt.

Noch in etwa 3 000 km Entfernung vom Brandherd waren die Rauchschwaden örtlich so dicht, dass eine nachtähnliche Verfinsterung eintrat. Hören wir hierzu einige Sätze aus der amerikanischen Zeitschrift »Life», Ausgabe vom 9. Okt. 1950.

»Last week in Ashtabula[3], Ohio . . . the sky suffused with a weird yellow light . . . Smoke blown from huge forest fires raging in Alberta and the District of Mackenzie had spread an enormous sun-stifling pall over the U. S. from Chicago to Philadelphia. In different localities the sky glowed with strange copper, pink and blue tones. In this unreal darkness at noon, birds retired for the night and airport beacons were lighted . . .«

Aufgrund der absoluten Topographien der 500 mb-Fläche zeigte H. Runge den Weg der »Rauchspitze» vom 24.—27.9.1950. Aus einer flüchtigen Durchsicht von Pressemeldungen ergaben sich hierzu noch folgende Ergänzungen.

»The Gazette», Montreal, 27.9.50. »The smoke reached Newfoundland Monday night and was reported over Bermuda later.«

Le Monde, Paris, 29.9.50. »Dans la journée de mardi[1] le soleil est apparu d'une couleur bleu saphir en Écosse. Et le même phénomène a été observé hier mercredi au Danemark dans la matinée, puis à Lyon, à Toulouse et jusqu'à Porto au cours de l'après-midi.«

Expressen, Stockholm, 27.9.50 — Deutsche Übersetzung[2] — »Als heute morgen die Sonne hervorbrach aus dem regenschweren Himmel, war sie von Schonen bis hinauf nach Härjedal kobaltblau!«

Die mittlere geographische Breite der schwedischen Landschaft Härjedal, des südlichen Teils des Läns Jämtland, ist etwa 62° Nord, diejenige von Porto, einer bekannten Hafenstadt Portugals, 41° Nord. Die ursprünglich etwa 300 km breite Rauchdecke hatte sich demnach bei ihrem Eintreffen in Europa bis zu einer Nordsüderstreckung von rund 2 500 km ausgebreitet; angesichts des zurückgelegten Weges von etwa 15 000 km erscheint dies durchaus plausibel.

Aufgrund der in H. Runges Mitteilung reproduzierten absoluten Topographien und der obigen Pressemeldungen wurde versucht, in Abb. 1 einen Überblick über die Ausbreitung und den Weg der Rauchdecke bis zu ihrem Eintreffen auf dem europäischen Festland zu geben. Wie gesagt, nur einen Überblick; Exaktheit oder Vollständigkeit konnte natürlich mit dieser Darstellung nicht angestrebt werden.

Durch die Blaufärbung der Sonne hervorgerufene Verkehrsstockungen meldeten die Zeitungen z. B. aus Hälsingborg (Schweden) und Basel (Schweiz). Offenbar interessierten sich die Verkehrsteilnehmer für die Farbänderung der Sonnenscheibe mehr als für den

[1] = 25. Sept.

[2] 80 Grad Fahrenheit = rund 27 Grad Celsius.

[3] Die Stadt Ashtabula liegt am Südufer des Erie-Sees.

[1] = 26. Sept.

[2] Der schwedische Originaltext lautet: »När solen i morse bröt fram ur regntunga skyar från Skåne upp till Härjedalen var den koboltblå!«

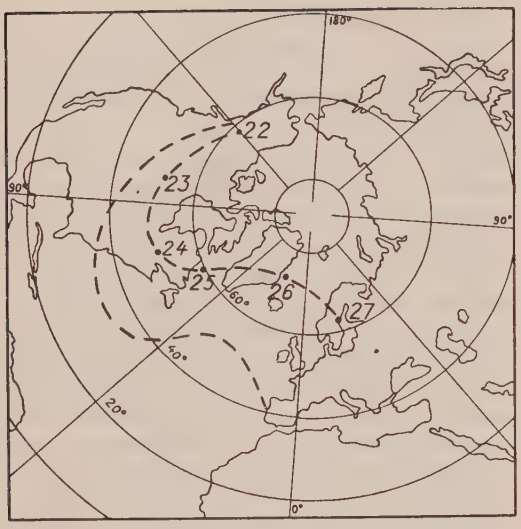

Abbildung 1. Weg der Rauchdecke vom 22.—27. Sept. 1950 jeweils 03 Uhr Weltzeit.

Farbwechsel der Verkehrsampeln, sodass an den Strassenkreuzungen Verkehrsstockungen leicht eintreten konnten.

II. Zur physikalischen Erklärung des Phänomens

Nach dem obigen kann es wohl keinem Zweifel mehr unterliegen, dass die Waldbrände im Nordwesten Kanadas die Ursache für das weit verbreitete Auftreten der Erscheinung in Europa waren. Im folgenden soll jedoch zunächst die Frage, in welcher Höhe sich die lufttrübenden Partikel über Europa befanden, einer eingehenderen Prüfung unterzogen werden.

Überwiegend wird berichtet, dass es sich eigentlich um mindestens zwei auffällige Phänomene handelte, die keineswegs in allen Fällen zusammen in Erscheinung traten. Erstens war die Sonne blauverfärbt; dies war die ungewöhnlichste und daher als besonders auffallend vielfach an erster Stelle hervorgehobene Erscheinung; zweitens konnte man in vielen Gegenden Europas die so verfärbte Sonnenscheibe trotz ziemlich hohen Sonnenstandes stundenlang ohne jede Blendung mit blossem Auge betrachten. Und als die Trübung nachgelassen hatte, erschien das Sonnenlicht in manchen Gegenden weiterhin merklich gedämpft und hatte einen bläulichen Schimmer,[1] »wie etwa eine Quarzlampe», ein nach meinen eigenen Wahrnehmungen sehr treffend gewählter Vergleich. In den Nächten kurz vor und kurz nach dem 27. Sept. 1950 erschien vielfach in Europa der volle oder nahezu volle Mond ebenfalls bläulich gefärbt. Stellenweise gab es noch bis zu acht Tagen später Verfärbungen. So schreibt z. B. P. Wellmann (1951) in dem Bericht über seine Beobachtungen in Hamburg-Bergedorf, wo das Phänomen am frühen Vormittag des 27.9.1950 am besten zu sehen war:

»Der anomalen Extinktion wurde im Laufe des Sept. 27 durch dichtere tiefe Bewölkung ihre Auffälligkeit genommen, sie blieb aber bis in den Anfang der Nacht hinein erhalten und äusserte sich in einer deutlichen Verfärbung des Mondes und der hellen Sterne, bis die trübende Schicht abzog. In viel geringerem Masse wiederholte sich die Erscheinung noch gelegentlich und wurde zuletzt am Abend des Okt. 5 gesehen . . .»

Die Erwähnung der Verfärbung der hellen Sterne, wobei eine Kontrastwirkung kaum in Frage kommen kann, spricht wohl stark gegen den nach W. Gelbke (1951) bei einem Greifswalder Kolloquium gemachten Versuch, die Blaufärbung rein physiologisch zu erklären.

Also, wie erwähnt, zwei ziemlich verschiedenartige Phänomene, einerseits Blaufärbung von Sonne und Mond, andererseits stundenlange blendungsfreie Beobachtungsmöglichkeit der Sonne. Zwei Wirkungen, vielleicht auch zwei Ursachen? Eine Meldung des »Daily Telegraph» in seiner Ausgabe vom 27. Sept. 1950 scheint diese Vermutung zu bestätigen:

»Glasgow, Dienstag[2]. — Allover Scotland for more than an hour this afternoon people saw a 'blue' sun. To-nights full moon looked sky-blue in colour. — The sun could be gazed at without dazzling the eyes. The blue hue changed constantly, as though smoke were drifting across the sun . . . The meteorological station at Renfrew, near here, later learned that an airplane had reported finding a thin layer of dust and sand at 43 000 ft[3] over the east of Scotland. At 20 000 to 30 000 ft it found a layer of ice particles in the thin cirrhus

[1] Vgl. den eingangs wiedergegebenen Beobachtungsbericht aus Schwerin in Mecklenburg.

[2] = 26. Sept.

[3] 1 foot (englischer Fuss) = 0,305 m.

cloud formation. — Experts believed that the two layers combined had the effect of filtering out the other colours in the sun's rays. The blue was left predominant. — One expert said the dust cloud was almost certainly part of a great American sandstorm of a few days ago. — The phenomenon is rare. It has been observed during dust storm conditions in Egypt . . .»

Nach dem Bericht des Piloten waren also über Schottland mindestens zwei lufttrübende Schichten vorhanden, eine relativ mächtige Schicht in der Troposhäre, zwischen 6 und 9 km Höhe,[1] eine dünne Schicht in der Stratosphäre, in etwa 13 km Höhe. Die Troposhären-Schicht bestand nach Angabe des Piloten aus »ice particles in the thin cirrhus cloud formation». Nun sind Cirruswolken bekanntlich immer Eiswolken; der Pilot wollte also damit vielleicht sagen, dass es sich um eine Ansammlung von Eispartikeln in auffallend starker Verdichtung handelte. Die bei den kanadischen Waldbränden entstandenen und durch die aufsteigenden Warmluftströme in grosse Höhe emporgerissenen Verbrennungsprodukte könnten bei der Bildung dieser Eispartikel als Sublimationskerne gewirkt haben. Dass nach den Beobachtungsberichten aus Schwerin, Hamburg-Bergedorf und Gotha keine sonst häufig mit Eiswolken verknüpften optischen Erscheinungen, wie z. B. Halos und Höfe, beobachtet wurden, spricht gegen diese Auslegung der Pilotangaben, ohne sie wohl gänzlich auszuschliessen.

Dagegen sagt der Pilot von der oberen, dünnen Schicht in 13 km Höhe, sie habe aus Staub und Sand — »dust and sand» — bestanden. Es erscheint daher möglich, dass diese in der Stratosphäre schwebende Schicht nicht von den erwähnten Waldbränden herrührte, sondern vielleicht von Vulkanausbrüchen oder Sandstürmen. Hierfür spricht u. a. die Mitteilung eines in Saporoshje, Ukraine, beheimateten Korrespondenten der Antwerpener Astronomischen Gesellschaft, M. V. Tshernov, wonach in Saporoshje bereits am 19. und 20. Juli 1950, also wochenlang vor dem Ausbruch der Waldbrände in Kanada, eine bläuliche Färbung des Mondes festzustellen war. Tshernov schrieb u. a.: »Les 19 et 20 juillet, par exemple, j'ai observé pour la première fois dans ma vie une teinte bleuâtre à la Lune et les 23 août et 22 septembre une teinte verdâtre. Il est probable qu'il faut voir dans ce curieux phénomène l'effet des dernières éruptions volcaniques importantes (Hécla, Paricutin 1943, Iles Hawai 1949, Japon 1950). D'autre part, j'ai remarqué que la lumière cendrée de la Lune a été plus faible que d'habitude.» Ferner hat, wie bereits erwähnt, P. Wellmann Verfärbungen der Sonne und der hellen Sterne noch bis zum 5. Okt. 1950 beobachtet, wo die untere Schicht kaum noch vorhanden gewesen sein dürfte. Es erscheint daher möglich, als Ursache der Blaufärbung in der Hauptsache die obere Schicht anzusehen, während die untere Schicht vor allem bewirkte, dass man die Blaufärbung der Sonne stundenlang ohne Blendung beobachten konnte.

Diese Annahme findet nach meiner Ansicht eine weitere Stütze in der theoretisch-physikalischen Erörterung, die P. Wellmann der Mitteilung seiner spektralphotographischen Beobachtungsergebnisse angefügt hat. Er nahm am 27. Sept. 1950 mit dem Zweiprismen-Spektrographen des 1 m-Spiegels der Sternwarte Hamburg-Bergedorf Sonnenspektren auf und verglich sie mit normalen Spektren vom 10. Okt. 1950, wobei speziell der Spektralbereich $\lambda\lambda$ 3 800—4 700 Å untersucht wurde. Die Ergebnisse dieser Untersuchung betrachtet er im Lichte der bekannten Theorie von Mie und Debye für kugelförmige dielektrische Teilchen; es zeigte sich, dass in dem untersuchten Spektralbereich der Extinktionskoeffizient der Wellenlänge proportional war. Die Teilchenradien a, für die dies möglich ist, liegen aber nach Untersuchungsergebnissen von Stratton und Houghton, sowie von Greenstein nur in einem sehr engen Bereich. Es könnte also nur dann Blaufärbung eintreten, wenn die trübende Schicht aus Teilchen nahezu gleicher Grösse besteht. P. Wellmann bemerkt dazu: »Gleichzeitig wird damit plausibel, warum diese Art von Trübung nur so ausnahmsweise selten auftritt.» Die geforderte Homogenität der störenden Schicht spricht wohl auch dafür, dass in der Hauptsache die obere Schicht die Blaufärbung bewirkte; denn in der Stratosphäre mit ihren gleichmässigen Strömungsverhältnissen ist Homogenität der störenden Schicht leichter vorstellbar als in der wesentlich unruhigeren Troposphäre.

Unter der Annahme eines Brechungsindex

[1] Mit den sonstigen Annahmen über die Höhe der Partikel stimmt dies einigermassen überein.

von $^4/_3$ (Wasser 1,33; Eis 1,31) erhält P. WELLMANN für das Verhältnis des Teilchenradius a zur Wellenlänge $\lambda = 4\,300$ Å (mittlere Wellenlänge des untersuchten Bereichs) die Abschätzung $\frac{a}{\lambda} = 1{,}24$.

Diesen Überlegungen liegt die Annahme kugelförmiger Teilchen zugrunde; sie führt für Teilchen, deren Radius klein ist gegen die Wellenlänge $\left(\frac{2\pi a}{\lambda} < 1\right)$, bekanntlich zum RAILEIGH'schen Gesetz, nach welchem der Extinktionskoeffizient umgekehrt proportional ist zur vierten Potenz der Wellenlänge. C. SCHAEFER und H. STALLWITZ zeigten (1916), dass für zylindrische Teilchen ein ähnliches Gesetz gilt, bei dem die dritte Potenz von λ im Nenner steht. Ob auch in diesem Falle, entsprechend den erwähnten Untersuchungen von STRATTON und HOUGHTON, Arbeiten vorliegen, die die gänzlich abweichende Abhängigkeit des Extinktionskoeffizienten von der Wellenlänge bei Vorhandensein grösserer Teilchen zeigen $\left(\frac{2\pi\varrho}{\lambda} > 1,\ \varrho = \text{Zylinderradius}\right)$, ist mir nicht bekannt.

Nach G. DIETZE dehnte sich bei den erwähnten Gothaer Messungen die verstärkte Extinktion im langwelligen Bereich des sichtbaren Spektrums nicht wesentlich auf das infrarote Spektralgebiet aus; er schliesst hieraus, ähnlich wie P. WELLMANN aus seinen spektralphotographischen Untersuchungen, auf Teilchen etwa von der Grösse der Lichtwellenlänge.

Zusatz bei der Korrektur

In einer mir erst nachträglich bekannt gewordenen Abhandlung, erschienen in Experientia, Verlag Birkhäuser, Basel, Bd. VI/12. 1950, S. 457 unter dem Titel »Beitrag zum Phänomen der Blauen Sonne» benutzt W. SCHÜEPP Beobachtungen, die er am Physikalisch-Meteorologischen Observatorium Davos angestellt hat, zur Führung des Nachweises, dass Rauchpartikel, Vulkanstaub, Wüstenstaub und Perlmutterwolken als Ursache der Blaufärbung der Sonne nicht in Frage kämen. Hierzu sei mir folgende Bemerkung gestattet. Es erscheint mir schwierig, den Umstand, dass die Sonne in grossen Teilen Europas stundenlang ohne Blendung betrachtet werden konnte, anders als durch die Kanadischen Waldbrände zu erklären; die Existenz einer dünnen störenden Schicht in der Stratosphäre wäre leichter auf andere Ursachen zurückzuführen.

Erwähnt sei noch W. SCHÜEPP's Mitteilung, dass eine Gruppe französischer Forscher die am 27. Sept. 1950 auf dem Jungfraujoch Sonnenbeobachtungen durchführten, nichts Abnormales festgestellt hat. Die störende Schicht wies also offenbar grössere Lücken auf.

Potsdam den 10. 8. 1951.

LITERATUR

DIETZE, G., 1951: Die anomale Trübung der Atmosphäre September/Oktober 1950. *Ztschr. f. Meteorol.* **5**. (z. Zt. im Druck.)

GELBKE, W., 1951: Bemerkungen zum Phänomen der blauen Sonne. *Ztschr. f. Meteorol.* **5**. (z. Zt. im Druck.)

JENNE, W., 1951: Beiträge zur Beobachtung und Erklärung des Phänomens »Blaue Sonne». *Ztschr. f. Meteorol.* **5**. (z. Zt. im Druck.)

RUNGE, H., 1951: Blaue Sonne — blauer Mond. *Ztschr. f. Meteorol.* **5**, 60.

SCHAEFER, C. und STALLWITZ, H., 1916: Ein zweidimensionales Dispersionsproblem. *Ann. d. Physik* **50**, 199.

SOCIETE D'ASTRONOMIE D'ANVERS, 1950: La Lune bleue. Gazette astronomique, *Bull. de la Soc.*, Nos. 371—372, p. 103.

WELLMANN, P., 1951: Die Blaufärbung der Sonne am 27. Sept. 1950. *Ztschr. f. Astrophys.* (z. Zt. im Druck.)

The Blue Sun of September 1950

By ANDERS ÅNGSTRÖM, Swedish Meteorological and Hydrological Institute

(Manuscript received 14 July 1951)

Abstract

Two causes for a coloured sun are discussed, namely refraction and absorption. The importance of integrating the refraction effects arising from different parts of the sun's disk as light sources is emphasized. It is shown that by such integration of ring phenomena around the sun, many observed peculiarities may be explained. Important conditions for that some types of coloured suns shall arise are homogeneity of the particles of the scattering medium, and also that the particles shall be large enough to give rise to rings of sufficiently small radius. Transfer of air masses at long distances but without a sideward mixture taking place is in favour of the creation of dust sheets of homogeneous character, as the vertical sedimentation has then time to come into action.

The sun, when seen through some absorbing medium — it may be clouds or dustlayers of different origin — generally takes on colour more or less different from the normal one. Absorption, as well as scattering, being in general different for different wave lengths, this effect is a natural one. Another possible cause for a change in the apparent colour of the sun may be found in the effects of refraction. During the end of September 1950 the sun appeared more or less distinctly blue to a number of European observers and also at many stations in the eastern parts of North America. As the blue sun represents a very unusual phenomenon it attracted great attention and aroused considerable interest. A number of rather exhaustive papers have already appeared on the subject.

According to generally accepted view, the colour effect resulted from cloud or smoke layers created in connection with great forest fires which had previously taken place in Canada during the period 17—25 Sept. 1940. An analysis of the upper air charts for the period 20—27 Sept. seemed to suggest this cause.

It is not the authors intention to repeat here large parts of the descriptions and observations published by others. For these, the reader is referred to the interesting material presented by JENNE (1951) in this issue of Tellus, and to a few other papers listed among the references. In making the following suggestions as regards the possible explanation, I simply presume that the essential facts are known. Before entering into a more theoretical discussion, I wish to add some few facts based upon observations in Sweden.

Table 1

Reports from Swedish Meteorogical Stations on the "Blue Sun" of 17th September 1950

Piteå { lat. 65°19′ / long. 21°28′ } On the 27th the sun broke through the clouds between 15 h and 15.30 h. It was blue in colour (cobolt blue), as seen by several observers in the vicinity.

Koskats { lat. 66°29′ / long. 20°18′ } Wednesday 27th Sept. the sun was strongly shimmering blue, in a very uncanny way.

Öjebyn { lat. 65°21′ / long. 21°23′ } Blue sun. The sun appeared silvergrey to blue. No glare from it.

Bruksvallarna { lat. 62°39′ / long. 12°25′ } The 27th September, the sun was bluish between about 8.45 h to 9.15 h; the light from it was feeble and could be looked at with the naked eye.

Kåreslätt { lat. 57°25′ / long. 14°29′ } The 27th Sept. at 9.30 h the sun appeared bluish.

Singshult { lat. 56°44′ / long. 13°22′ } The 27th Sept. the sun blue in colour at 8.50 h.

Törneryd { lat. 56°14′ / long. 15°01′ } The 27th Sept. the sun bluish "like a day light lamp".

Kristianstad { lat. 56°02′ / long. 14°09′ } The 27th Sept., the sun blue-white.

Lyngsjö { lat. 55°56′ / long. 14°05′ } Cobolt blue sun 9.10 h to 11.20 h, Sept. 27th.

Malmö airport { lat. 55°36′ / long. 13°03′ } The 27th September a peculiar phenomenon was observed between 9 h and 9.30 h. The disk of the sun appeared a clear light-blue colour through the cloud sheet, which consisted of Cist, Cu and Scu. It seems doubtful, however, but whether the Ci-Str did not actually consist of a sheet of dry haze. At about 9.15 h the cloud elements at about 10° distance from the sun showed a dusky red colour. At 15.35 h—15.55 h a similar phenomenon was observed, but the solar disk was then not so decidedly blue but had more the colour of a flame used for welding. The colour of the clouds had by then disappeared.

Lund { lat. 55°42′ / long. 13°12′ } Sun blue 8.30 h—10.30 h the 27th.

Björka { lat. 55°39′ / long. 13°38′ } Sun bluish grey, most conspicuously at 9.40 h the 27th Sept.

Alnarp { lat. 55°39′ / long. 13°05′ } The 27th: Sun blue between 9 h and 10 h.

Svalöv { lat. 55°55′ / long. 13°07′ } The 27th, sun blue between 8 h and 9.30 h.

Ven { lat. 55°55′ / long. 12°44′ } The 27th: Sun clearly light blue at 8.10 h—9.15 h.

Hörby { lat. 55°51′ / long. 13°40′ } Sun blue behind light cloud sheet at 9 h—10 h, the 27th.

Morups tånge { lat. 56°55′ / long. 12°22′ } The 27th, sun appeared blue between 8.30 h to 9.15 h.

The Table 1 gives a complete list of the reports on the "blue sun" received from the Swedish meteorological stations. It ought to be noted that the first appearance of the phenomenon occurred almost simultaneously at all stations from Bruksvallarna at lat. 62° 39 N, down to Malmö airport at lat. 55° 36 N. The slightly later observation at Piteå, 65° 19 N, can possibly be due to the fact that the sun broke through the lower cloud layers first at 15^h in the afternoon at that station.

In Table 2 are given the results of some actinometric observations at Stockholm. These observations were taken at a considerably later date than the first appearance of the blue sun, because of the fact that earlier observations were made dubious by a rather large variability of the sun's radiation. However, during the actinometric observations the sun appeared decidedly blue at times. From the measurements of the total radiation together with those determined with aid of red and yellow filters, the quantities β and α are computed according to the method devised by myself and later further developed by SCHÜEPP (1949). It may be remembered that the scattering by dust and other solid or liquid particles in the air, is in the fundamental considerations on which this method is based, expressed by the empirical formula:

$$I = I_0 \cdot e^{-\frac{\beta}{\lambda^\alpha} \cdot m}$$

where I_0 and I are the incoming and outgoing radiations respectively, β is the scattering coefficient and α an exponent, which reflects the dependence of the scattering upon wave length. In the case of purely molecular scattering, α has a value equal to 4.015. The scattering by ordinary dust in the atmosphere is characterized by a value of α of about 1.3; after volcanic outbreaks (like that of Mount Katmai in 1912) α goes down to values as low as about 0.5 or even less, showing the particles to be considerably larger than normal. Over the deserts, especially after sand storms, values of α have been found which are also very low (see for instance F. ALBRECHT 1941).

It is evident that for a value of $\alpha > 0$ the scattering is larger the shorter the wave length, viz. a larger detoriation for instance in blue than in red. If on the other hand α assumes a

Table 2
Place: Stockholm 59° 11′ N, 18° 4′ E

Date	Hour	Radiation from sun gr cal/cm²				
		Total	OG 1	RG 2	α	$10^3\ \beta$
1950						
29/9	13.12	0.622	0.452	0.376	—0.8	163
	13.20	0.622	0.452	0.372	—0.5	160
	13.28	0.717	0.523	0.427	0.3	124
	13.36	0.780	0.562	0.460	—1.2	99
	13.44	0.897	0.658	0.532	0.2	82
	13.53	1.031	0.748	0.602	—0.5	46
30/9	10.03	0.963	0.727	0.604	0.6	107
	10.11	0.978	0.738	0.620	0.3	93
	10.46	1.070	0.793	0.653	0.5	83
	10.54	1.098	0.799	0.658	—0.8	70
	11.42	1.070	0.789	0.645	0.5	84
	11.50	1.070	0.790	0.643	1.1	83
	12.40	0.991	0.737	0.606	0.6	105
5/10	12.37	1.192	0.866	0.682	2.3	29
	12.45	1.210	0.881	0.702	1.4	30

negative value, the dependence of the scattering effect upon wave length is reversed, viz. the red is reduced more rapidly than the blue. Apart from the question of whether the supposition of a constant α throughout the spectrum is valid here (and probably it is not), we may however conclude from the way in which the computation is made that the observations on which it is based have given a much larger reduction for waves longer than 0.525 than for shorter wave lengths. The blue has consequently been represented in the sun light more strongly than is normal. From Table 2 in the doctorate thesis of SCHÜEPP, a table based on the theoretical considerations of MIE (1908), it is clear that while the ordinary scattering particles in the atmosphere have a diameter less than 2.0 μ, the particles in this actual case must have had a much larger diameter, probably greater than 15 μ. I will return to this subject later on.

From what has been said above it seems evident, that the bluish colour of the sun *can* have arisen through the scattering and absorption by a cloud or dust layer containing rather large particles compared with those present in the clear atmosphere. But the question is whether this statement represents the whole truth. A silverblue or grayish blue sun light might have arisen in this way, but can it explain the rather clear blue sun observed at many places? Before attempting an answer it may be worth while to consider for a moment the possible effects of refraction.

As has been shown theoretically as well as practically, the refraction of the light from a luminous point source, under certain conditions, gives rise to luminous ring phenomena: circular spectra with the light source as the centre. The radii of these rings are in general inversely proportional to the diameter of the particles and directly proportional to the wave length. Kämtz (PERNTER-EXNER 1922) has made a large number of measurements on such rings round the sun, when the sun light is passing through thin cloud sheets consisting of water droplets. Similar measurements have also been made by Hilding Köhler. The largest drops found by Kämtz in this way have a diameter of 61 μ, giving rise to rings which for red light (about 0.65 μ) had a radius of 0°39′. For blue light these particles would consequently be expected to give rings with radii of just the same order of size as the diameter of the sun itself (about 0°32′).

What will now occur if the radii of these rings get so small as to be comparable with the sun's diameter itself? It seems evident that colour effects in the neighbourhood of the sun must then result as an integral effect of all the rings which we can imagine to be produced with the different elements of the sun's disk as centres. Let us take a simple case with the radius of the first ring of blue light equal

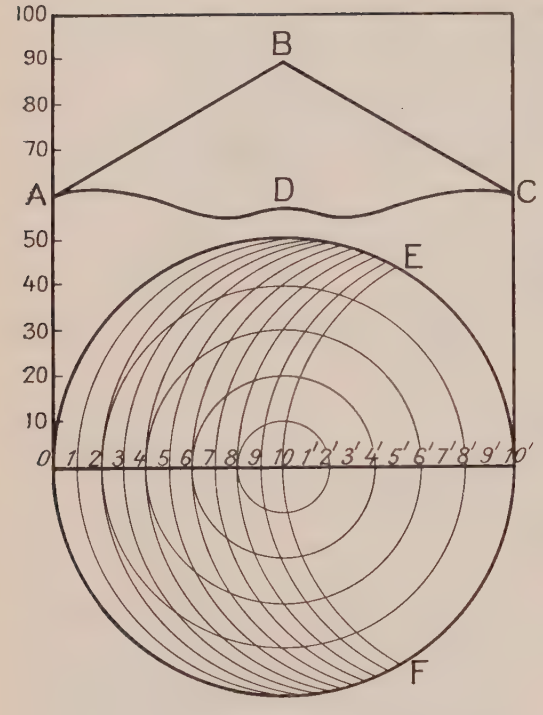

Fig. 1

Colour distribution of "additional" refracted light over the sun's disk under the assumption that first blue ring has the same radius as the sun's disk. If the blue light (wave length 4,200 Å) in sun radiation would be uniformly distributed over the sun's disk, the *additional* light at point 10′ would be proportional to the length of the arc EF, the light at point 9′ proportional to the arc through 9 and so on. The distribution of additional blue light over the sun's disk would then be according to the line ABC, the intensity being largest at the centre and uniformly decreasing against the edges. If due regard is also taken to the fact that the blue light in the direct sun radiation is subjected to a rapid decrease from the centre to the edges the distribution of the additional blue light will be given through the curve ADC showing the blue to be strongest at the periferic parts of the disk. A tendency to a blue ring thus is apparent also in this case. (Distribution of radiation over sun's disk, see Smithsonian Physical Tables 1910, p. 179).

to the sun's radius (r). Then a point at the distance a from the centre of the sun will additional blue light from all elements on a segment AB of a circle which has a radius r and the point in question as a centre. The apparent illumination with blue light of the various points of the sun's disk may for this simple case simply be expressed by $I \simeq \arccos \gamma$; where $\gamma = \frac{a}{r}$.

Fig. 1 demonstrates how this extra illumination of blue light is distributed over the sun's disk. It falls off from the centre to about 20 per cent at edges. If we take account also of the fact that the blue light of the sun's disk is decreasing from centre to edges and that the integral "additional" light on the points far from the centre has its source, to a larger extent, at elements near the sun's centre than is the case for points near the sun's centre, we find an almost uniform distribution of additional blue light over the sun's disk. On the other hand additional red light can only occur at points for which γ is larger than about 0.60, which means that the central parts of the sun up to about 0.6 of the radius must appear decidedly blue or green.

If the radius of the first blue ring is larger than the radius of the sun, a peculiar phenomenon ought to occur. Then the central parts of the sun can not obtain additional blue light from any parts of the sun. A darker spot ought to occur in the centre of the sun's disk and around it a clear blue circle ought to appear. As no red light probably in that case will add itself to the direct light from the sun's disk, the sun will appear blue or blue green as a whole, with exception for the dark centre.

To these considerations we may add from a paper by GELBKE (1951) the following description taken from Pernter-Exner of some experiments by Kiessling who, in view of some peculiar light phenomena following the eruption of Krakataua, made experiments on the optical effect of dust and powders on sun light: "In einem Glaskolben wurden nach Belieben, Staub- oder Dampfwolken verschiedenster Art erzeugt. Die künstlich durch Zerkleinern fester Stoffe hergestellten Staubmassen waren nicht geeignet, im durchfallenden Licht besondere Farbenphänomene zu erzeugen... offenbar weil die Grösse der Teilchen sehr ungleich war . . . Mit den Sporen von *Boletus cervini*, die einen Durchmesser von 0,026 bis 0,031 mm haben, also recht gross sind, gelang es hingegen, sehr farbenprächtige Beugungerscheinungen zu erzielen, offenbar deshalb, weil alle Teilchen die gleiche Grösse hatten. Ebenso zeigten verschiedene Kondensationsprodukte, wie Salmiaknebel und Wassernebel sehr schöne Farben, desgleichen alle durch Verbrennung entstandenen Rauch-

arten. . ." "Aus der Veränderung der Farben in kurzer Zeit nach Entstehen des Nebels — die Sonne erschien durch denselben zu Anfang rot oder braunrot, dann trat ein violetter Farbenton hinzu, und nach wenigen Minuten ging die Farbe in ein reines, zuletzt blendend leuchtendes Azurblau über — lässt sich auf eine Änderung der Grösse der Nebelteilchen schliessen."

Further I also wish to cite from the paper af Gelbke the following description of early observations of blue- or green-coloured suns.

"1465 In diesem Jahre ist die Sonne um den heiligen Creuztag gar dunkel am Himmel gestanden und ein blauer Cirkel (vgl. Greifswalder Beobachtungen.) rings umher/so blau als ein Kornblume gesehen worden.

1554 Grüne Sonne und auffallenden Dämmerungserscheinungen in Thüringen.

1571 Grüner Mond am 27. Oktober. (Ohne Ortsangabe)

1815 Nach dem Ausbruch des Tambora grüne Sonnenfärbung im Indischen Ozean."

The first of these cases, the one of 1465, seems to present an instance where the peculiar case of a dark centre with a blue ring has actually been observed.

It is evident that we can not further apply the theoretical considerations holding for small droplets to the particles giving rise to these phenomena. On the other hand the experiments of Kiessling and others show that quite similar phenomena of refraction occur when light is passing through powder and dust sheets from solid substances. From theory and experiments and from what is known from earlier observations, it may be proposed that two conditions ought to be fullfilled in order to produce the blue- or green coloured sun, namely:

(1) The particles ought to be of rather uniform size,

(2) The particles ought to be large enough, probably of a size larger than 0,050 mm in diameter.

It is perhaps doubtful whether the first condition is really necessary for producing the blue colour of the sun's disk or of rings around it. It is clear that if particles of rather different size are present in the cloud or dust sheet, the smallest blue ring arising through refraction must result from the largest particles present and that the blue colour must be rather pure, since no other particles can produce a mixture with other longer waves just at that angular distance from the centre. If the particles are not of uniform size the other colours, as for instance red, must appear rather dusky and be spread out over a wider area around the sun. Compare here the figure published by Gelbke in his paper mentioned above. The only condition necessary that a clear blue colour shall be produced at the disk or in its immediate surroundings seems then to be that particles large enough shall be present in sufficient amount to produce a visible effect.

Since it seems evident that refraction can produce effects very similar to those observed, it may be asked whether the observed surplus of blue in the transmitted radiation does not simply result from the refraction effect and the apparent high transmission of blue simply is a result of the fact that only blue refracted light falls within the opening angle of the actinometer. As, however, the opening angle of the Michelson actinometer is 8°—20°, and consequently covers the essential part of the area within which the refraction phenomenon takes place, I think that in the present case this explanation does not include the whole truth. It seems therefore safe to conclude that an abnormal transmission of blue light has taken place. On account of the fact that the difference in transmission between short and long waves is not very large, I doubt on the other hand that the transmission conditions alone would have been able to produce the optical sensation observed. We have here probably a case where the *two causes together* have been necessary to produce the impression of a clearly blue sun.

Finally some few words concerning the origin of the refracting and scattering particles. Evidently they have been abnormally large and they have occured at a level where in general such large particles seldom occur, namely at a height of 10,000 to 13,000 meters. The explanation that they have originated from the large and intense forest fires in Canada seems acceptable, even if it appears quite remarkable that smoke from these fires should have been able to rise to such a height. The

possibility of some other origin should not, however, be overlooked. The trajectories of the air masses which passed over Europe during the period 27—30 September also pass over the Canadian forest fire region at the proper time, but it seems possible to extrapolate them further back in time to the region of the Japanese Islands. The unsafety and scarcity of observations from the Pacific Ocean makes the extrapolation not very dependable. In Japan, however, there was observed a violent outbreak of the Volkano Asama on September 23. *Hamburger Abendblatt*, on Sunday, September 24, carried the following notice from Associated Press: "Eine 10000 m hohe Rauchsäule stieg zum Himmel auf, als der 2780 m hohe Vulkan *Asama*, etwa 110 km nordwestlich von Tokio am Sonnabend früh ausbrach. In dem Naheliegenden Kurort Karnizama wurden von der Gewalt der Explosion zahlreiche Fensterscheiben eingedrückt."

It is perhaps doubtful whether dust particles from this volcano could have reached Europe already by the 27 of September, but on the other hand there are indications of other volcanic activity in the Japanese region at a somewhat earlier time. The wind reports from the upper air layers over the Pacific, however, do not permit conclusive statements concerning these possibilities. In this respect it would be highly interesting to know whether reports of a blue sun have come in from any points west of Canada. If the answer is negative, the volcanic hypothesis, as regards the origin of the causative particles, is eliminated. That it should be seriously considered, however, seems evident from the fact that in most cases where "blue suns" have been earlier reported heavy volcanic outbreaks (for instance that of Krakataua) had recently taken place in the same region.

REFERENCES

Albrecht, F., 1941: Ergebnisse von Dr Haudes Beobachtungen der Strahlung und des Wärmehaushaltes der Erdoberfläche. *Sino-Schwed. Exp. IX 2.*

Ashmore, S. E., 1951: Blue sun and moon. *Weather*, **6**, 4.

Elsley, E. M., 1951: Alberta forest fire smoke — 24 Sept. 1950. *Weather*, **6**, 1.

Gelbke, W., 1951: Bemerkungen zum Phänomen der blauen Sonne. *Zeitschrift f. Meteorologie*, **5**, 3.

Jenne, W., 1951: Das Phänomen "Blaue Sonne". *Tellus*, **3**, 3.

Mie, G., 1908: Annalen der Physik. 25, par. 377.

Pernter-Exner, 1922: Meteorologische Optik. Wien u. Leipzig.

Runge, H., 1951: Blaue Sonne — blauer Mond. *Zeitschrift f. Meteorologie*, **5**, 2.

Schüepp, W., 1949: Die Bestimmung der Komponenten der atmosphärischen Trübung aus Aktinometer-Messungen. Inanguraldiss. Springer-Verlag. Wien.

Wexler, H., 1950: The great Smoke Pall, Sept. 24—30, 1950. *Weatherwise*, **10**, 12.

Forecasting Minimum Temperatures

By HEINZ REUTER, Zentralanstalt für Meteorologie, Wien[1]

(Manuscript received 14 March 1951)

Abstract

Because of the fact that too many factors influence the nocturnal cooling of the ground surface, simplifications are necessary in order to derive a convenient formula giving the amount of cooling from sunset to sunrise. These simplifications must be justified both theoretically and practically. The solution is finally found by semiempirical methods. For the practical application of this cooling formula a diagram is constructed. A test of the results using observations for Vienna shows a good agreement between the predicted and observed temperature minima.

Introduction

The importance of calculation of minimum temperatures and the prediction of ground frost for agriculture, especially for the so-called frost districts is obvious. For this purpose a vast number of more or less empirical formulae have been produced by various authors. For a discussion of empirical formulae for forecasting the minimum temperature the reader is referred to E. S. Ellison (1928). Some details can also be found in the textbook by Geiger (1942). Other formulae and diagrams have been developed from Brunt's (1939) expression for the net loss of heat by radiation from ground [see Dufour (1938), Jacobs (1940) and Lönnqvist (1946)], but actually these formulae have not given a satisfactory solution of the problem. One difficulty is that a particular formula may give excellent results in one locality but not in another. The whole problem is made complex by the many factors which influence the nocturnal cooling. If we consider all these factors in a mathematical treatment the solution, if any can be given at all, would be too complex for practical purposes. If we oversimplify the problem on the other hand we can not expect accurate results.

Theory of nocturnal cooling of the earth's surface

The conditions which favour nocturnal cooling of the ground surface are well known from experience. These conditions are;

a) Clear skies,
b) Absence of wind,
c) Low vapour pressure in the atmosphere, and
d) Low thermal conductivity and specific heat of the ground.

All these factors have to be considered in a mathematical treatment for calculating the drop of temperature at the ground during the night.

A first theoretical approach is due to Brunt (1939). His well known formula can be written as follows;

[1] Most of the work for this study was done during a visit to the Training and Research Section of the Canadian Meteorological Service at Toronto under an Unesco fellowship granted by the Canadian Council for Reconstruction.

$$\Delta T_0 = \frac{2}{\sqrt{\pi}} \frac{E}{\sqrt{k_g \varrho_g c_g}} \sqrt{L} \qquad (1)$$

where ΔT_0 is the amount of the cooling at the ground surface from sunset to sunrise during a night of length L. E is the effective outgoing radiation, which is assumed to be constant during the cooling process and k_g, c_g and ϱ_g are the coefficient of heat conductivity, the specific heat and the density of the soil respectively. It is supposed that k_g, c_g and ϱ_g are constant both with respect to time and with depth. In order to derive equation (1) the effect of transport of heat by eddies from the atmosphere to the ground must be neglected. A further necessary simplification is that we consider only the vertical transport of heat and that we assume an isothermy in the ground at sunset as an initial condition.

Although some of these simplifications are rather restrictive and exclude many practical cases, BRUNT's formula has been used with remarkable success for the construction of frost prediction diagrams as has been stated before. The assumption, E = constant, seems to be a rather close approximation, at least for the beginning of the cooling process as was shown by SAUBERER (1936) by direct measurements. If the length of the night increases it might be necessary to consider a variation of E. As GROEN (1947) pointed out it is not too difficult to allow for a linear variation of E. For practical purposes however the assumption, E = constant, can be justified as long as no advection takes place and there is clear sky or no change in the cloudiness. In order to evaluate E we can use empirical formulae which give in general a close fit to the observations obtained by different authors. It is also possible to calculate the downward flux of the atmospheric radiation by means of a radiation chart whenever a radiosonde ascent is available. For different seasons in 1949 CZEPA and REUTER (1950) have evaluated the effective outgoing radiation in Vienna using ELASSER's radiation chart. A comparison of these results with values obtained by the empirical formula of ÅNGSTRÖM showed that the latter frequently overestimated E by as much as 20%. The same result was obtained by SAUBERER (1936) from measurements using a radiometer designed by ALBRECHT. In a recent study, LÖNNQVIST (1950) came to the same conclusions. On the other hand ROBINSON (1950) was able to show that values of E obtained by means of ELSASSER's chart are in general too low compared with measurements. In practice usually no measurements of E at sunset are available so that an empirical formula or a diagram has to be used. The assumption of dealing only with a vertical transport of heat in the ground and of considering k_g, c_g and ϱ_g as constants can be justified in general since only relatively small layers of the ground are affected by the nocturnal cooling.

To assume isothermal conditions in the ground at sunset seems to be rather arbitrary, but actually it has been shown by several investigations (BRACHT 1949) that near isothermy is observed in the highest layers of the ground at sunset. It is however not difficult to allow for a linear variation of temperature in the ground as will be seen later. In most cases the resultant cooling of the surface is only slightly modified.

As may be seen from (1) the cooling of the surface depends essentially upon the soil constants. Therefore we must expect a variation of ΔT_0 from one place to the other. Since furthermore the conductivity of heat changes to a high degree with the water content of soil, ΔT_0 at a given station will depend upon the moisture conditions in the soil. Since the value of k_g in snow is very small we get a much larger cooling at a snow surface than on ground even if the radiation is the same. For details the reader is referred to a paper by the author (REUTER 1948).

As we have seen most of the assumptions made by BRUNT in deriving equation (1) can be justified. As BRUNT has stated, equation (1) cannot be a final solution of the problem as long as we neglect the effect of heat transport from the air to the ground. Therefore the diagrams based upon (1) can be used for clear calm nights only. Following a study by PHILIPPS (1940) the author (REUTER 1947) has introduced the eddy transport of heat in the atmosphere into the theory. In so doing the whole problem becomes more complex and further simplifications are necessary. The solution becomes relatively simple under the assumption that the coefficient of eddy conductivity may be considered as constant.

If we allow for a linear variation of the

temperature T as an initial condition both in the ground and in the atmosphere and if we make the same simplifications as regard to E and the soil constants as before, our problem can be expressed by the following differential equations, where z is the vertical coordinate and t the time.

$$z < 0 \qquad \frac{\partial T_1}{\partial t} = \frac{k_g}{c_g \varrho_g} \frac{\partial^2 T_1}{\partial z^2} \text{ soil} \qquad (2\,a)$$

$$t = 0,\ T_1 = T_i - B(-z);$$

where B is the lapse rate of temperature in the soil and T_i the temperature of the surface at sunset.

$$z > 0 \qquad \frac{\partial T_2}{\partial t} = \frac{A}{\varrho} \frac{\partial^2 T_2}{\partial z^2} \text{ atmosphere} \qquad (2\,b)$$

$$t = 0,\ T_2 = T_i - \gamma z;$$

where γ is the lapse rate of temperature in the atmosphere at sunset and ϱ the density of the air which is assumed to be constant.

The boundary conditions are;

$$(T_1)_{z=0} = (T_2)_{z=0} \text{ for any time} \qquad (3\,a)$$

and

$$E + k_g \left(\frac{\partial T_1}{\partial z}\right)_{z=0} - c_p A \left(\frac{\partial T_2}{\partial z} + \gamma_d\right)_{z=0} = 0; \qquad (3\,b)$$

where A is the coefficient of eddy conductivity in the air ($A = K\varrho$ where K is the coefficient of eddy diffusivity), c_p is the specific heat of the air and γ_d the dry adiabatic lapse rate. The condition (3 b) states simply that the sum of the effective outgoing radiation, the flow of heat from below to the surface and the flow of heat from the atmosphere to the surface is equal to zero. The solution of (2 a) and (2 b) with (3 a) and (3 b) can be found following a study by the author (REUTER 1947) in which the solution of a similar system of equations with slightly different initial and boundary conditions was given.[1] For the surface it yields;

$$\Delta T_0 = T_i - T_0 =$$

$$= \frac{2}{\sqrt{\pi}} \frac{E + Bk_g + (\gamma - \gamma_d)\, c_p A}{\sqrt{k_g \varrho_g c_g} + c_p \sqrt{A\varrho}} \sqrt{L}, \qquad (4)$$

where the meaning of the different quantities is the same as in equation (1). Putting $A = 0$ and $B = 0$ in (4) we arrive at BRUNT's formula (1).

The assumption under which (4) is derived, namely A = constant, is only a rough approximation. Attempts were made by J. G. JAEGER (1945) and R. FROST (1948) to allow for a variation of A in the form of a power law according to SUTTON's well known theory. The treatment then becomes so complicated that it cannot be successfully used for practical purposes. As JAEGER pointed out, it is only possible to describe in this way the temperature distribution in atmospheric layers near the ground assuming that the surface temperature is kept at a temperature given by equation (4). Starting from isothermal conditions both in the ground and in the atmosphere, R. FROST neglects the transport of heat from below to the ground surface which seems to be in many cases a rather crude approximation. Furthermore the assumption of an increasing A with height holds only for layers near the ground; in higher levels the eddy coefficient will again decrease. Actually, in many cases, layers up to several hundred meters are influenced by the nocturnal cooling of the earth's surface. The author (REUTER 1947 and 1948 b) was able to show that, with the assumption A = constant, the formation of the ground inversion can be described sufficiently. Therefore it seems to be more convenient for practical purposes to take a mean value of A estimated from the observed horizontal wind velocity. As PEASCHKE (1937) showed, the value of A at a certain level can be expressed as a linear function of the horizontal wind velocity. A final justification of the simplifying assumption A = constant can be given only by a verification in practice as it will be seen later.

---

[1] In the previous investigation the third term in (3 b) was assumed to be $-c_p A \left(\frac{\partial T_2}{\partial z}\right)_{z=0}$. The flow of heat from the atmosphere to the surface however depends on the gradient of the potential temperature i.e. $\frac{\partial \Theta}{\partial z} = \frac{\partial (T_2 + \gamma_d z)}{\partial z} = \frac{\partial T_2}{\partial z} + \gamma_d$, so that the third term of the boundary condition (3 b) may be included in its present form.

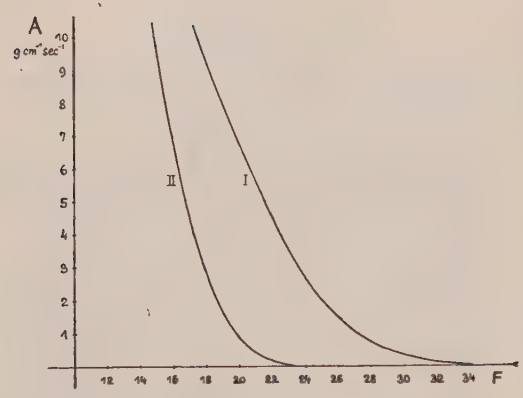

Fig. 1. The characteristic function F plotted against the eddy coefficient A. Curve I — normal ground; Curve II — after remarkable rainfall.

For a detailed study of the *temperature distribution* near the ground the assumption of a constant coefficient of eddy conductivity is of course not a close approximation. We are mostly interested however in the drop of temperature at the *surface* during the night so we may use equation (4) with some hope of success. Before we deal with practical applications of equation (4) it must be emphasized that the method outlined above gives only the static drop of temperature from sunset to sunrise and cannot include temperature changes produced by advection; upslope or downslope motion; and the effect of freezing or melting processes, evaporation and the formation of dew.

Practical application of the cooling formula

In order to apply equation (4) for practical purposes it is convenient to separate three factors on the right side. Equation (4) may then be written;

$$\Delta T_0 = F \cdot [E + Bk_g + (\gamma - \gamma_d)\, c_p A] \cdot \sqrt{L}, \qquad (5)$$

where F is given by

$$F = \frac{2}{\sqrt{\pi}} \frac{1}{\sqrt{k_g \varrho_g c_g} + c_p \sqrt{A \varrho}}. \qquad (6)$$

We will denote the characteristic function of the ground as F and plot F against A for given soil constants (Fig. 1). The function F varies from place to place and depends, to a certain extent, on the water content of the soil. The curves shown in Fig. 1 are plotted, using soil constants given in the textbok of Meteorology by HANN-SÜRING (1937). The effect of water content on the variation of heat conductivity in the ground has not yet been investigated sufficiently, although some progress has been made in recent studies by BRACHT (1949) and ALBRECHT (1948). Therefore Curve II in fig. 1 represents only a rough approximation showing how F will change after a remarkable rainfall.

In practice however we usually do not know the value of the soil constants. Therefore it might be possible and convenient to find the proper function F for a particular place and for certain ground conditions by using the observed values of ΔT_0 and computing F as will be shown later. Furthermore we can try to plot F against the horizontal wind velocity rather than against the mean value of A.

The diagram in fig. 2 shows $\Delta T_0 = F^\star \sqrt{L}$ for different seasons and for different values of

$$F^\star = F \cdot [E + Bk_g + (\gamma - \gamma_d)]\, c_p A \qquad (7)$$

using for L the length of the night for a latitude of 48 degrees. As the radiation is usually measured in cal per cm² per minute we will for convenience express the term $[E + B \cdot k_g + (\gamma - \gamma_d)\, c_p A]$ in this unit. If furthermore we express the length of the night L in hours we express F in the same units as in Fig. 1 (i.e. the c.g.s.system).

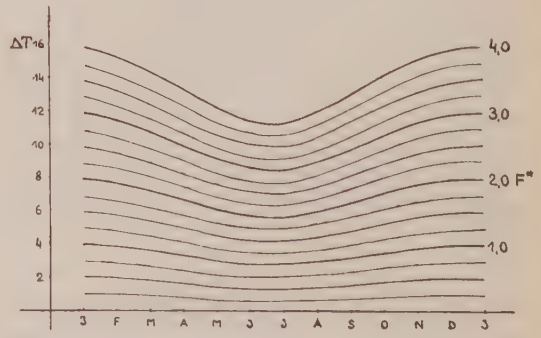

Fig. 2. Seasonal variation of nocturnal cooling for various values of $F^\star$ (latitude 48 degres).

In order to find the amount of nocturnal cooling at the surface in the course of a night we have to start with fig. 1. We obtain the amount of F for a certain value of A. Multiplying F by the observed or calculated effective outgoing radiation E (expressed in cal/cm² min), which should be corrected by the usually small quantity $Bk_g + (\gamma - \gamma_d)\, c_p A$, we can immediately read off from the diagram (Fig. 2) the possible drop in temperature for the particular case.

The order of magnitude of $(\gamma - \gamma_d)\, c_p A$ can be illustrated by assuming relatively high values. Let

$$A = 10 \text{ g cm}^{-1} \text{ sec}^{-1} = 600 \text{ g cm}^{-1} \text{ min}^{-1}$$
$$\gamma = 0$$
$$\gamma_d = 10^{-1} \text{ deg cm}^{-1}$$
$$c_p = 0.24 \text{ cal } g^{-1} \text{ deg}^{-1}$$

then $\gamma_d c_p A = 0.014$ cal cm^{-2} min^{-1} whereas E is of the order of 0.10—0.15 in the same units. Therefore $(\gamma - \gamma_d)\, c_p A$ is negligible unless the cooling period is very long.

The order of magnitude of $B \cdot k_g$ can be illustrated by assuming values for B and k_g as obtained by BRACHT (1949). Let

$$k_g = 0.0018 - 0.0025 \text{ cal cm}^{-1} \text{ sec}^{-1} \text{ deg}^{-1} =$$
$$= 0.11 - 0.15 \text{ cal cm}^{-1} \text{ min}^{-1} \text{ deg}^{-1}$$
$$B = 0.1 - 0.2 \text{ deg cm}^{-1},$$

then $B \cdot k_g = 0.011$—0.015 which is of the same order of magnitude as $\gamma_d c_p A$. In some cases it would be necessary to consider this term if observations of the temperature in the ground were available. If a ground inversion exists at sunset γ becomes negative. This means that the cooling is diminished. For a detailed discussion the reader is referred to REUTER (1947).

Summarizing the results of a practical application of the cooling formula we come to the following conclusion; because of our lack of knowledge of the physical constants of soil we have to use first of all the observational material to find the function F for a particular place. We may then use a graph like fig. 1 and a diagram like fig. 2 to predict the temperature fall (we will illustrate this method in the next section which deals with a practical test of the theoretical formula).

Practical test of the theory

In order to test the theory outlined above for a particular case, temperature observations for Vienna have been used. According to the strict theory, the ground surface temperatures should be used; in many cases however the amount of ΔT_0 at the screen level will not differ too much from that at the surface.[1] The difference between air and ground surface temperature at sunset may occasionally be noticeable, especially in summer.

Table 1. Nocturnal cooling for days with clear skies at Vienna — March, August and September 1949

Date	Temperature difference Sunset to Sunrise	F^*	E cal/cm² min.	F	Mean wind velocity km/h
March					
9—10	4.9	1.37	0.174	7.9	16.3
21—22	3.5	1.00	0.169	5.9	24.1
23—24	7.9	2.33	0.179	13.0	10.0
24—25	10.4	3.08	0.178	17.3	3.7
25—26	10.0	2.93	0.180	16.3	7.8
26—27	12.0	3.55	0.187	19.0	4.1
27—28	9.8	2.90	0.184	15.8	5.1
August					
6— 7	8.3	2.75	0.150	18.3	4.3
7— 8	10.1	3.33	0.154	21.6	2.6
Sept.					
24—25	6.7	1.68	0.152	11.1	11.6
25—26	8.3	2.42	0.169	14.3	8.0
26—27	10.5	3.00	0.158	19.0	3.5
27—28	9.5	2.62	0.151	17.3	3.1
28—29	10.0	2.92	0.153	19.1	2.5

In Table 1 a selection of observations for nights with clear sky conditions only, in different seasons in 1949, are shown. The amount of F is obtained from fig. 2 with the known value of ΔT_0 (the night time cooling). The effective outgoing radiation was computed with the aid of ÅNGSTRÖM's formula;

$$E = \sigma T_0^4 \, (0.194 + 0.236 \cdot 10^{-0.069\, e_0}) \quad (8)$$

[1] From the complete solution of equations (2 a) and (2 b) the author (REUTER 1948 b) came to the conclusion that for $A \geqq 1$ g. cm^{-1} sec^{-1} the temperature difference between screen and surface must be considered as almost constant during the night. Observations of the temperature difference between screen and surface for Vienna (to be published later) show *in the mean* over a long period the same result.

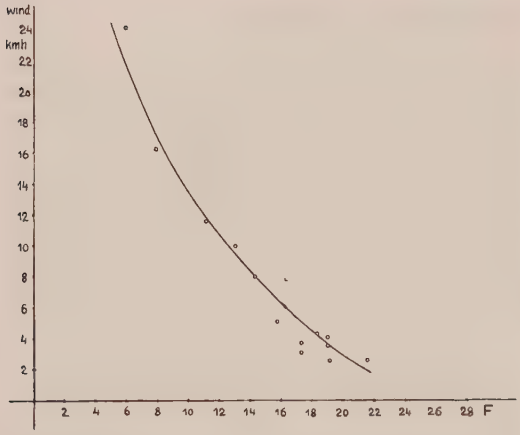

Fig. 3. The characteristic function F plotted against wind velocity. Data are for Vienna for clear nights, March—September 1949.

where σT_0^4 is the black body radiation in cal cm^{-2} min^{-1} and e_0 is the vapour pressure in mm. The value of E may also be obtained graphically using the temperature and relative humidity at sunset.[1]

The value of E obtained from (8) might be incorrect as has been pointed out previously; also it should be corrected by the factor $B \cdot k_g + + (\gamma - \gamma_d)\, c_p A$. This factor is neglected here. The error made by too high a value of E is however not too serious so long as we exclude observations where the wind velocity is either too high or is changing in direction (advection). It is important that we use in any one period the same method for evaluating E [for instance equation (8)]. Naturally the best way to obtain E is by direct measurement, but unfortunatly such measurements were not available.

We have used the observational material of 1949 to find the function F. The result is illustrated in fig. 3. It must be emphasized that for convenience the wind velocity is expressed in km/h whereas F remains in the same units as in fig. 1. As is apparent from the graph, a close relation exists between wind velocity and the function F. fig. 3 together with the diagram (fig. 2) enables us to predict minimum temperatures for any other period. We have only to read off the amount of F from fig. 3 for a given wind velocity. Multiplying this value with the effective outgoung radiation E, evaluated from (8) in cal/cm^2 min, we obtain immediately from the diagram in fig. 2 the possible drop in temperature for the particular case. The advantage of this semiempirical method is that the graph of fig. 3 can be modified by continually using the most recent observations. A graph for F should be obtained from observations for both dry and wet ground conditions. Then the value of F used in the forecast could be adjusted

[1] A convenient diagram for computing E can be found in the November issue 1948 of the Periodical *Wetter und Leben* (Zeitschrift für praktische Bioklimatologie, Vienna)

Table 2. Forecast and observed temperature minima at Vienna — August and September 1950

Date	Temp. Sunset C°	Vapour pressure Sunset mm	Cloudiness	E (formulae 8 and 9) cal/cm^2 min.	Mean wind velocity km/h	Forecast temperature Sunrise C°	Observed temperature Minima C°
August							
20—21	20.4	9.4	clear	0.151	3.0	11.1	12.7
21—22	22.3	9.9	clear	0.158	2.5	12.8	13.1
22—23	25.7	10.0	clear	0.159	2.0	15.0	15.3
23—24	25.8	13.8	clear	0.146	2.0	16.0	15.7
24—25	26.6	12.4	clear	0.151	10.2	20.8	19.2
27—28	24.8	13.3	3/10 As	0.118	2.5	17.3	17.8
28—29	25.6	15.4	clear	0.142	2.0	16.1	16.4
30—31	21.2	11.4	3/10 As	0.115	2.9	14.0	14.0
31— 1	23.5	10.3	4/10 Cs	0.134	4.6	15.7	15.5
September							
3— 4	13.5	8.3	4/10 As	0.109	15.0	12.2	12.0
4— 5	14.5	8.7	2/10 As	0.125	13.2	10.6	10.2
10—11	20.9	14.8	9/10 St	0.066	10.6	18.1	17.8
11—12	22.0	12.6	clear	0.139	1.2	12.0	14.2
13—14	20.2	9.8	clear	0.144	2.7	10.7	11.5

in individual cases by considering the moisture conditions in the ground.

The result of the prediction of minimum temperatures for a period in the summer 1950 can be read off from Table II. Excluded are those nights when precipitation occurred or when the wind velocity was too high. The cloudiness has been considered using a formula due to DORNO, namely;

$$E_w = E\,(1 - k\,w), \qquad (9)$$

where E_w is the observed net loss of radiation from the ground when w tenths of the sky are covered with clouds. E being the net loss of radiation (effective outgoing radiation) to a clear sky under the same conditions of temperature and humidity given by equation (8). The factor k has the following values; for Cs — 0.031, for As — 0.063, for St — 0.085 and for Ns — 0.099.

Table 2 shows that the objective method outlined in this study gives rather accurate results. As has been mentioned before, the results of Table 2 might be used to modify the graph of fig. 3 before we commence predictions for another period. Again it must be emphasized that the function F depends essentially upon the special features of a particular place. Therefore the graph of fig. 3 can be used for Vienna only. A similar application for another place was given by the author in a Technical Circular of the Canadian Meteorological Service (1950), using data for Toronto.

Acknowledgments

The author wishes to express his gratitude to Dr Andrew Thomson, Controller of the Canadian Meteorological Service, for many suggestions and his interest during the preparation of the study. Also sincere thanks are due to Mr C. M. Penner of the Training and Research Section of the Canadian Meteorological Service for his help and advice during the course of the work.

REFERENCES

ALBRECHT, F., 1948: Die Weiterentwicklung der Messtechnik des Wassergehaltes des Bodens auf thermischer Grundlage. *Arch. Met. Geophys. u. Bioklim.*, B I, pp. 149—155,

BRACHT, J., 1949: Untersuchungen über die Wärmeleitfähigkeit des Bodens. *Veröff. d. Geophys. Inst. Leipzig*, XIV.

BRUNT, D., 1939: Physical and Dynamical Meteorology, 2d ed. Cambridge, University Press.

CZEPA, O. and REUTER, H., 1950: Über den Betrag der effektiven Ausstrahlung in Bodennähe bei klarem Himmel. *Arch. Met. Geophys. u. Bioklim.*, B II, pp. 250—258.

DUFOUR, L., 1938: Notes sur le problème de la gelée nocturne. *Inst. Roy. Met. de Belgique*, Mem. Vol. IX.

ELLISON, E. S., 1928: A critique on the construction and use of minimum-temperatures formulas. *Monthly Weather Review.*, **56**., pp. 485—495.

FROST, R., 1948: Calculation of night minimum temperatures. *Prof. Notes.* **95**., London.

GEIGER, R., 1942: *Das Klima der bodennahen Luftschicht.* Fr. Vieweg und Sohn. Braunschweig.

GROEN, P., 1947: On radiational cooling of earth's surface during the night, especially with regard to the prediction of ground frost. *Mededeelingen en Verh., S. B. J.*, No: 9., Kon. Ned. Met. Inst.

HANN—SÜRING, 1937: *Lehrbuch der Meteorologie.* 5. Aufl. Willibald Keller. Leipzig.

JACOBS, W. C., 1940: A convenient minimum temperature diagram. *Bull. Am. Met. Soc.*, **21**. pp. 297—301.

JAEGER, J. C., 1945: Note on the effect of wind on nocturnal cooling. *Quart.. Journ. Roy. Met. Soc.*, **71**, pp. 388—390.

LÖNNQVIST, O., 1946: A frost prediction diagram. *Arkiv f. Mat., Astr. och Fysik*, **32**, A, 13.

— 1950: A general method and a simplified formula for calculating effective radiation. *Arkiv f. Geofysik*, **1**. 4, pp. 79—115.

PAESCHKE, W., 1937: Experimentelle Untersuchungen zum Rauhigkeits-und Stabilitätsproblem in der bodennahen Luftschicht. *Beitr. Phys. fr. Atm.*, **24**, pp. 163—189.

PHILIPPS, H., 1940: Zur Theorie der Wärmestrahlung in Bodennähe. *Gerlands Beitr.*, **56**, pp. 229—319.

REUTER, H., 1947: Zur Theorie der nächtlichen Abkühlung der bodennahen Luftschicht und Ausbildung der Bodeninversion. *Sitz. Ber. Akad. Wiss. Wien*, IIa, 155, pp. 334—358.

— 1948 a: Über die Theorie des Wärmehaushaltes einer Schneedecke. *Arch. Met. Geophys. u. Bioklim.*, A I, pp. 62—92.

— 1948 b: Die Modifikation einer Luftmasse durch die nächtliche Abkühlung der Erdoberfläche. *Arch. Met. Geophys. u. Bioklim.*, AI, pp. 252—263.

ROBINSON, G. D., 1950: Notes on the measurement and estimation of atmospheric radiation. *Quart. Journ. Roy. Met. Soc.*, **76**, pp. 37—51.

SAUBERER, F., 1936: Messungen des nächtlichen Strahlungshaushaltes der Erdoberfläche. *Meteorol. Z.*, **53**, pp. 296—302.

On the Effective Radiation to Various Parts of a Cloudless Sky

By OLOV LÖNNQVIST, Swedish Meteorological and Hydrological Institute

(Manuscript received 13 June 1951)

Abstract

From the author's formula for the relative radiation as a function of temperature and humidity conditions in the atmosphere, a formula is deduced for the zenith distance variation of the effective radiation. This formula is compared with observational data and empirical formulae. Finally, the constancy of the representative zenith distance, for which the effective radiation equals the effective radiation integrated over the whole hemisphere, is investigated.

Introduction

The long-wave radiation from the sky may be characterized in quite different, but closely related, ways. We could either give the figure for *the downward radiation D* itself, or the figure for the difference between the black-body radiation at the surface temperature and the downward radiation, i.e. *the effective radiation F*. To eliminate, at least to a very large extent, the temperature dependence of the radiation, we could thirdly give the percentage figure for the ratio between the effective radiation and the earth's black-body radiation. This ratio has been called *the relative radiation r* by the present author (1950).[1]

Observational data and empirical formulae

Measurements of the effective radiation towards various parts of a cloudless sky by means of small-aperture instruments have been carried out by several investigators. Apart from the rather primitive measurements by HOMÉN (1897), the first measurements of this kind were made by ÅNGSTRÖM (1915). Since then investigations have been made by DINES & DINES (1927), DUBOIS (1929), SÜSSENBERGER (1935) and RAMDAS, SREENIVASIAH & RAMAN (1937). From all such investigations it is obvious that the effective radiation, and so the relative one, is largest in the vertical direction and that it decreases with increasing zenith distance.

LINKE (1931) found an empirical formula (1), i.e. a trigonometric power law, which fitted very closely the measurements by DUBOIS, at least for zenith distances up to about 70°, viz.:

$$\frac{F(z)}{F(0)} = \frac{r(z)}{r(0)} = \cos^{L} z, \qquad (1)$$

where $F(z)$ is the effective radiation and $r(z)$ the relative radiation at the zenith distance z. The exponent L was supposed by LINKE to depend upon the humidity at surface. It has a value generally between 0.2 and 0.5. In fig. 1 are shown curves for these two values of L as well as for $L = 1$, i.e. the simple cosine function. The solid dots represent observed values by RAMDAS and collaborators (see Table II), for which L approximately equals 0.4.

SÜSSENBERGER (1935) tried to find a more

[1] Also the figure for (1—*r*) could be used and defined as e.g. *the relative downward radiation*.

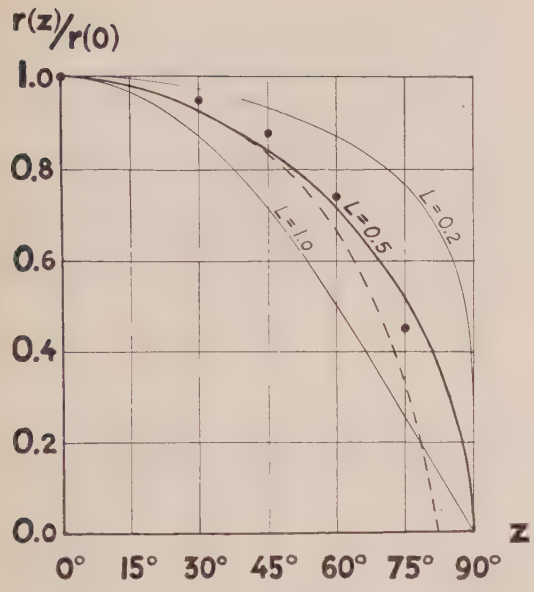

Fig. 1. The ratio $r(z)/r(0)$ given as a function of the zenith distance z. Full lines represent LINKE's formula (1) for various values for the exponent L. The broken line represents our formula (7) for $L = 0.5$, while the dotted line gives a correction to this curve, arising from certain limitations of our basic formula (3). Solid dots show values observed by RAMDAS, SREENIVASIAH & RAMAN.

accurate formula, and he found one, which followed the empirical data up to about 85°, viz.:

$$\frac{r(z)}{r(0)} = 1.1 - 0.1 \left\{ \frac{90}{100 - z} \right\}^S, \qquad (2)$$

where z is given in degrees(!) and where S has values generally between 1.0 and 1.6. The formula was pointed out by SÜSSENBERGER not to be valid for $z < 10°$, where instead $r(z)/r(0) = 1.00$.

Formulae previously given by the present author

In a recent paper (1950) the author presented a general method, based on the water-vapour spectrum, for calculating effective radiation. The method was applied to a set of cloudless atmospheres, where the temperatures and humidities were varied systematically. It was then possible to deduce a formula, which for all these atmospheres gave values in good agreement with the results obtained by the general method. As the computations were made under the assumption of purely vertical radiation, the formula was properly valid only for $z = 0$:

$$r(0) = A + 0.06\, t_0 + (0.18 + 0.12\, w)\, \gamma_m - \\ - 10 \ln w\varrho_0 \,\%, \qquad (3)$$

where A is a constant, somewhat uncertain as to its numerical value, and t_0 is the temperature (in °C). ϱ_0 is the absolute humidity (in gram/m³) at the surface, γ_m is the mean value (up to about 2 km) of the temperature lapse-rate (in °C/km), and w is the "humidity factor", defined as

$$w = \frac{1}{\varrho_0} \int_0^\infty \varrho \sqrt{\frac{p}{1000}}\, dh,$$

where p is the pressure in mb and h is the height in km. It is readily seen that $w\varrho_0 \approx 0.9\, W$, where W is the amount of precipitable water, given in mm.

To obtain now a formula for $r(z)$ we must introduce the apparent lapse-rate $\gamma_m \cos z$ in place of γ_m in (3), and $w/\cos z$ for w, as shown by the author (1951). We then find

$$r(z) = r(0) - 0.18\, \gamma_m + 0.18\, \gamma_m \cos z + \\ + 10 \ln \cos z \qquad (4)$$

Denoting the relative radiation integrated over the whole hemisphere by r, we have

$$r = 2 \int_0^{\frac{\pi}{2}} r(z) \sin z \cos z\, dz \qquad (5)$$

From (4) and (5) we obtain

$$r = r(0) - 0.18\, \gamma_m + \frac{2}{3}\, (0.18\, \gamma_m) + \frac{1}{2}\, (10),$$

which can be written

$$r(0) - r = 5.0 + 0.06\, \gamma_m \qquad (6)$$

Derived formulae for the ratio r(z)/r(0)

Dividing equation (4) with $r(0)$, we obtain

$$\frac{r(z)}{r(0)} = 1 - \frac{0.18\, \gamma_m}{r(0)} (1 - \cos z) - \\ - \frac{10}{r(0)} \ln \frac{1}{\cos z} \qquad (7)$$

But

$$-L \ln \frac{1}{\cos z} = \ln \cos^L z = \cos^L z - 1 - \\ - 1/2 (\cos^L z - 1)^2 + 1/3 (\cos^L z - 1)^3 - \ldots$$

Substituting in (7)

$$L = \frac{10}{r(0)} \tag{8}$$

and ignoring terms of third and higher order, we obtain

$$\frac{r(z)}{r(0)} = \cos^L z - 1/2 \ (\cos^L z - 1)^2 - \\ - 0.018 \ L \gamma_m (1 - \cos z), \tag{9}$$

where L takes values generally between 0.2 and 0.5, corresponding to $r(0) = 50\,\%$ and 20 %, respectively. At least for small zenith distances we may neglect the last two terms in (9), thus obtaining LINKE's empirical formula (1). We have also shown by (8) and (9) that his exponent L is a function of $r(0)$ and thus chiefly depends on ϱ_0, as supposed by LINKE. We have further obtained in (9) two correction terms to LINKE's formula; the maximum magnitudes of these terms are as follows (computed for $L = 0.5$ and $\gamma_m = 10$):

Table I. Maximum magnitudes of correction terms to Linke's formula

z	$1/2 (\cos^L z - 1)^2$	$0.018 L \gamma_m (1 - \cos z)$
10	0.00	0.00
20	0.00	0.01
30	0.00	0.01
40	0.01	0.02
50	0.02	0.03
60	0.04[1]	0.05
70	0.09[1]	0.06
80	0.17[1]	0.07

[1] These figures are somewhat increased (to 0.05, 0.13 and 0.29, respectively) by terms ignored in (9), viz. $-1/3 (\cos^L z - 1)^3$, etc.

We see from the table that also under extreme conditions, the LINKE formula is valid with good approximation up to about 60° or even 70°, which was the value found empirically by LINKE himself, when determining L from the observed ratio $r(z)/r(0)$ at $z = 60°$.

In fig. 1 we have also drawn a broken curve representing equation (7) for $L = 10/r(0) = 0.5$ and $\gamma_m = 0$. We see that according to this curve the ratio $r(z)/r(0)$ equals zero for a zenith distance less than 90°. The author has given in his last paper (1951) an explanation of this fact, viz. the basic formula (3) is not valid for the very large values of the apparent humidity factor $w/\cos z$, which occur when the zenith distance approaches 90°. The author has also given a formula, viz.

$$r(z) = K_1 \cdot e^{-0.0124 \frac{w \varrho_0}{\cos z}},$$

which holds for $z > z_Q$, where z_Q is called the critical zenith distance, defined by

$$\cos z_Q = \frac{w \varrho_0}{K_2}$$

The above quantities K_1 and K_2 vary somewhat with the temperature of the atmosphere but take values approximately equal to 25 and 80, respectively.

For the case studied in fig. 1, the critical zenith distance approximates 69°. The dotted curve in the figure gives that correction to the broken curve, which results from the above discussion. It can be seen from the figure that this correction to formula (7) is of very small significance.

Comparisons with empirical data

As mentioned above, LINKE recommends that L be determined with $z = 60°$. In fig. 2 we have plotted values of L, obtained in this way, as a function of the surface humidity, using measurements of DUBOIS (according to LINKE, 1931), SÜSSENBERGER (1935) and RAMDAS and collaborators (1937). Also shown are curves for extreme values of L, obtained from (8) by aid of (3) when using those extreme values of w, γ_m and t_0, which were found by the author (1950) from Swedish data. We find from the figure that most of the empirical data fall within the theoretical spread; the SÜSSENBERGER data, however, are too low to lie within the spread area.

To supplement the empirical formulae (1) and (2) we have obtained a third formula for the zenith distance dependence of the relative radiation, viz. equation (7). The three formulae

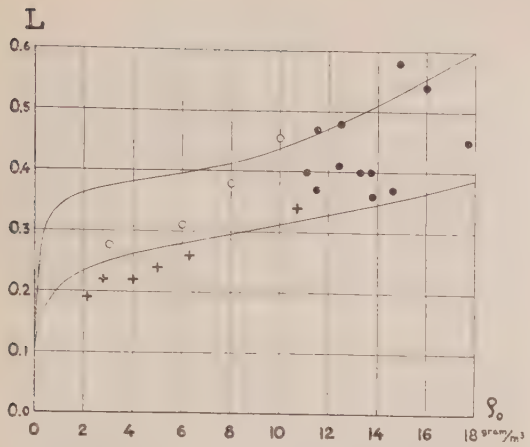

Fig. 2. The exponent L in LINKE's formula given as a function of the absolute humidity at the surface. Circles represent values observed by DUBOIS; crosses refer to SÜSSENBERGER and solid dots to RAMDAS, SREENIVASIAH & RAMAN. The curves bound the area of extreme spread, according to our theory.

will now be compared between themselves and with empirical data. The first series of such data is the one by RAMDAS and collaborators which was mentioned above. The measurements were all made during one single night (May 2, 1936) under "ideal conditions" as the authors say. In Table II we find in the first column average values computed from these twelve observations. The values for L and S, used in the columns to the right, have been obtained with $z = 60°$. It is seen from the table that up to this zenith distance there are no significant differences between empirical and computed values. For greater zenith distances, however, our values seem to be more accurate than values obtained from (1) and (2).

Table II. Comparison between computed values and Ramdas' data for the ratio r(z)/r(0)

z	Observed by RAMDAS and coll.	Calculated from (1) $L = 0.43$	(2) $S = 1.58$	(7) $L = 0.38$[1]
0	1.00	1.00	(1.00)	1.00
30	0.95	0.94	0.95	0.95
45	0.88	0.86	0.88	0.87
60	0.74	0.74	0.74	0.74
75	0.45	0.56	0.34	0.49

[1] $\gamma_m = 0$. This assumption influences the results but slightly.

Another comparison can be made with measurements by DINES & DINES (1927), viz. their annual means of the radiation to various parts of the sky. Here again we have obtained L and S with $z = 52{,}5°$. We see here, too, that there are no significant differences up to this value. For $z = 67.5°$ however, our formula gives the closest agreement with empirical data, while SÜSSENBERGER's formula seems to be the best one for $z = 82.5°$.

Table III. Comparison between computed values and the data by Dines & Dines for the ratio r(z)/r(0)

z	Observed by DINES & DINES	Calculated from (1) $L = 0.30$	(2) $S = 1.37$	(7) $L = 0.28$[1]
7.5	1.00	1.00	(1.00)	1.00
22.5	0.99	0.97	0.98	0.98
37.5	0.94	0.93	0.94	0.94
52.5	0.86	0.86	0.86,	0.86
67.5	0.73	0.75	0.70	0.73
82.5	0.20	0.54	0.15	0.43

[1] $\gamma_m = 0$. This assumption influences the results but slightly.

The representative zenith distance

DINES & DINES (1927) have pointed out that the downward radiation from the cloudless atmosphere as a whole is very closely the same as the radiation at the zenith distance 52.5°[2]. They also refer to RICHARDSON (1922), who found by some kind of deduction that what we call the representative zenith distance has a value about 55°. What is here said as to downward radiation, obviously holds for effective and relative radiation as well.

It is clear that the relative radiation $r(z)$ of necessity equals r for a certain z, as it is, for $z = 0$, larger than the hemispherical value r, and approaches zero for $z = 90°$. We denote this zenith distance z_r and will attempt to deduce it from the equations given above. Then the question is if this representative zenith distance may be treated as a constant.

[2] In fact it is seen from their data that the representative zenith distance has a variation between 52° and 57°. ROBINSON (1947) has obtained the same result.

Starting from the formula by LINKE (1), we have according to (5):

$$r = \frac{2\, r(0)}{L+2},$$

which was indeed found by LINKE himself.

By definition $r(z_r) = r$ we find from (1)

$$r = r(0) \cos^L z_r,$$

and eliminating $r(0)$ in these two equations, we obtain

$$\cos z_r = \sqrt[L]{\frac{2}{L+2}}. \qquad (10)$$

For $L = 0.2$ equation (10) gives $z_r = 51.6°$, and for $L = 0.5$ it gives $z_r = 50.2°$; values not too far from the empirical result, given above.

As SÜSSENBERGER (1935) has himself pointed out, his formula (2) is not as suitable as LINKE's for deriving a formula for the hemispherical radiation r, nor could we obtain one like (10) for the representative zenith distance. By graphical integration for certain values of S, however, we find that z_r equals 54°, apart from a small variation with S.

We can also start from (4) and insert there the value of $r(0)$ to be found in (6). For $z = z_r$ we then obtain

$$r(z_r) = r + 5.0 + 0.18\ \gamma_m \cos z_r - 0.12\,\gamma_m + \\ + 10 \ln \cos z_r,$$

and again setting $r = r(z_r)$, we find

$$10 \ln \cos z_r + 0.18\ \gamma_m \cos z_r = \\ 0.12\ \gamma_m - 5.0$$

Inserting $\gamma_m = +8°$/km, we obtain $z_r = 52.2°$, while a lapse-rate of $-8°$/km gives $z_r = 53.0°$. In the simple case with isothermal conditions, we find $z_r = 52.7°$.[1]

Obviously both the constancy of the representative zenith distance and the empirical value itself seem to be well confirmed. We may then echo these words of DINES & DINES, viz.: "This result is a very fortunate one, for it renders it possible to get a good idea of the sky radiation as a whole — an important meteorological quantity — from one single observation, and will greatly faciliate the possibility of using a self-recording radiometer."

Conclusion

Concerning the empirical formula given by LINKE for the zenith distance variation of the effective radiation, we have shown that his formula may be derived from the author's formula for the effective radiation, but that it is strictly valid for very small zenith distances only. For larger zenith distances we have given the necessary correction terms. As to the exponent L in LINKE's formula, it has been shown that it varies with the relative radiation and thus essentially with the humidity at surface. The formula empirically given by SÜSSENBERGER, on the other hand, has no theoretical background.

From comparisons made between observed data and computed values from our formula and from the empirical ones, we find a good agreement, at least for $z \leq 60°$. Our formula and that of SÜSSENBERGER seem to be the most accurate ones.

Finally we have shown that there exists an almost constant zenith distance which is representative in the sense that parallel radiation in that direction equals the integrated hemispherical radiation.

[1] ROBINSON (1947) has called attention to the connection between what we call the representative zenith distance and the factor 1.66, found by ELSASSER (1942); a factor which makes computations based on the assumption of vertical radiation applicable to diffuse radiation. The present author (1951) found for the same factor the mean value 1.65, which for isothermal atmospheres could also be found from the equation

$$x = \frac{1}{\cos z_r}.$$

REFERENCES

Ångström, A., 1915: A study of the radiation of the atmosphere. *Smiths. Misc. Coll.*, **65**, 3, pp. 1—106.

Dines, W. H., and Dines, L. H. G., 1927: Monthly Mean Values of Radiation from Various Parts of the Sky at Benson, Oxfordshire. *Mem. Roy. Met. Soc.*, **2**, 11, pp. 1—8.

Dubois, P., 1929: Nächtliche effektive Strahlung. *Gerl. Beitr. z. Geophys.* **22**, pp. 41—99.

Elsasser, W. M., 1942: Heat Transfer by Infrared Radiation in the Atmosphere. *Harvard Met. Studies*, **6**, 107 pp.

Homén, T., 1897: *Der tägliche Wärmeumsatz im Boden und die Wärmestrahlung zwischen Himmel und Erde.* Leipzig, Wilhelm Engelmann. 147 pp.

Linke, F., 1931: Die nächtliche effektive Ausstrahlung unter verschiedenen Zenitdistanzen. *Met. Zeitschr.*, **48**, pp. 25—31.

Lönnqvist, O., 1950: A general method and a simplified formula for calculating effective radiation. *Arkiv för geofys.*, **1**, 4, pp. 79—115.

— 1951: Calculating effective radiation with due regard to its diffuse nature. *Arkiv för geofys.*, **1**, 15, pp. 441—451.

Ramdas, L. A., Sreenivasiah, B. N., and Raman, P. K., 1937: Variation in the nocturnal radiation from the sky with zenith distance and with time during the night. *Proc. Indian Acad. Sci.* (*Bangalore*) *A.*, **5**, 1. pp. 45—55.

Richardson, L. F., 1922: *Weather Prediction by Numerical Process.* Cambridge, University Press. 236 pp.

Robinson, G. D., 1947: Notes on the measurement and estimation of atmospheric radiation. *Q. J. Roy. Met. Soc.*, **73**, pp. 127—150.

Süssenberger, E., 1935: Die nächtliche effektive Ausstrahlung unter verschiedenen Zenitdistanzen. *Met. Zeitschr.*, **52**, pp. 129—132.

Structure of Shear Lines near the Tropopause in Summer

C. W. NEWTON, N. A. PHILLIPS, J. E. CARSON, and D. L. BRADBURY
University of Chicago[1]

(First manuscript received 25 March 1951, revised 27 July 1951)

Abstract

A detailed study is made of a shear line in the tropopause region. A summer case was purposely selected, in which the lower half of the atmosphere was relatively barotropic, in order to minimize the role that could possibly be played by a subsiding cold air mass in producing a vertical stretching and consequent concentration of vorticity in the higher atmosphere.

During the period studied, the circulation over North America was characterized by the existence of two distinct jet streams, the southernmost of which, though initially having the form of a sinusoidal trough, appears to "buckle", forming a very sharp trough separating two jet streams of opposite direction. A possible mechanism is suggested for the production of strong northerly flow leading up to shear-line formation, which depends upon a mutual interaction between the mass and velocity fields of the jet-stream systems located at different latitudes.

An attempt to determine whether potential absolute vorticity is conserved during formation of the shear line is not wholly conclusive, but indicates a reasonable possibility that vorticity may be generated in the free atmosphere.

Introduction

Although much has been published regarding the importance of such phenomena as cut-off lows and higher-latitude warm highs as cells for the meridional exchange of air masses, certain related features of the circulation have received little attention in the literature. One of these is the shear line frequently found near the tropopause level, with which this paper will be concerned.

For purposes of this discussion, the shear line may be defined as a line of more-or-less abrupt discontinuity of wind direction in the free atmosphere, somewhat analogous to the wind shift found at surface fronts. The free-atmosphere shear line, however, is not generally associated directly with a density discontinuity, but is, in the troposphere, more likely to be associated with a temperature minimum relative to the environment.

Two principal questions prompted interest in this subject: (1) what causes the breakdown of the westerlies into a shear line, rather than the more commonly observed type of trough with continuous flow of air through it, and (2) can the high values of vorticity observed in shear lines be accounted for by conservative processes? The latter question appears to be of fundamental importance not only from the general standpoint of fluid dynamics, but in particular because of the increasing interest in numerical weather prediction, present methods of which are based upon the assumption that potential absolute vorticity is conserved (CHARNEY, 1949); (CHARNEY, FJÖRTOFT and VON NEUMANN, 1950).

[1] Published as a contribution to a research project on the general circulation of the atmosphere, sponsored by the Office of Naval Research.

Direct evidence that vorticity may not be conserved in limited regions of the free atmosphere has recently been presented by R. FRITH (1950). Photographs of a rift brought about by dry-ice seeding of supercooled Sc clouds over southern England showed a narrow zone with cyclonic shear estimated to be 15 mph in 0.25 mi (1.7×10^{-2} sec^{-1}), two orders of magnitude greater than the shear commonly observed in the higher atmosphere near the jet stream. In this instance, the cloud base was at 2,000 ft and the tops 4,500 ft, with no evidence of a front nearby.

Examinations of time and space variations of upper winds indicate that the strongest wind in the vicinity of a shear line is usually found 200 to 400 km from it, with wind decreasing to calm just in the shear line. The detailed distribution of wind shear is at present indeterminable because of sparsity of observations, but in most cases the mean absolute vorticity over a broad zone spanning the shear line is about three times, and occasionally up to five or six times, the Coriolis parameter. The shear line therefore seems to be a likely place to look for the possible generation of vorticity by nonconservative processes.

Three possibilities exist for the origin of high vorticities: vertical stretching, advection, or generation *in situ*. It is one of the purposes of this study to determine whether the high vorticity observed in shear lines can be accounted for by the first two (conservative) processes, or whether generation of potential absolute vorticity takes place locally.

Some previous investigators (e. g., HSIEH, 1950) have attempted to explain the formation of regions of strong vorticity in shear lines as being the result of vertical stretching above a subsiding cold air mass. Undoubtedly this mechanism is operative in many cases of shear line formation; however, shear lines are also observed to form on occasions when such a cold air mass is lacking. A basic difficulty is also encountered in this explanation in that the subsidence of such a cold dome would lead to a more barotropic distribution of temperature, while actually increased baroclinity is required to achieve quasigeostrophic balance since the vertical wind shear in the bounding currents often increases during the formation of a shear line. It is obvious from the circulation theorem and considerations of continuity, that a purely local process which increases the barocline field cannot at the same time concentrate vorticity in the shear line region.

In order to minimize the possibility that subsidence could play an important rôle in the formation of the shear lines to be studied, summer cases were selected in which frontal activity was weak and confined to the lowest layers. Two cases were studied in detail, of which only part of one is presented in this paper because of the excessive number of diagrams which would otherwise be involved. The conclusions reached were consistent between the two cases, which were very similar in their general features.

Case of 6—10 July 1950

Shear lines are characteristically most pronounced near the tropopause level, which in the present case is most nearly represented by the 200-mb surface over the United States. As the basic charts in the synoptic description a series of 200-mb charts is presented in figs. 1—6, embracing the period 1500 GCT 6 July to 0300 GCT 10 July 1950.

Certain broad-scale features of the circulation pattern are persistent throughout the development considered here: a major trough extending southward from a cold low center near the Canadian west coast, followed downstream by a slowly progressive (until fig. 5) ridge extending from a closed warm high near the southwest border of the United States, and a slow-moving trough in the region south of the Great Lakes.

Near the Arctic Circle, there are two principal quasistationary systems: a cut-off warm tropospheric high over Alaska and a deep cold low north of Hudson Bay. The sparse observations indicate the probable existence of a rather extensive west-wind belt south of latitudes 15—25° N. A series of high centers strung out in an E—W direction between latitudes 25 and 40° N is separated from the lower-latitude westerlies by a series of shear lines or sharp troughs, particularly well developed in the southwest Atlantic and Caribbean.

The major changes during this period are the intensification and eastward movement of the middle-latitude ridge over the western

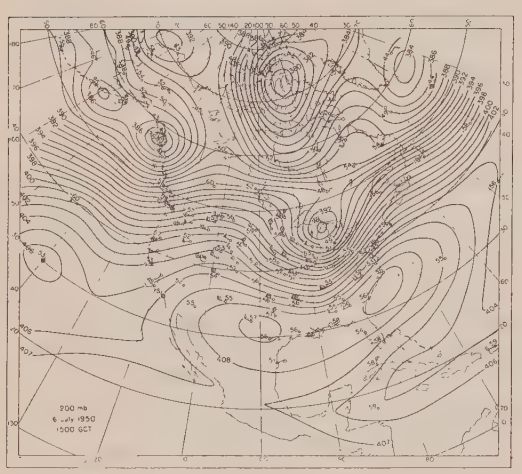

Fig. 1. 200-mb chart at 1500 GCT 6 July 1950. Contours labelled in hundreds of feet, contour interval 100 ft. At stations, temperature in degrees C, wind in knots (full barb 10 knots, solid triangle 50 knots; dashed wind shafts and open triangles represent winds at 35,000 ft).

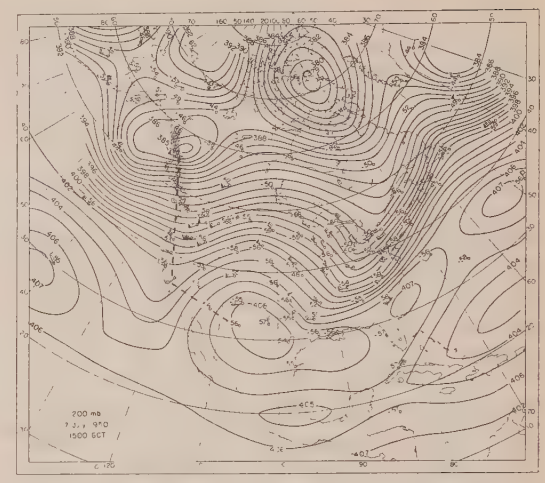

Fig. 2. 200-mb chart, 1500 GCT 7 July 1950.

United States, concurrent with a slow deepening of the west-coast trough. Simultaneously with the intensification of this ridge, the trough over the east central United States underwent a sharpening, at first rather gradual (figs. 1—3, interval between charts 24 hrs), then quite rapidly until a distinct NNE—SSW shear line appeared in the chart for 1500 GCT 9 July (fig. 5). During the first part of the period, there was a considerable flow of air through the trough line at all times, but by 9 July the winds bordering the shear line are almost parallel to it, so the latter time is characterized by only nominal flow through the trough line at 200 mb. The flow pattern in this region may thus be considered as relatively stable and slowly changing up until shortly before 1500 GCT 8 July (fig. 3) and for some time after 1500 GCT 9 July (fig. 5), with a rapid breakdown from one type of flow to the other during the short intervening period.

Even before the complete breakdown of the trough into a clear-cut shear line, there must evidently have been a pronounced cross-contour flow toward higher contours (deceleration) on the immediate southwest side, and probably a corresponding flow toward lower contours on the southeast side of the trough, since air cannot pass through a sharp trough at a high kinetic-energy level because of the excessive centrifugal force which would be involved. The rapid deepening of the southern part of the shear line trough might be considered as the effect of a tendency to mutual adjustment between the mass and velocity fields as a result of the feeding into the region west of the trough, of a northerly current possessing high momentum. To find an explanation for the generation of these strong northerly winds would therefore seem to be a basic problem in getting at the mechanism of shear line formation.

Twelve hours after the time of fig. 1, the high-latitude trough over Hudson Bay had amalgamated with the trough south of the Great Lakes, forming the extensive trough seen in fig. 2 over the eastern part of the continent. The northern part of this trough moved steadily eastward, eventually shearing off and again (figs. 5 and 6) assuming an identity entirely separate from the lower-latitude part. The latter is evidently retarded by the persistent lower middle-latitude warm high over the western Atlantic.

As often observed in the case of cut-off lows (University of Chicago, 1947), (Cressman, 1948), the northern part of this shear line is, in the fully-developed stage, bridged across by strong westerly flow, and the shear line trough is out of phase with the long-wave pattern

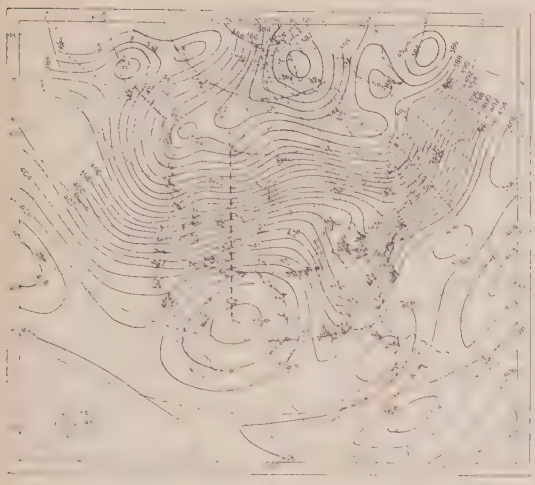

Fig. 3. 200-mb chart, 1500 GCT 8 July 1950.

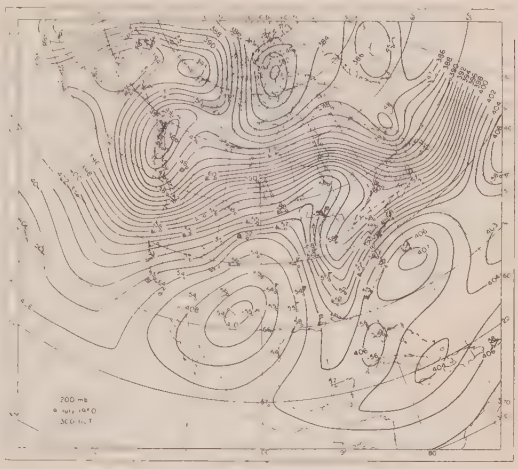

Fig. 4. 200-mb chart, 0300 GCT 9 July 1950.

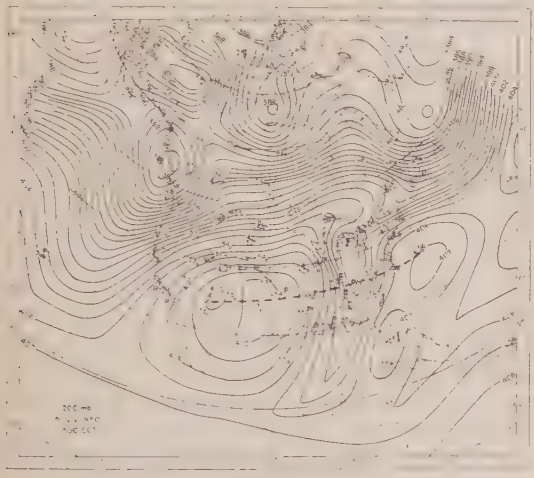

Fig. 5. 200-mb chart, 1500 GCT 9 July 1950.

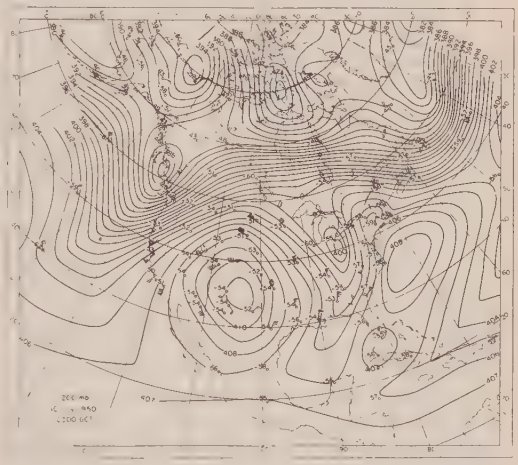

Fig. 6. 200-mb chart, 0300 GCT 10 July 1950.

in the main belt of westerlies. In the early stages (fig. 1), the principal belt of westerlies passes almost entirely south of the low centered over the Great Lakes. This low subsequently fills, but a splitting of the belt of westerlies remains, with successively more of the westerly current passing north of the split in response to an increase in strength of the southwesterly flow over western Canada as the major west-coast trough deepens.

The lower middle latitudes are in the last stages characterized by a series of large-amplitude disturbances bearing some resemblance to "blocking" situations of the higher latitudes described by Rex (1950) and others. In this case, the block starting the train of meandering disturbances is furnished by the strongly developed closed warm high centered over west Texas and New Mexico late in the series. The principal point of dissimilarity between the flow pattern illustrated here, and the typical higher-latitude blocking situation, is that in this case the meandering takes place entirely south of the principal belt of westerlies, which continues eastward without much diminution of the total level of its kinetic energy. In the higher-latitude blocking type, on the other hand, the initial blocking high

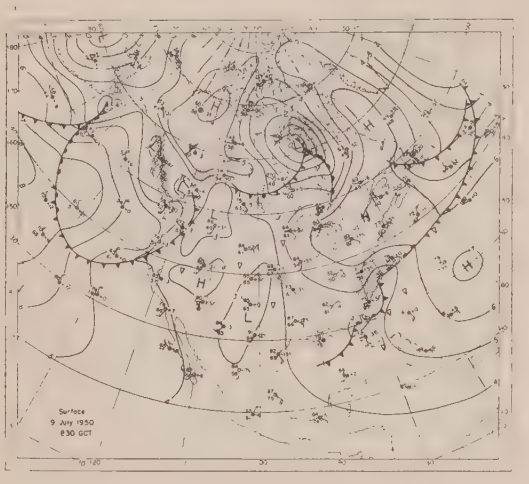

Fig. 7. Surface chart, 1830 GCT 9 July 1950. Contours of the 1000-mb surface in hundreds of feet; fronts indicated by standard symbols.

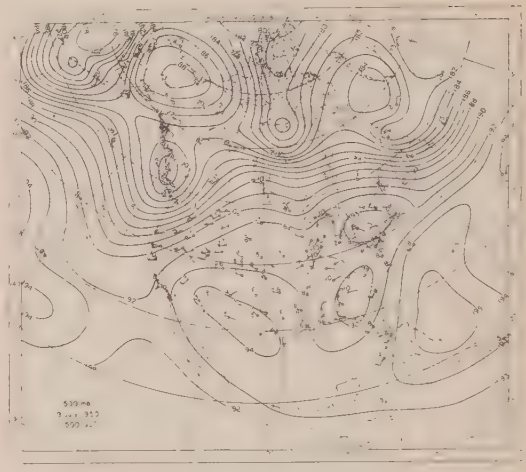

Fig. 8. 500-mb chart, 1500 GCT 9 July 1950.

forms north of the latitude of the strong current upstream, and the kinetic energy level is considerably diminished downstream from the block.

Rex states that the prime requisites for development of a high-latitude blocking situation are (1) a high kinetic energy level in the basic current and (2) interference from an external perturbation, namely a strong cyclone upstream from the blocking region. There is therefore a certain similarity with the present situation from this point of view, since the development of the block, shear line, and the rest of the meandering disturbances downstream occurs during a period when the trough upstream off the west coast of North America is increasing in amplitude.

The increased amplitude of the shear trough obviously cannot be considered simply as an effect of the change of constant-vorticity paths as a result of the deepening upstream, since the amplitude of the downstream disturbance is considerably greater than that observed upstream. However, it does appear likely that the building-up of the blocking high is at least partly a result of mutual adjustments of the mass and velocity fields as consequence of increased amplitude of the upstream trough.

Certain experiments conducted in the Hydrodynamics Laboratory of the Department of Meteorology of the University of Chicago produce a flow pattern very similar to that observed here (FULTZ and LONG, 1951). One of these experiments consists of placing a circular obstacle of about 20° latitude diameter in the middle-latitude region of a fluid-filled rotating hemispherical shell, and moving the obstacle upstream with respect to the bowl so that a flow is created analogous to a west wind with respect to the obstacle. When this is done, the fluid flows completely around the northern and eastern sides and reaches a stagnation point just east of the south side of the obstacle. The lines of flow observed east of the obstacle show a remarkable similarity to a NE—SW shear line. The obstacle used in this experiment is of a size approximately equivalent to that of the warm high over the southwest United States in the present case (fig. 6).

Associated flow patterns at lower levels. — Figs. 7 and 8 show the surface chart at 1830 GCT and the 500-mb chart at 1500 GCT 9 July, the time of greatest shear line intensity at 200 mb (cf. fig. 5). The surface chart is quite typical of the weather patterns commonly associated with high-level shear lines; a surface ridge beneath the shear line and a series of open waves along a SW—NE oriented cold front to the east. Weak development of surface low-pressure centers is characteristic of the frontal systems associated with shear lines; these ordinarily do not intensify appreciably until they move sufficiently far north to come under the influence of the main belt of westerlies north of the shear-line trough.

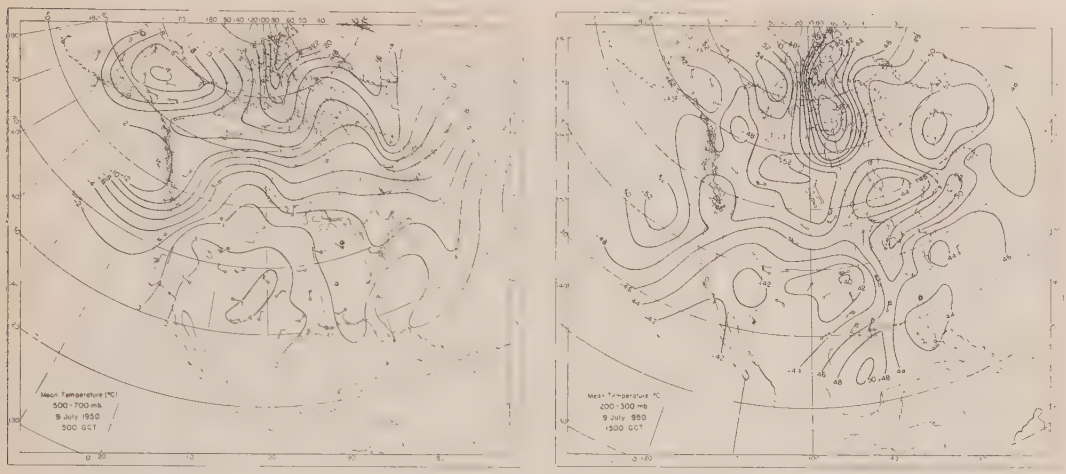

9 a 9 b

Fig. 9. Relative topography charts for (a) layer between 500 and 700 mb, and (b) layer between 200 and 300 mb. Isolines labelled as degrees C mean virtual temperature. Wind symbols indicate vectorial wind shear between top and bottom of layer.

At 500 mb (fig. 8), the large-scale perturbations are in general similar to those at 200 mb. However, at the lower level there is little indication of the strong deformation found near the tropopause, the only evidence being a rather weak closed low. The strong winds and concentration of solenoids at 500 mb over southern Canada stand out in striking contrast to conditions over the eastern United States at this level. The concentration of baroclinity in the higher part of the troposphere near the shear line is emphasized by the "relative topography" charts of fig. 9. The gradient of mean temperature in the layer between 500 and 700 mb (fig. 9 a) is very weak in the region south of the Great Lakes. In the same region, however, an extremely strong mean temperature gradient is found in the layer between 300 and 200 mb (fig. 9 b). There is correspondingly a very great difference between the vectorial vertical wind shears (indicated by plotted wind symbols) in these two layers of almost equal thickness.

If the deepening of surface cyclones is in any way dependent upon the presence of a jet stream, as some synoptic studies suggest (Riehl, 1948), the failure of waves to deepen until they move northward beneath the main (northern) belt of westerlies is readily understood from comparison of the structures of the northern and southern jet stream systems. The latter being almost nonexistent in the middle and lower troposphere even though it is quite pronounced at higher levels over the wave systems on the east coast, it seems logical to expect it to have very little effect upon surface cyclogenesis. This might, of course, be interpreted also as a failure to deepen because of the absence of available potential energy in the lower and middle troposphere.

Structure of wind field. — In order to show some variations of the wind field in space and time, the three vertical cross sections of figs. 10, 11, and 12 are presented. These show the isentropes and distribution of the wind component normal to the lines along which the cross sections were drawn (nearly the total wind speed). Isotachs on these sections were constructed from observed winds, supplemented by gradient winds computed from pressure profiles taking trajectory curvature into account[2]. The successive sections are so spaced that an air particle travelling at about 30 m sec^{-1} (60 knots) near the right-hand jet would be found successively at the different cross sections at the appropriate times.

[2] The apparent inconsistency between the strong vertical shear and the weak solenoid concentration between 200 and 300 mb on the cold-air side of the jet near Nashville is balanced by differences of path curvature at these levels. The current is almost straight at 300 mb but anticyclonic at 200 mb, giving a centrifugal circulation acceleration in the same sense as the solenoids.

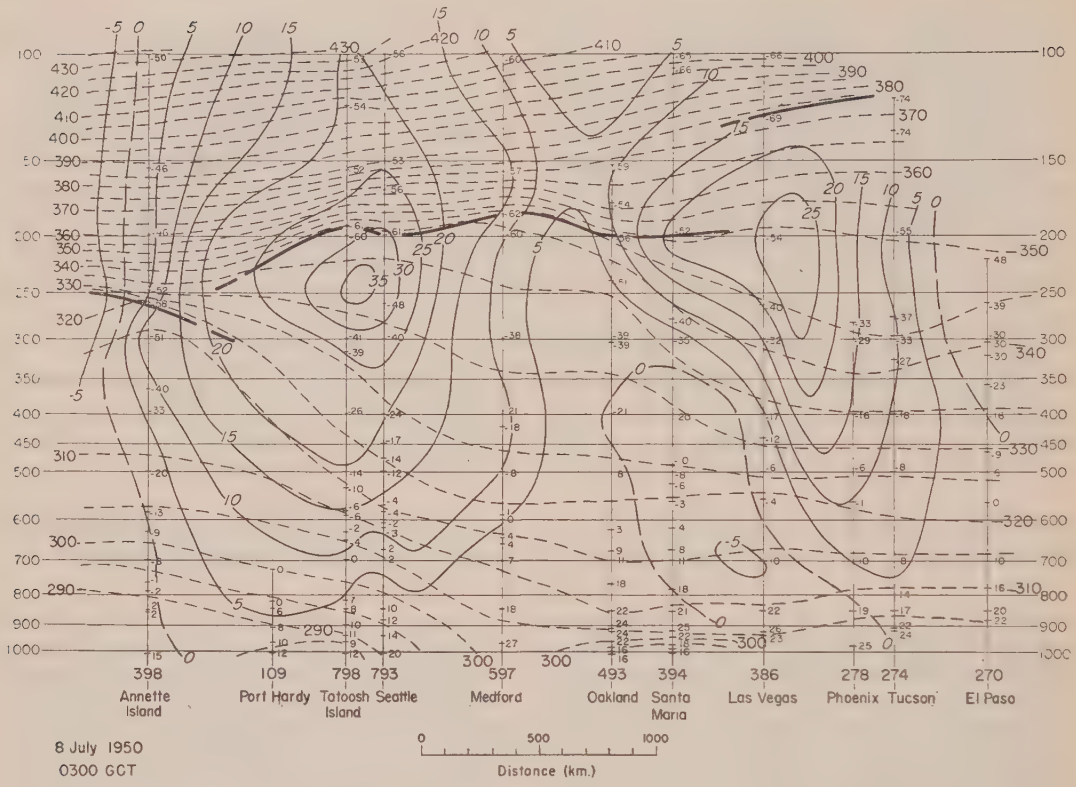

Fig. 10. Vertical cross section from Annette Island to Oakland to El Paso, 0300 GCT 8 July 1950, along heavy dashed line in fig. 2 (note times are 12 hours different). Thin dashed lines, potential temperature (deg. K.); thin solid lines, isotachs of wind component (m sec^{-1}) normal to cross section; heavy lines, tropopauses.

The immediately striking feature of the wind distribution shown here is the pronounced concentration of momentum near the tropopause level in the vicinity of the southern jet stream; particularly in the case of fig. 12, the section through the fully-developed shear line. This is quite different from the vertical wind distribution normally observed in the middle latitudes during winter months, which generally shows rather uniform vertical shear through the troposphere, outside of frontal layers. In the case shown here, no frontal layer was present. There is, however, a marked tendency for the strong vertical shear to be concentrated in a sloping barocline layer entirely within the upper third of the troposphere (upper fourth by weight). While in the typical winter case the strong solenoid concentration and vertical wind shear are found mostly below 400 mb, in the case examined here these properties are found almost entirely above that level. The strongest shear, both vertical and horizontal, is located on the cold-air side of the axis of the jet. The axis of the jet stream at 200 mb west of the shear line (right-hand side in fig. 12) is actually some 500 km distant from the corresponding axis at 500 mb. This type of velocity distribution is not peculiar to this case, but has been noted in a number of summer cases not involving shear lines.

The structure of the southern jet on the west coast and over the Rockies (right-hand sides of figs. 10 and 11) is qualitatively similar to that observed further downstream in the shear line region (fig. 12). All three regions are characterized by a marked tilt of the jet axis and by pronounced concentration of the vertical wind shear in the highest troposphere on the cold-air side of the jet.

Upper wind observations were too sparse to construct a completely reliable picture of the

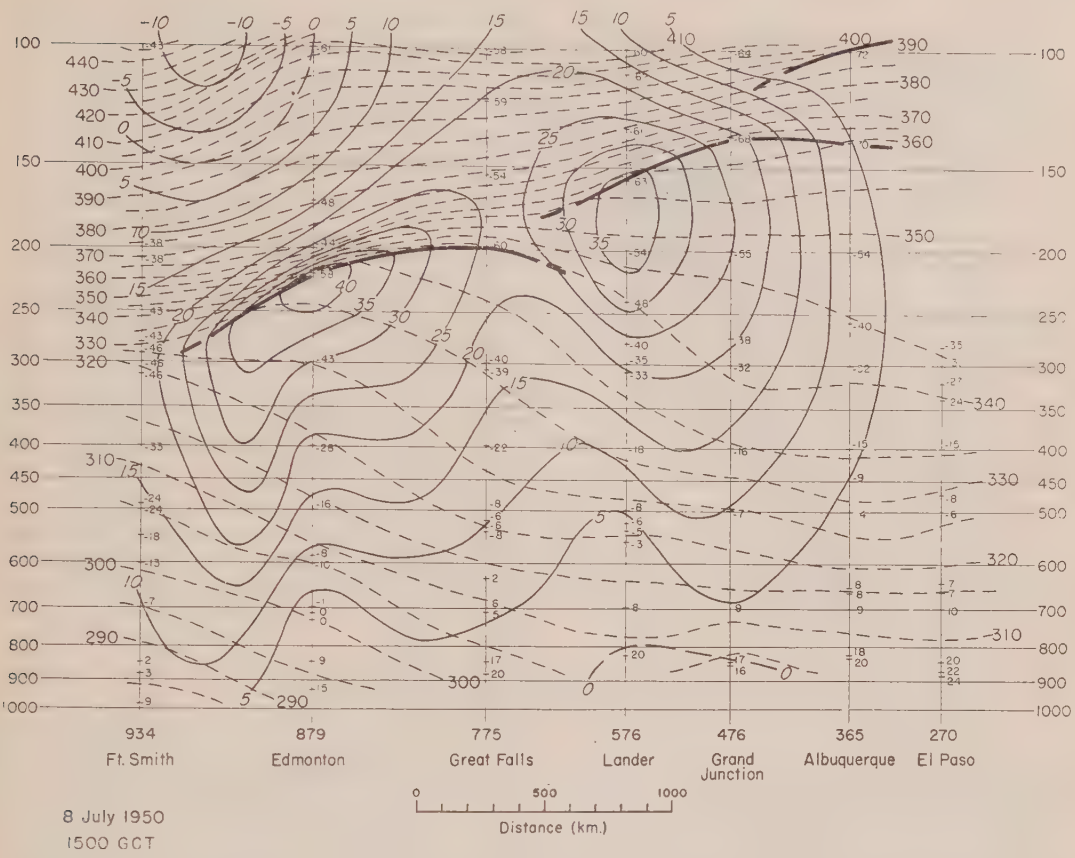

Fig. 11. Vertical cross section from Ft. Smith (Yukon) to El Paso, 1500 GCT 8 July 1950, along heavy dashed line in fig. 3. Legend as in fig. 10.

northernmost jet in figs. 10 and 11, which corresponds to the main belt of westerlies passing north of the shear-line region. Pronounced baroclinity is evident from the earth's surface throughout the troposphere, however, indicating a rather uniform vertical wind shear. Thus the kinematic structure of the northern belt of westerlies is fundamentally different in character from that of the southern wind belt.

Several wind-speed profiles near the axis of the southern 200-mb jet are shown in fig. 13. All of these soundings show the same type of velocity distribution; almost complete absence of vertical shear up to around 30,000 ft and a sharp increase in shear near that level. At Nashville, the 30,000-ft wind is only 6 m sec^{-1}, while at the 200-mb level the wind speed is 58 m sec^{-1}. Theoretical aspects of this type of vertical variation of velocity are dealt with in two papers by Rossby (1951 a, b).

Although the distribution of wind velocity in the southern jet in figs. 10 and 11 is qualitatively similar to that found later on in the shear-line region (fig. 12), quantitatively there is a great difference. In the latter cross section, a very marked increase in velocity has taken place at the levels near the tropopause, with very little change in the velocity at levels below about 300 mb. This is emphasized by the profiles of kinetic energy taken from the cross sections of figs. 10 to 12 and shown in fig. 14 a along the sloping jet axis and in fig. 14 b at the 200-mb level. The total kinetic energy changes relatively little between the first two cross sections, but an extremely large increase takes place between the latter two. This increase is almost entirely confined to a

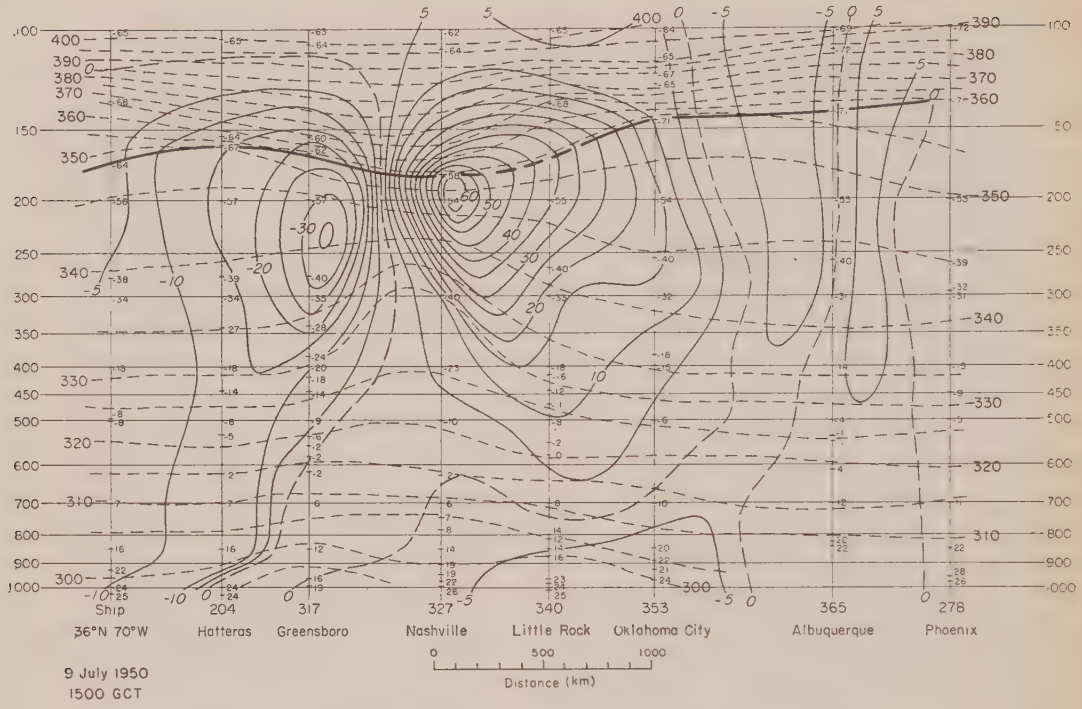

Fig. 12. Vertical cross section from ship located at 36° N 70° W to Phoenix, 1500 GCT 9 July 1950, along heavy dashed line in fig. 5. Legend as in fig. 10.

Fig. 13. Profiles of wind speed at various locations (time and location indicated in figure) near axis of 200-mb jet stream, 8—9 July 1950.

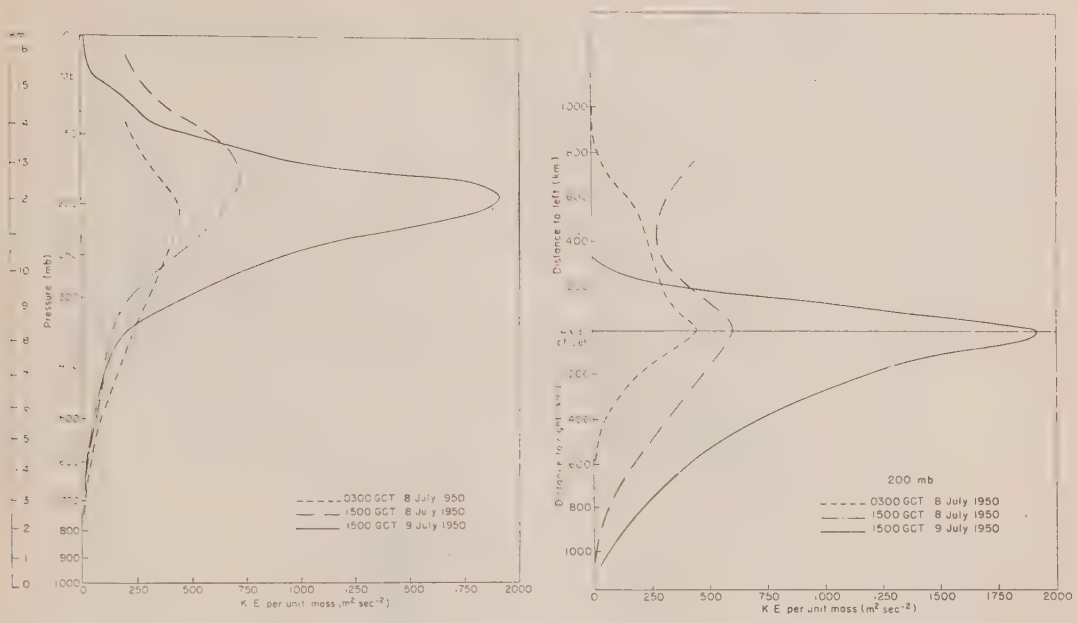
Pressure (mb)
0300 GCT 8 July 950
1500 GCT 8 July 1950
1500 GCT 9 July 1950
K E per unit mass (m² sec⁻²)
Distance to left (km)
200 mb
0300 GCT 8 July 1950
1500 GCT 8 July 1950
1500 GCT 9 July 1950
K E per unit mass (m² sec⁻²)

14 a 14 b

Fig. 14. (a) Profiles of wind speed along sloping axis of maximum wind, taken from southernmost jet in figs. 10, 11, and 12; (b) profiles of wind speed at 200-mb level through same jet.

layer about 150 mb (4.5 km) thick and 1,000 km wide[3]. Wind observations were too sparse to construct an intermediate cross section along the ridge line at 0300 GCT 9 July (fig. 4), but available observations seem to indicate that the increase in kinetic energy took place almost entirely on the east side of this ridge.

The structure of the 200-mb wind field over North America at the time of maximum shear line development is shown by the isotachs of fig. 15. The coexistence of two distinct jet-stream systems at different latitudes is clearly shown by this figure. The double jet structure was evident from a careful examination of the wind observations throughout the series from fig. 1 to fig. 6. At 1500 GCT 9 July (figs. 12 and 15), the maximum wind speed on the west side of the shear line was approximately twice that observed on the east side. This is not an invariant feature, though it is commonly observed during the earlier stages of shear line formation. Available wind observations and the contour analyses clearly show a marked acceleration of the air on the east side of the ridge just upstream from the shear line; that is, it is plainly evident that the strong concentration of momentum in this region did not originate wholly by advection from points further west[4].

Distribution of vorticity in shear line region. — Fig. 16 shows the distribution of the vertical component of absolute vorticity at various levels, taken from the cross section through the shear line (fig. 12). The high degree of concentration of the strong vorticity, both in a vertical and horizontal sense, is strikingly evident from this figure. At 200 mb, Nashville had a wind of 360° 112 knots, while

3 Since the velocity does vary along the profile, comparing these profiles in fig. 14 does not really indicate changes in velocity of the same particles at the different cross sections. However, the flow in the lower-velocity boundary regions of the jet was sufficiently close to steady-state to allow a comparison to be qualitatively correct.

4 J. Bjerknes, in an article to be published in the Compendium of Meteorology of the American Meteorological Society, has suggested that strong acceleration occurs east of sharp ridges due to the fact that curvature of the pressure-contours in such ridges often exceeds a critical anticyclonic curvature for the velocity of the air passing through the ridge, this necessitating a flow toward lower contours and therefore an acceleration east of the ridge. This appears to be a significant factor in the present case.

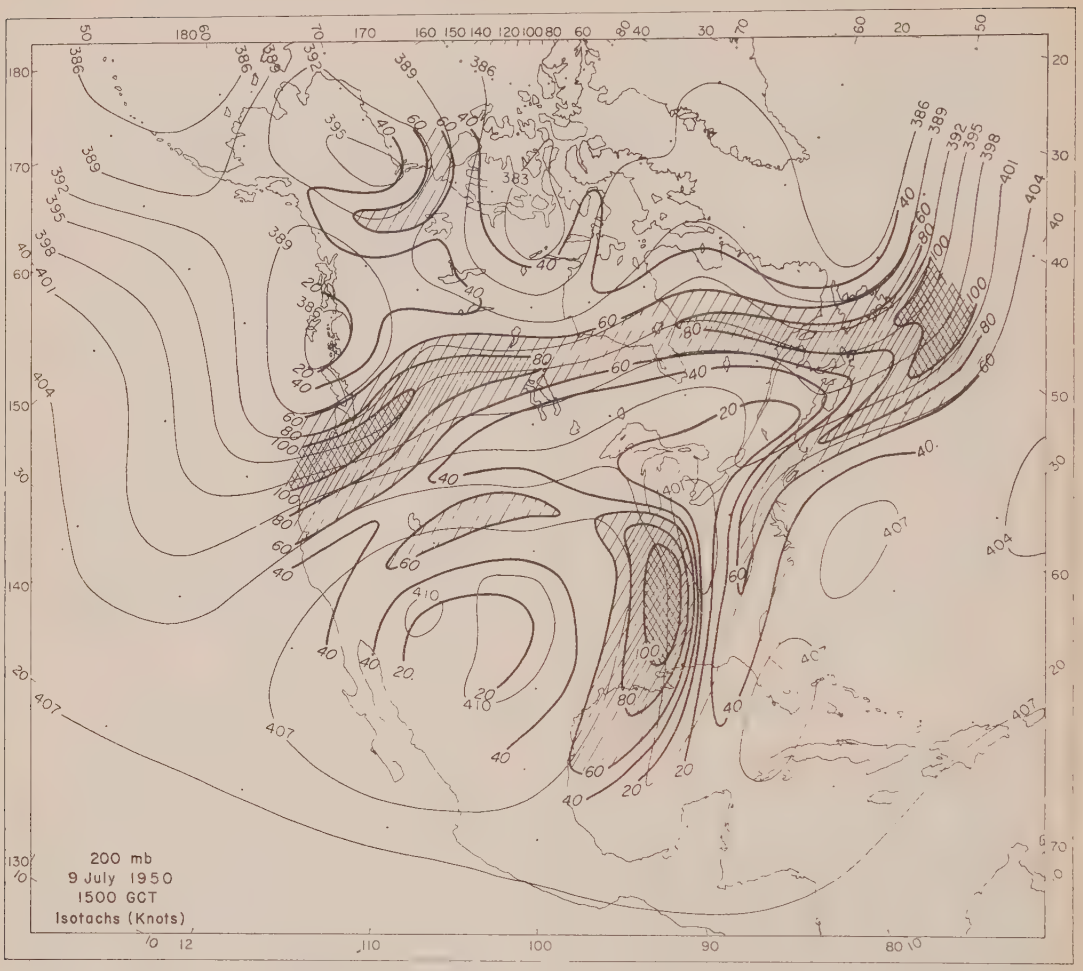

Fig. 15. 200-mb chart, 1500 GCT 9 July 1950. Thin lines, contours of 200-mb surface, contour interval 300 feet. Heavy lines, isotachs (knots). Hatching indicates regions of wind speed greater than 60 knots, cross hatching speed greater than 100 knots.

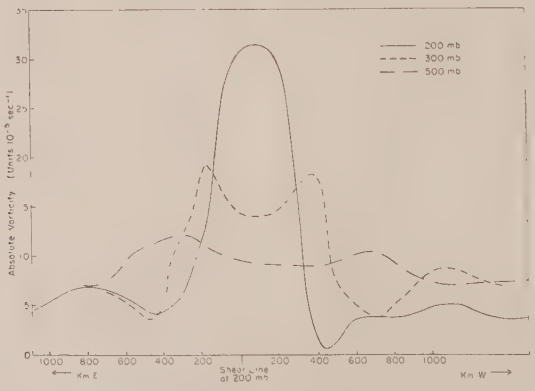

Fig. 16. Profiles of the vertical component of absolute vorticity at 200 mb (solid line), 300 mb (dashed line), and 500 mb (dash-dotted line), across the shear line at 1500 GCT 9 July 1950, taken from fig. 12. Units 10^{-5} sec^{-1}.

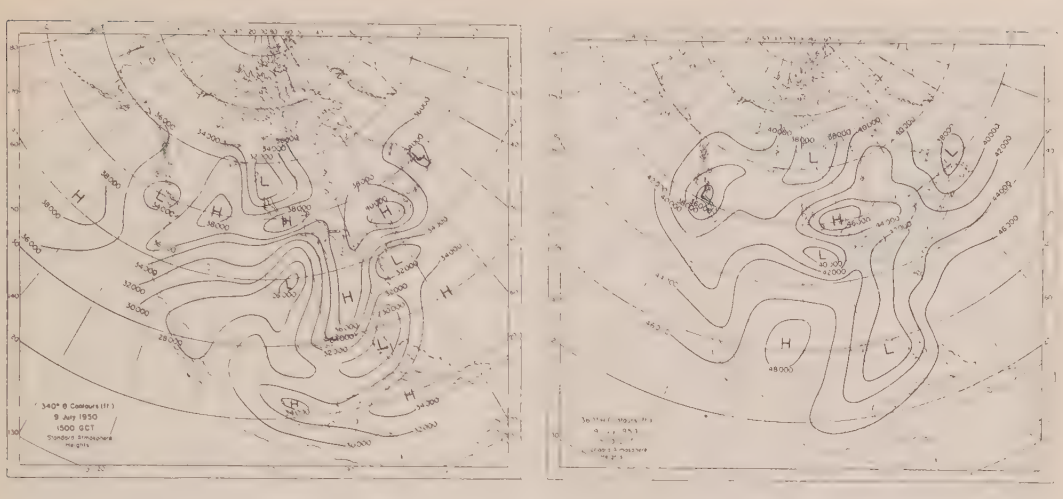

17 a 17 b

Fig. 17. Contours (feet) of isentropic surfaces at 1500 GCT 9 July 1950, (a) 340K and (b) 360K potential temperature. H and L indicate regions of high and low elevation.

Knoxville, 260 km farther east, had a wind of 40° 2 knots. Making the too-conservative assumption of a linear variation of wind speed between these two stations, an average absolute vorticity of 30.4×10^{-5} sec^{-1}, or 3.6 times the Coriolis parameter, is obtained.

Comparing the distribution of vorticity with that of stability as shown by the vertical packing of isentropes in fig. 12, we see that the strongest vorticity is located, in the upper troposphere, just in that region where the vertical stability is most pronounced. The weakest vertical stability in the vicinity of the shear line is found at lower levels (300—400 mb) where the horizontal shear is weak.

In order to find out whether the high vorticity was generated locally or transferred advectively from other regions, an attempt was made to estimate paths of particles in relation to the potential absolute vorticity field. Since the 340 and 360K isentropic surfaces in this case straddle the tropopause, envelope a semi-nodal surface and also enclose the layer wherein the greatest vorticity and momentum concentrations are found, this layer was chosen as the most logical to examine for the purposes of this study.

Fig. 17 illustrates the topography (standard atmosphere heights) of the 340 and 360K surfaces at the time of maximum shear line intensity. The outstanding feature is the almost complete out-of-phase relationship of the troughs and ridges of these two surfaces over the United States. Over the major anticyclonic regions, the 360K surface is found at high, and the 340K surface at low elevations, while the opposite is observed in the vicinity of the shear line. This implies, as does the cross section of fig. 12, that regions of high absolute vorticity are, near the tropopause, associated generally with pronounced thermal stability, while the anticyclones, regions of

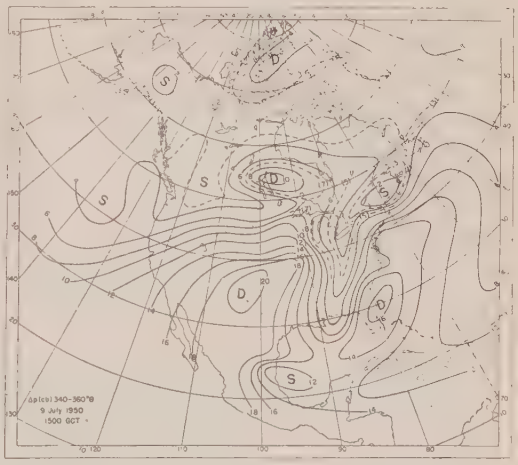

Fig. 18. Isentropic "weight chart" for the layer 340 to 360K at 1500 GCT 9 July 1950. Contours labelled in centibars. S, "shallow" and D, "deep" represent regions of small and large pressure differences respectively.

low vorticity, are relatively unstable in their upper parts. Thus both the horizontal and vertical gradients of potential vorticity are in general in the same direction and of greater magnitude than the gradients of absolute vorticity.

As an aid in the analysis of the potential absolute vorticity field, a series of isentropic weight charts (340 to 360K) was analyzed at 12-hourly intervals. Fig. 18, showing the weight distribution at 1500 GCT 9 July, the time of maximum development of the shear line, is reproduced from this series[5]. The preceding charts showed considerable irregularity of smaller-scale features, but the continuity of the broadscale features was fairly well preserved. During the three days preceding fig. 18, a gradual amplification of the "deep" thickness tongue over the southwest was observed, together with the extension southward of the "shallow" tongue in the shear line region which at first appeared upstream as a much smaller perturbation. South of latitude 45° N, there was close parallelism between the isentropic thickness pattern and the contours of the 200-mb surface, throughout the development (compare figs. 5 and 18).

The conservation of potential absolute vorticity. — The equation expressing the conservation of potential absolute vorticity and potential temperature may be written in the form

$$\frac{d}{dt}\left(\frac{f+\zeta}{\triangle p}\right) = 0, \qquad (1)$$

where f is the Coriolis parameter, ζ is the vertical component of the relative vorticity, and $\triangle p$ is the pressure difference between two isentropic surfaces[6]. This equation is valid only when the non-conservative "frictional" forces are negligible and the motion is adiabatic. Thus in the absence of frictional and non-adiabatic effects, air columns contained between two isentropic surfaces can increase their absolute rate of rotation about the vertical only when the isentropic surfaces move farther apart (so that $\triangle p$ increases).

Application of this theorem to the cross section through the shear line (fig. 12) implies that the appearance of high absolute vorticities in the fully-developed shear line must have previously been associated with even smaller values of isentropic thickness (or greater vertical stability) than they are associated with on the cross section. The isentropic weight charts showed that there were regions to the north of this shear line where the pressure difference $\triangle p$ between the potential temperature surfaces 340 K and 360 K was smaller than the smallest value of $\triangle p$ in the cross section through the fully-developed shear line (fig. 12). It may therefore be possible that the shear line was formed by a process whereby columns of air with great stability ($\triangle p \sim 20$ mb) and normal values of absolute vorticity stretched vertically and increased their absolute vorticity at least approximately in conformance with the vorticity equation (1).

One way in which this possibility can be tested is to analyze synoptic charts of the potential absolute vorticity, $(f+\zeta)/\triangle p$. Charts of $(f+\zeta)/\triangle p$ at the 200-mb level were constructed for the six observation times preceding and including the time of maximum development of the shear line at 1500 GCT 9 July. For these charts, the relative vorticity was computed geostrophically, using the relation

$$\zeta = \text{scale factor} \times \nabla^2 z_{200},$$

where z_{200} is the height of the 200-mb surface. $\nabla^2 z_{200}$ was evaluated by finite differences from the analyzed 200-mb contours, using an overlapping rectangular grid with intervals of approximately 500 km (except over the eastern part of the United States where a non-overlapping grid interval of 250 km was used). It must be pointed out that this method will tend to minimize extreme vorticity values if they exist over a small region — as is the case with the shear line. After adding the relative vorticity to the Coriolis parameter, the potential absolute vorticity $(f+\zeta)/\triangle p$ was then obtained by dividing the absolute vorticity $f+\zeta$ (in units of 10^{-5} sec^{-1}) by $\triangle p$ (in cb) for the isentropic layer 340—360 K.

[5] As a qualitative guide in the analysis of these charts, $\partial^2 \mathbf{v}/\partial z^2$ (parallel to the weight lines) was computed from wind observations at the 35-, 40-, and 45-thousand foot levels.

[6] In general, the conservation theorem must also include the horizontal components of the absolute vorticity vector and potential temperature gradient, as shown by ERTEL (1942), but these may ordinarily be disregarded when the isentropic surfaces are not excessively steep.

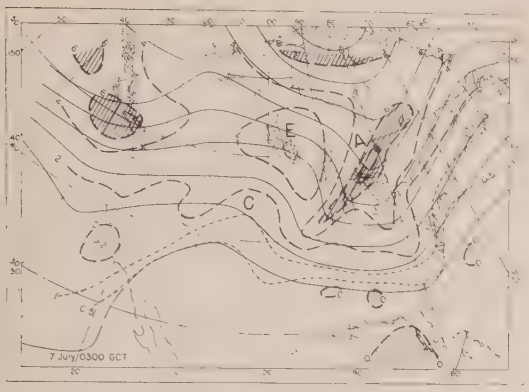

19 a

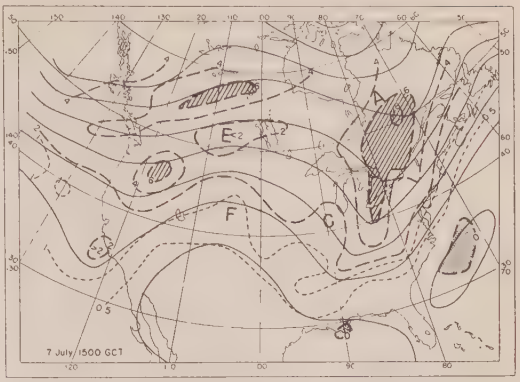

19 b

19 c

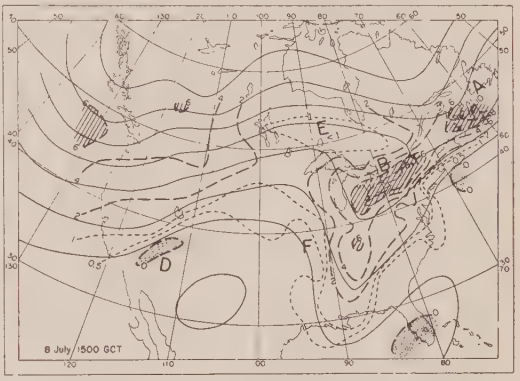

19 d

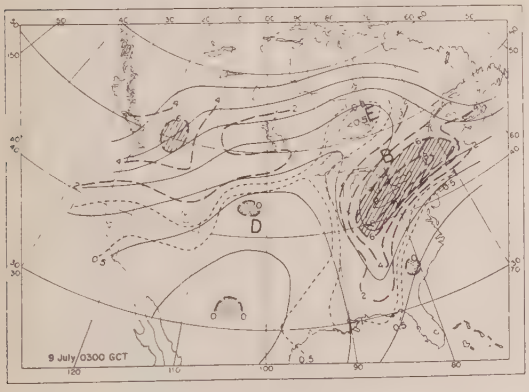

19 e

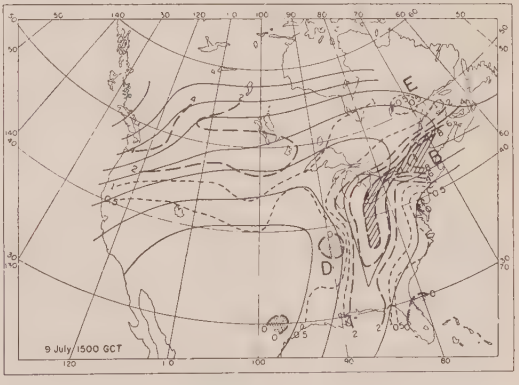

19 f

Fig. 19. Charts of potential absolute vorticity, $[(f + \zeta)/\Delta p]$, 0300 GCT 7 July to 1500 GCT 9 July 1950. Dashed lines are isolines of potential vorticity (units of 10^{-5} sec^{-1} cb^{-1}) and thin continuous lines are contours of 200-mb surface at intervals of 300 feet. Regions of maximum (> 6) and minimum (< 0) potential vorticity are indicated by hatched and stippled areas respectively.

The charts prepared in this manner are reproduced in fig. 19.

An examination of these charts shows that in general the continuity of the isolines of $(f + \zeta)/\Delta p$ was quite good in the central part of the region. For example, the features indi-

cated by the letters A, C, D and F show very good continuity on successive charts. On the other hand the center of minimum potential vorticity (indicated by E) that is present near the Canadian-United States border throughout the series, exhibits little tendency to move with the flow pattern. Similarly, the center of maximum potential vorticity indicated by B appears suddenly on the chart for 0300 GCT 8 July (fig. 19c) with no previous history. There are two possibilities of explaining these two discrepancies: (*a*) The analysis of potential vorticity in southern Canada is essentially correct and the anomalous behavior of systems B and E is to be explained by the non-conservative processes neglected in (1); (*b*) the more scattered aerological observations over southern Canada make a sufficiently accurate analysis of the potential absolute vorticity impossible at this level. It is difficult to conceive of non-conservative processes sufficiently intense to explain completely the sudden appearance of center B, but it is possible that a combination of the two possibilities (*a*) and (*b*) can account for its appearance.

The marked intensification of the shear line occurs between 1500 GCT on the 8th and 9th, corresponding to the last three charts in fig. 19. The simultaneous formation of the strong but shallow meridional jet on the west side of the shear line is associated with the increase of the zonal gradient of potential vorticity in the same region. At least a part of this increase (and thus in a sense the formation of the jet itself) can be explained by advection of potential vorticity since the center of minimum $(f+\zeta)/\triangle p$ (letter D) shows excellent continuity from 1500 GCT 8 July to 1500 GCT 9 July. During this 24-hr period there is also a local increase of potential vorticity in the region of the shear line itself. It is quite possible that this also can be explained qualitatively by advection since the charts for 1500 GCT 8 July and 0300 GCT 9 July show that the "ridge" in potential vorticity lagged slightly behind the trough in the contour lines. A more detailed analysis of this last point is not possible, however, because of the relatively long time- and space-intervals between observations.

Especially important with respect to the conservation of potential vorticity is an exact determination of the velocity field in the vicinity of the shear line. As pointed out previously, the most conservative assumption (that of a quasi-linear field) gives the smallest possible value of the maximum absolute potential vorticity in the shear zone. If the velocity field is not this simple, the maximum values of potential absolute vorticity in the shear zone may be considerably larger than the values indicated on the charts. It would then be very difficult, if not impossible, to explain the final formation of the shear line by a process compatible with the individual conservation of potential absolute vorticity.

Interpretation of mechanism of shear-line formation. — As pointed out earlier, the most significant event connected with the shear-line formation appears to be the initial generation of a strong northerly current on its west side. Once such a current has been established, the wave trough in which it is initiated must become unstable, since a large amount of momentum is then injected into lower latitudes where the pressure gradient is insufficient to balance the Coriolis force acting upon the current. Deepening of the pressure trough comes about through a tendency to mutual adjustment of the mass and velocity fields, and the generation of an oppositely-directed current east of the shear line follows from intensification of the zonal pressure gradient as a result of this deepening[7].

Although an increase in amplitude took place in the trough off the west coast at about the time of most pronounced development of the shear-line trough (figs. 1 to 6), the dispersion of energy from such a deepening trough could not in itself cause the formation of a trough of even greater amplitude downstream (see YEH, 1949). The deepening likewise did not seem to take place through local barocline processes of the type ordinarily associated with concentration of vorticity; baroclinity in the lower troposphere was very weak, while baroclinity in the upper troposphere increased with time in the shear-line region.

It was concluded from the analyses presented earlier (e. g., fig. 15) that the pronounced local

[7] It should be pointed out that the discussion here refers only to the type of shear line that develops initially in a single westerly current. The type that forms, e. g., between a strong W or SW current of considerable extent upstream, and an initially separate E or NE current flowing around an anticyclone located at a higher latitude, appears to be of a fundamentally different character.

increase of northerly winds in the region west of the shear line did not evolve through advection from other regions. Since none of the above processes appears to furnish a complete explanation for the local acceleration, it is clearly necessary to look for a possible mechanism due to some other external influence. Since such an influence is not apparent in the southern jet-stream system alone, it is logical to consider what possible interactions could take place between the momentum and pressure fields in the vicinity of the jet stream further north, and the wind field of the southern jet-stream system.

To determine what this interaction might be, an attempt was made to study the isallohyptic and wind-velocity fields. For the case described above, this attempt was unsuccessful because of lacunae or inaccuracies of data in certain critical regions. A second case was therefore studied (31 July to 5 August 1949), in which it was possible to arrive at a satisfactory analysis of these fields. The flow patterns in the two cases were quite similar, and qualitatively the velocity and height-change fields in the July 1950 case were similar to those of the August 1949 case, insofar as the points discussed below were concerned. In order to conserve space, the charts already presented for the former case will be referred to in this discussion, together with a schematic diagram prepared with the help of more adequate data from the latter case.

Examination of the 200-mb charts between 1500 GCT 7 July and 0300 GCT 9 July shows that during this period the southwesterly flow over western and central Canada, in the northern jet-stream system, increased strongly as the major ridge in the northern belt of westerlies moved eastward to a position north of the shear line. This suggests that the height rise SW of James Bay (figs. 3 and 4) may be considered as the result of the amplification and eastward movement of the major ridge in response to deepening of the west-coast trough, in combination with a "banking" or mutual adjustment of pressure and velocity fields as suggested by Rossby (1937), following the injection of a current possessing high momentum into a region initially possessing a pressure-gradient field insufficient to balance the Coriolis force acting upon the injected stream.

The field of height changes imposed in this manner is illustrated by the dashed lines in fig. 20, in relation to the two jet-stream systems. The greatest rises are found just to the right of the northern jet, and the greatest total rises over a longer period of time (but not necessarily in a given 12-hr period) take place at approximatively the half-wave length $\frac{1}{2}\lambda_s$ of a stationary wave from the upstream trough, given (Rossby, 1940) by

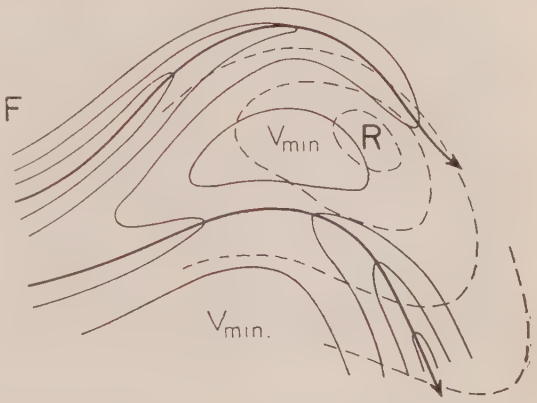

Fig. 20. Schematic diagram of height-change field accompanying increase in a amplitude of northern part of complex ridge due to processes acting upstream in northern jet-stream system. Solid heavy lines, axes of jet streams; light solid lines, isotachs; light dashed lines, lines of equal height rise decreasing in magnitude away from rise center *R*. V_{min} denotes regions of slow wind speeds.

$$\frac{1}{2}\lambda_s = 90\sqrt{\frac{2U}{\omega a \cos^3\varphi}},$$

where U is the speed of the basic westerly current, a is the radius of the earth and ω its angular rotation, and λ_s is measured in degrees longitude.

The rise-center R thus imposed in the northern part of the ridge relaxes the height gradient across the southern jet near the ridge line. In the case of a ridge moving at a speed much less than that of the wind in the center of the jet, the radius of trajectory curvature R_T is approximately given by the gradient wind equation

$$R_T = \frac{v^2}{f(v - v_g)}, \qquad (2)$$

where R_T is taken as positive for anticyclonic curvature, v is the actual and v_g the geostrophic wind speed. The relaxation of the height gradient due to the rises centered at R in fig. 20 must, by decreasing v_g, also decrease R_T. In the limiting case ($v_g \to 0$), the trajectory curvature approaches that of an inertia circle of radius v/f. As seen from figs. 2 to 4, the relaxation of the height gradient in the southern part of the ridge was very pronounced, so the progressive clockwise turning of the southern jet east of the ridge is in accord with the conclusion from equation (2). This conclusion assumes that v does not decrease with time in the vicinity of the ridge, an assumption that appears to be borne out by the observations and would be expected from the nearly constant input of momentum into the ridge region from farther upstream.

In both of the cases studied, it was clear that an axial acceleration of the winds developed east of the ridge upstream from the shear line, as indicated schematically by the isotachs in the lower right-hand portion of fig. 20. This implies that a pronounced cross-contour flow developed where previously it was negligible. The magnitude of the movement across contours may be estimated from the energy equation for adiabatic motion on an isobaric surface,

$$\frac{c^2}{2} + gz = \text{const.}$$

For the air to accelerate from 60 to 100 knots, a total height change of 80 m toward lower heights is necessary. This is approximately in agreement with the amount determined by inspection from fig. 15 in the region SW of Lake Michigan, along the axis of maximum wind speed. Since fig. 15 does not represent a steady-state condition, however, the angle of flow across contours as estimated from this figure alone is somewhat exaggerated. This angle may be computed from the equation

$$\frac{dv}{dt} = -g\left(\frac{\partial z}{\partial s}\right)_p = fv_g \tan \alpha,$$

where v is the total wind speed along the direction s of a streamline and α is the angle measured counterclockwise from contour to streamline. This angle was computed to be about 15° in the region of strong acceleration SW of Lake Michigan in fig. 15.

No satisfactory explanation for the development of this pronounced axial acceleration has been found. It is recognized, of course, that the imposition of a localized region of height rises such as indicated in fig. 20 contributes not only to increasing the anticyclonic curvature of the streamlines according to equation (2), but also to increasing the curvature of the contours in the southern part of the ridge. If the increase in contour curvature through this process exceeds the increase in streamline curvature, the required axial acceleration can be produced east of the ridge in the southern jet. It is by no means obvious how this condition can be produced. Thus the simple mechanism proposed above for the interaction between jet streams at different latitudes appears to partially answer the question of how the strong northerly winds can be produced in the region west of the incipient shear-line formation, insofar as a turning of the winds is involved, but does not provide an explanation for the simultaneous increase in total momentum of the northerly current.

Conclusion. — No claim can be made that a completely satisfactory answer has been given to either of the questions stated in the opening paragraphs. Through the expedient of choosing cases at the outset in which no pronounced lower-tropospheric cold dome was present, it is believed that the process of vertical stretching of the warm air above such a subsiding cold dome has been eliminated as a significant factor in the formation of the shear lines or the production of the strong vorticity observed therein. The study of changes in the potential absolute vorticity field, while not wholly conclusive because of limitations in the data, at least suggests that potential vorticity may have been generated through nonconservative processes in the free atmosphere.

A possible mechanism has been suggested for the production of a strong meridional current leading to instability of the shear line trough; this mechanism may have more general application in understanding the interference patterns of waves in westerly currents

at different latitudes. The question as to why the instability should take on the form of a shear line rather than simply an increase in amplitude of a continuous current flowing around a trough, needs further investigation. The answer appears to be connected with the initially weak baroclinity throughout the troposphere in the lower latitudes into which the strong meridional current is injected; the rapidity with which changes in the kinematic field take place may make it impossible to build up a solenoid concentration rapidly enough and of sufficient intensity to deflect the current eastward.

The extreme concentration of momentum in a shallow layer near the tropopause observed in the case discussed above, appears to be of great synoptic as well as theoretical interest. Particularly in view of the interest shown by synoptic meteorologists in the connection between the jet stream and cyclogenesis, it would appear profitable to study the differences in behaviour of jets characterized by this concentration of momentum, and those characterized by more even distribution of baroclinity throughout the troposphere. Lastly, studies of this nature emphasize the need for more adequate observational data in the higher troposphere and lower stratosphere; particularly wind data, since it is difficult if not impossible to construct a completely satisfactory picture of the kinematic field from the sparse data now available in the higher levels over North America.

Acknowledgement. — The writers are greatly indebted to Dr C.-G. Rossby, who initially suggested the various phases of this investigation, for his generous guidance throughout its progress.

REFERENCES

Charney, J., 1949: On a physical basis for numerical prediction of large-scale motions in the atmosphere. *J. Meteor.*, **6**, 371—385.

— R. Fjörtoft and J. von Neumann, 1950: Numerical integration of the barotropic vorticity equation. *Tellus*, **2**, 237—254.

Cressman, G. P., 1948: On the forecasting of long waves in the upper westerlies. *J. Meteor.*, **5**, 44—57.

Ertel, H., 1942: Ein neuer hydrodynamische Wirbelsatz. . *Meteor. Zeits.* **59**, 277—281.

Fultz, D., and Long, R. R., 1951: Two-dimensional flow around a circular barrier in a rotating spherical shell. *Tellus*, **3**, 61—68.

Fultz, D., 1950: Experimental studies related to atmospheric flow around obstacles. *Geofisica Pura e Applicata*, **17**, 88—93.

Frith, R., 1950: Details of wind structure revealed by artificial nucleation of supercooled cloud. *Nature*, **165**, 899.

Hsieh, Y.-P., 1950: On the formation of shear lines in the upper atmosphere. *J. Meteor.*, **7**, 382—387.

Rex, D. F., 1950: Blocking action in the middle troposphere and its effect upon regional climate. I, *Tellus*, **2**, 196—211; II, *Tellus*, **2**, 275—301.

Riehl, H., 1948: Jet stream in upper troposphere and cyclone formation. *Trans. Amer. Geophys. Union.*, **29**, 175—186.

Rossby, C.-G., 1937: On the mutual adjustment of pressure and velocity distributions in certain simple current systems. *J. Marine Res.*, **1**, 15—28.

— 1940: Planetary flow patterns in the atmosphere. *Quart. J. R. Meteor. Soc.*, **66**, *Supplement*, 68—87.

— 1951a: On the vertical and horizontal concentration of momentum in air and ocean currents I. Introductory comments and basic principles, with particular reference to the vertical concentration of momentum in ocean currents. *Tellus*, **3**, 15—27.

— 1951b: Über die Vertikalverteilung von Windgeschwindigkeit und Schwerestabilität in Freistrahlbewegungen der oberen Troposphäre. *Arch. f. Met. Geoph. und Biohl.* Serie A. Band IV.

Staff members, Dept. of Meteorology, University of Chicago, 1947: On the general circulation of the atmosphere in middle latitudes. *Bull. Amer. Meteor. Soc.*, **28**, 255—280.

Yeh, T.-C., 1949: On energy dispersion in the atmosphere. *J. Meteor.* **6**, 1—16.

A Synoptic-Aerological Study of Interaction between Vortices

By F. A. BERSON, Swedish Meteorological and Hydrological Institute

(Manuscript received 1 Oct. 1950; revised 15 Jan. 1951)

Abstract

The displacement and intensity changes of a cyclone and anticyclone over the Northeastern Atlantic in October 1945 are investigated. An attempt is made to explain the motion of the cells as an analogue to the vortex pair in hydrodynamics. The observed paths and translational velocities are compared with those computed from theoretical relationships derived on simplifying assumptions involving a.o. conservation of absolute vorticity and an hypothesis of equivalent vortex strength. With reference to the third day after the genesis of the system, the result of this comparison is satisfactory and is considered significant in view of a concurrent transient reduction of horizontal divergence inferred from observed variations in the thermal structure of the cyclone.

The genesis and behaviour of the system of vortices is also discussed in relation to a recent theory of composite baroclinic vortices. In part this theory is confirmed by observational evidence as e.g. an accelerated equatorward drift of the cyclone in its early stage and an intensification of its upper part in a later stage when the centre of the system of vortices is stationary.

1. Introduction

During the last three decades theoretical discussion of dynamical problems in extratropical synoptic meteorology has been largely concerned with the genesis, development and and movement of disturbances in the pressure field associated with fronts and wave-like flow patterns in the middle and upper troposphere. In recent years the interest in atmospheric vortices, especially their motion across the surface of the earth, has been strongly revived, chiefly because of the important rôle they play as links in the general circulation. Synoptic-aerological descriptions of long-lived cyclonically rotating high-tropospheric pools of cold air breaking away from the circumpolar whirl of westerlies (Scherhag, 1948), were followed by studies of these vortices — and their counterparts, warm anticyclones to the north of the maximum upper westerlies — with a view to throwing light on their part in the mechanism of the meridional transport of heat and zonal angular momentum (University of Chicago 1947; Palmén 1949).

The dynamics of vortices of this kind has been also explored from a theoretical viewpoint by other writers employing simplified kinematic models (see references in next section). The present investigation is a synoptic aerological study of an observed remarkable motion of vortex-like systems: of a Low and a High moving in quasi-circular paths of unequal radii about a fixed point. For a preliminary view of the displacement of the pressure cells, the reader may at this point turn to the 500 mb contour charts (Fig. 3), cells A_3 and C_3, and to the track diagrams (Figs. 5 and 6). The representation of the observational data and the proposed explanation of the phenomenon as an analogue to the

two-vortex model in hydrodynamics will be facilitated by a prior review of recent theories of large-scale vortex motion in the atmosphere.

2. Review of theories

In an attempt to clarify the problem of the dynamical control of pressure in the atmosphere from a principal standpoint, PRIESTLEY (1948) has a.o. dealt with adjacent large-scale, quasi-circular baroclinic cyclones and anticyclones centred in a latitude circle. By using analytical methods similar to those employed in a theory of the wave-cyclone (BJERKNES and HOLMBOE 1944) and based on the semi-empirical concept of local gradient wind motion, the displacement in the line of centres or the zonal drift of such systems is derived from an appropriate approximation of the field of horizontal divergence.

The theory of motion and mutual interaction of circular vortices of various standard types, i.e. of different radial pressure profiles, has been developed by JAMES (1950). The velocity is taken as the sum of geostrophic, cyclostrophic and isallobaric components, which is however not a general truth.[1] A theory of quasi-geostrophic vortex interaction is forwarded, based on the hypothesis that in mutual interaction the pressure profile of individual vortices is conserved, and permits vortex interaction to be considered as the motion of attracting and repelling "centres of action". Pertinent to the problem in the present study is, in particular, the author's conclusion that "*if two vortices are rotating about some point with constant separation, such motion could persist without violating the energy equation, as the mutual energy is a function of the separation only*". Although the equation of energy balance for the two-vortex case, as given by James, may well serve as a basis for a quantitative verification of the vortex paths in the present case, it is perhaps more desirable to take recourse to a hydrodynamic theorem due to VON HELMHOLTZ (1858) and LORD KELVIN (1866), revealing in the same manner an exact analogy to the similar equations in the dynamics of attracting bodies and electric charges.

However, as the movement of atmospheric vortices is observed in a system rotating with the earth, certain effects must be entirely due to its rotation and its spherical shape. It has been shown (DAVIES 1948, ROSSBY 1948, 1949) that *solitary* vortices with vertical axes in an environment at rest relatively to the earth are subjected to a force directed polewards in the case af a cyclone, equatorwards in the case of an anticyclone. This force is readily determined when it is assumed that the lateral extent of the vortex be small (viz. its radius of cross section R small in comparison with the earth's radius a) and that the motion inside the vortex as well as the escape motion in the environment be non-divergent. The force is then proportional to the gradient of absolute vorticity Z_0 in the environment, which in this case is equal to the (mean) variation of the Coriolis parameter with latitude,

$$\partial Z_0/a\partial\varphi = \partial f/a\partial\varphi = 2\Omega\cos\varphi/a \equiv \beta.$$

ROSSBY found for this force, per unit square of a horizontal slice of unit thickness, acting on a vortex in *solid rotation* having vorticity $\zeta = 2\omega$, where ω is the angular velocity (counted positive for cyclonic rotation):

$$Fy = \frac{1}{4} R^2 \omega \beta = \frac{1}{8} R^2 \zeta \beta \qquad (1)$$

In the derivation of this expression it is implied that the velocity has a jump at the outer boundary of the vortex from the value ωR to zero. It is noteworthy that when an appropriate annular zone of lateral shear at the outer boundary is taken into consideration the result is almost the same, since e.g. in the case of a cyclone the factor 1/4 is replaced by 5/16. This has been shown by KUO (1950) who points out that these, however, are only approximate results, because rigorous solutions satisfying the vorticity equation for non-divergent motion in a barotropic fluid are only possible if the absolute vorticity ($Z_0 = f + \zeta_0$) in the environment of the vortex is uniformly distributed — whereas in the seemingly simple case of a solitary vortex in an environment at rest this is clearly *not* satisfied. When $\partial Z_0/a\partial\varphi = 0$, but f and ζ

[1] From an analysis of the relation between the ageostrophic wind component and the isallobaric field it is possible to show (BERSON 1939) that the isallobaric and cyclostrophic components are mutually interdependent.

are linear functions of latitude so that $\beta =$ const. and $\zeta_0 = \zeta_{00} - \beta a \delta\varphi$ where ζ_{00} is the vorticity at the centre of the vortex, the force driving a vortex with solid boundary across the latitude has two principal components: one, a rotor effect, stems from the motion of the vortex relative to the environment and from the circulation around the vortex; the other is due to the distribution of relative vorticity in the surrounding fluid. (In the case of a superimposed basic zonal current, this distribution would then correspond to a poleward decreasing cyclonic, or increasing anticyclonic lateral shear $\partial U_0/a\partial\varphi$. The corresponding force F_x is in this case due to the rotor effect only.)

It is to be noted that although in the above theory it is assumed that the vortex possesses a solid boundary, the motion *inside* the vortex may be of any kind, provided it has the same (relative) vorticity as the surrounding fluid. Yet even if its vorticity differs from that of the latter — as is usually the case in the atmosphere — *the effect of a superposed circulation is only to give an irrotational cyclic motion to the surrounding fluid.* This irrotational motion is represented by an additional logarithmic stream function, $\Psi_1 = 1/2\ R^2(\zeta - \zeta_0)\ \ln r$, where r is the distance from the centre of the vortex. This stream function satisfies the vorticity equation and the boundary condition that $\Psi_1 =$ const when $r = R$.

In the next section it will be seen that the earlier mentioned vortex theory due to VON HELMHOLTZ and KELVIN, which permits one to determine the velocity at every point in an incompressible fluid containing a discrete number of vortex filaments and at rest at infinity, may be taken as both a simplification and generalization of the foregoing treatment; for if it be assumed that no basic current exists and the effect of the earth's rotation be disregarded (U_0 and β vanishing), the rotor effect as well as the effect from the distribution of vorticity in the environment vanish. We are left with the reaction to the surrounding irrotational circulation given by the stream-function $\Psi = 1/2\ R^2\zeta\ \ln r$ and so, between two or more adjacent vortices, only with their interaction. Presumably in the case of two or more vortices, for these conditions there also ought to exist an effect on each from the variation of the Coriolis parameter with latitude; but if we arbitrarily disregard the relevant forces *Fy*, our problem is reduced to a simple kinematic vortex interaction in a rotating system with constant Coriolis parameter, i.e. on a rotating disc.

There is another important aspect of the displacement of solitary vortices across the latitude circles, due to a non-uniform distribution of absolute vorticity in the environment. Because of the latter the vorticity and thus also the flow in the vortex must readjust themselves whereby a certain amount of energy will be released. This *kineto-potential* energy supply is, as ROSSBY has shown, not necessarily converted into translational energy only, but provides (in favourable conditions) for the creation of *rotational* energy as well. A baroclinic system, as e.g. an anticyclonically rotating cold dome, will sink and spread out along the surface of the earth during its displacement equatorward and a cyclonic circulation above the sinking dome will be created. A verification of this process from synoptic and statistical evidence has been given (ROSSBY, 1949 and KOO, 1950). In the present study of vortex motion there is certain evidence that the rotary motion of the pressure cells has been preceded by a process of this kind. Data supporting this conclusion will be given in § 7.

3. Application of "vortex pair" theory

If in particular we restrict our attention to two rectilinear vortex filaments in an incompressible non-viscous fluid at rest at infinity, it is possible to derive relationships for the displacement of the filaments relative to a fixed point. When the strengths of the vortices, whose separation D is large in comparison with their radius of cross section ($D \gg R$), are equal and of opposite sign, viz. $I_1 = 2\pi R^2\omega = -I_2$, the system is called a "*vortex pair*" par excellence. The filaments in this case propel each other in a direction perpendicular to the line of their centres. In the following we shall use the term "vortex pair" even for the case when $|I_1| \neq |I_2|$.

We shall next give a brief derivation of the relationships for vortex filaments which will be subsequently applied to large-scale pressure systems. The deductions will be based mainly on a summary of the HELMHOLTZ-KELVIN

theory given by LAMB (1932), but the notations are altered so as to bring them into line with accepted meteorological conventions.

When the motion is in two dimensions (rectilinear vortices) the Cartesian components of the velocity, $\boldsymbol{V}_2$, are u and v and are functions of x and y only. The vortex lines are straight lines parallel to the z axis and the vorticity $\zeta = \partial v / \partial x - \partial u / \partial y$. The velocity outside the vortex filaments is determined by a streamfunction Ψ, as the motion is assumed to be nondivergent, whence

$$\boldsymbol{V}_2 = \boldsymbol{k} \times \boldsymbol{\nabla}_2 \Psi \qquad (2)$$

where $\boldsymbol{k}$ is the unit vertical vector directed along the positive z-axis (pointing upward) and $\boldsymbol{\nabla}_2$ is the horizontal ascendent. The stream function is found from a solution of the differential equation

$$\Delta_2 \Psi = \zeta \qquad (3)$$

where Δ_2 denotes the two-dimensional Laplacian operator. This solution is in virtue of the assumptions mentioned in the preceding section

$$\Psi = \frac{1}{2\pi} \iint \zeta' \ln r \, dx' \, dy' + \Psi_0 \qquad (4)$$

where ζ' is the vorticity at the point (x', y') at which the volume integral is taken (extended over that part of the two-dimensional space in which $\zeta' \neq 0$) and r is the distance between that point and the point (x, y) at which the velocity $\boldsymbol{V}_2$ is required; Ψ_0 is a complementary function which is any arbitrary solution of $\Delta_2 \Psi_0 = 0$ which satisfies the boundary conditions. In virtue of the restrictions imposed upon the fluid (u and v assumed vanishing at infinity), Ψ_0 reduces to a constant and one obtains then for the velocity

$$\boldsymbol{V}_2 = \frac{1}{2\pi} \iint (\boldsymbol{k} \times \boldsymbol{\nabla}_2 \ln r) \, dx' \, dy' \qquad (5)$$

or

$$u = -\frac{1}{2\pi} \iint \zeta' \left[\frac{y - y'}{r^2} \right] dx' \, dy'$$

$$v = \frac{1}{2\pi} \iint \zeta' \left[\frac{x - x'}{r^2} \right] dx' \, dy'$$

These relations show that any vortex filament situated at (x', y') and possessing strength $I' = \zeta \sigma'$, where σ' is the small cross section $\delta x' \delta y'$, contributes to the motion at (x, y) a velocity

$$\boldsymbol{V}_2 = \frac{I'}{2\pi} (\boldsymbol{k} \times \boldsymbol{\nabla}_2 \ln r) \qquad (6)$$

being thus directed at right angle to the line joining the points (x', y') and (x, y) and having the value $I'/2\pi r$ (See fig. 1 — The vector $\boldsymbol{k}$ turns the vector $\boldsymbol{\nabla}_2 r$ counterclockwise by 90° in our right-handed system of coordinates).

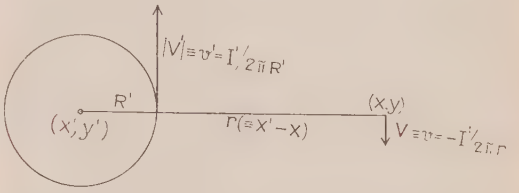

Fig. 1. Illustrating the motion at a point (x, y) due to a neighbouring vortex filament at (x', y'). For simplicity the line joining these points is made to coincide with the x-axis.

Taking the integral of the product of vorticity and velocity, extended over the sections of all the vortices present in the fluid, viz. $\iint \zeta V_2 \, dx \, dy$ and substituting from (5), it is easy to show that this integral vanishes identically, whence

$$\Sigma I' u = \Sigma I' v = 0 \qquad (7)$$

These equations permit one to fix the "*centre of inertia*" of the system of vortices which is analogous to the centre of a film of substance distributed over the xy-plane with the surface density ϱ (corresponding to ζ). This analogy is already embodied in the equation for the streamfunction, eq. (4), which is in form identical with the corresponding equation in the theory of attraction (between gravitating rods).

The coordinates of the centre of inertia are readily obtained from equations (7). In view of the assumptions of nondivergence and barotropy the vorticity is individually conserved or $d\zeta/dt = 0$; and the cross sections are unchanged during the displacements of the

filaments. Therefore the strengths I' are also invariants so that, as $u = \frac{dx}{dt}$, $v = \frac{dy}{dt}$ we have

$$\Sigma I'x = \text{constant}$$

or

$$x_i \Sigma I' = \Sigma I'x$$

whence

$$x_i = \frac{\Sigma I'x}{\Sigma I'} \text{ and similarily } y_i = \frac{\Sigma I'y}{\Sigma I'} \qquad (8)$$

the point (x_i, y_i) representing the centre of inertia.

Referring back to the case of *two* vortex filaments of strengths I_1 and I_2 resp., it is evident from the foregoing that the motion of each filament must be entirely due to the other and is therefore perpendicular to the line joining their centre (compare also Fig. 1). The two filaments remain at a constant distance apart and *rotate about the centre of inertia which is fixed*. It is easy to prove that the angular velocity of this rotation is determined by the identity

$$\omega^\star \equiv \frac{I_1 + I_2}{2\pi D^2} = \frac{R_1^2\omega_1 + R_2^2\omega_2}{D^2} \qquad (9)$$

where D is the separation of the centres. It follows from eq. (8), after rewriting it for the two-vortex case, that if the sense of rotation in the two vortices is the same the centre of inertia lies *between* the filaments whereas in the case of opposing rotation it lies *beyond* one of these, in the line joining them (extended). It is readily seen that the filaments of a "vortex-pair" par excellence will propel each other in the direction perpendicular to the line joining their centres, since in this case $\omega^\star = 0$.

Application of vortex pair theory and in particular equation (9) to barotropic vortices with vertical axes in the atmosphere seems a priori feasible when, as required by one of the premises underlying the theory, $D \gg R$ and when $\omega \gg f/2$. Attempts have in fact been made in this direction with a view to explaining certain characteristics of the motion of small atmospheric vortices such as dust-whirls a.o. (WILLIAMS, 1948).

Serious objections may be raised against any attempt to apply the above relations to phenomena characterized through that simultenaously ω and $f/2$, as well as D and R are respectively of the same order of magnitude. This is true for most large vortex-like pressure systems of comparable size and so also for the cells A_3 and C_3 in the present investigation. When ω and $\Omega \sin\varphi$ $(= f/2)$ are of the same o.o.m., equations (8) and (9) are still applicable, provided R is much smaller than the earth's radius so that the variation of the Coriolis parameter with latitude may be neglected. We have then to insert in the place of the strength I the absolute strength $I_a = 2\pi R^2 (\omega + f/2)$, and for the angular velocity of rotation about the inertia centre to take the absolute angular velocity, viz. $\omega_a^\star = \omega^\star + f/2$, whence from eq. (9)

$$\omega^\star = \frac{(I_a)_1 + (I_a)_2}{2\pi D^2} - \Omega \sin\varphi \qquad (9\,a)$$

However, when D and R are actually of the same o.o.m., in view of the proximity of the cells the velocity field, resulting from a superposition of the rotational field of one cell and a circulation pertaining to the environment of the other, will be rather complex. Strictly the application of the above relation would be permissible, if it could be shown from observational data that the velocity field is in fact composed of these components. An investigation of this kind would, however, ultimatively lead to the well known concept of a vortex-like disturbance being *steered* by the velocity field of an adjacent circulation system. When the latter itself is being displaced at a comparable rate — as is in fact the case in our "vortex pair" — not much could be profited from following up this line of approach.

The above elucidated difficulties, as well as others arising from the non-uniform distribution of vorticity within the pressure cells, may be overcome by making a hypothesis based on the exact correspondence between the centre of a film of mass and the centre of inertia of a system of (rectilinear) vortices, to which we have referred earlier. We shall assume that with regard to the specific interaction of two vortices, viz. their rotation about a fixed point, there is an equivalence between filaments of cross section πR^2, $(R \ll D)$ possessing vorticity ζ, and large adjacent

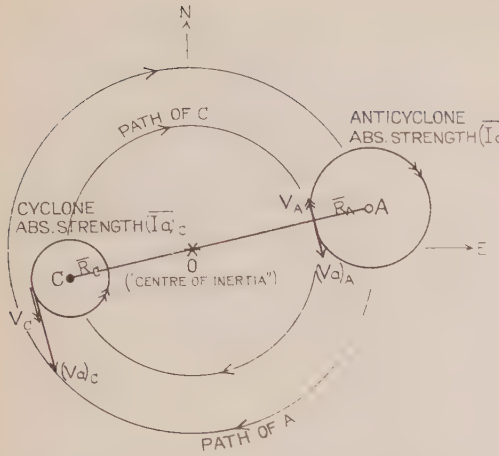

Fig. 2. Schematic representation of the path of circular vortices with vertical axes (cyclone centered at C, anticyclone at A) about their "centre of inertia" (at o). The ratio of the absolute vortex strengths is assumed as $I_{aC}/I_{aA} = 1.5$, the ratio of the radii of cross sections as 0.67. From equations (8) one obtains for the ratio AO/AC the value 0.6 and for the ratio of the absolute peripheral velocities V_{aC}/V_{aA} the value 2.25. V_C and V_A are the peripherical velocities relative to the earth's surface (not drawn to scale).

circulation systems with cross section $\pi \overline{R}^2$, $(\overline{R} \approx D)$, possessing an average vorticity $\overline{\zeta} = \zeta \dfrac{\pi R^2}{\pi \overline{R}^2} = 2\,\omega\,(R/\overline{R})^2$. This hypothesis may be also formulated as follows: "*Arbitrary vortices (solid bodies) may be contracted to filaments (gravitating rods) with strength (mass) equalling that of the former, without affecting thereby the interaction with (attraction exerted on) a second vortex (body) situate at finite distance from the centre of the first.*"

Accepting this hypothesis we may apply equations (8) and (9 a) to adjacent irregular systems such as the cyclonic and anticyclonic cells C_3 and A_3 of the present study. Giving the corresponding equivalent quantities $\bar{I}$, $\bar{\omega}$ and $\overline{R}$ the subscripts A and C (anticyclone and cyclone), equation (9 a) may be written as

$$\omega^\star = \frac{(\bar{I}_a)_A + (\bar{I}_a)_C}{2\pi D^2} - \Omega \sin \overline{\varphi}$$

$$= \frac{(\overline{\omega}_A + \overline{f}/2)\,R_A^2 + (\overline{\omega}_C + \overline{f}/2)\,\overline{R}_C^2}{D^2} - \Omega \sin \overline{\varphi} \qquad (10)$$

where $\overline{\varphi}$ is the latitude at which the inertia centre (point x_i, y_i) is situate. The geometry of the vortex pair and of the paths of its cells are schematically illustrated in fig. 2.

In order to illustrate the usefulness of the theory by means of a concrete example, let us for simplicity assume that there are two vortices with equal cross sections and that their separation is 3 $\bar{R}$, the cyclone having an equivalent vorticity equalling twice the Coriolis parameter, or $\overline{\omega}_C = \overline{f}$, the anticyclone having an equivalent vorticity equalling one half of the critical (minimum) value — which is obtained from the criterion for inertial instability of horizontal flow, viz. $\omega_a = 0$, thus $\overline{\omega}_A = -\overline{f}/4$. With these assumptions it follows from equation (10) that the cells would rotate about their inertia centre with an angular velocity $\omega^\star = -0.3\,\overline{f}$ or, taking the latitude as 55°, $= -0.35 \times 10^{-4}$ sec^{-1}. The vortices move therefore in *anticyclonic paths* of unequal radii. (The radii are the respective distances from the vortex centres to the inertia centre, and are readily calculated from the relations (8)). The corresponding period of revolution is for this case appr. 50 hours, a rather low value but of a reasonable order of magnitude.

The choice of the values for the dimension ratios $\overline{R}_A/\overline{R}_C$ and $\overline{R}/D$ and of the rotation ratios $\overline{\omega}_A/\Omega \sin\varphi$ and $\overline{\omega}_C/\Omega \sin\varphi$ does not affect the sense of curvature of the path, because for a wide range of values for these ratios one obtains negative $\omega^\star$ and thus *anticyclonic paths*. E.g. with prescribed values for the first three of the above ratios, taken as in the above example, *cyclonic paths* would result for an equivalent angular velocity of the cyclonic vortex exceeding the value 15/4 $\overline{f}$. The corresponding equivalent absolute vorticity $\overline{Z}$ would be 8.5 $\overline{f}$, but such high values are not observed in extratropical cyclones. Clearly, a certain combination of a reasonably large ratio $\omega_C/\Omega \sin \overline{\varphi}$ with a large ratio $\overline{R}_C/D$ may also reverse the sign of $\omega^\star$, so that a cyclonic path would result. We shall not here go into further details regarding this question, but it may be useful to compute roughly the angular velocity in the case of a cyclone being "captured" by a larger anticyclone (both cells, however, being of comparable seize). This is

not unlike the kind of system observed in the present case. Assuming $R_A = 2\,\overline{R}_C$, $D \approx \overline{R}_A + \overline{R}_C$, $\overline{\omega}_A = -\overline{f}/4$ and $\overline{\omega}_C = \overline{f}/4$, one obtains for ω^* approx. $-f/3$ or very nearly the same value as in the first exemple above and, incidentally, corresponding roughly to the mean values obtained in the calculations from the observational data, given below.

4. The flow pattern — "vortex pair" of October 4—7, 1945

The purpose of presenting the observational data in this, and the results of the calculations in the following, section is to show that the displacement of pressure systems may be determined to a large extent by the kind of interaction discussed in the foregoing. In this connection it is necessary to stress that the mutual dependency of the velocity field in the environment of adjacent vortices and of their displacement is usually overshadowed, not only by the effects which have been discussed in par. 2, but also by processes which cannot be accounted for by any theory of rectilinear (barotropic) vortices. In view of baroclinity in the pressure field, almost always present, such processes can only be understood from a study of the distribution of motion and mass (temperature) in three dimensions; and over an area exceding by far the area covered by the system as a whole. Nevertheless, the present case appears to bring out the mutual dependency rather clearly; it lends itself also for a discussion of the discrepancy between the proposed theory and the observed displacements (see §§ 6 and 7).

In order to provide a basic orientation with regard to the large-scale flow patterns constituting the environment of the "vortex pair", the analysis is chiefly restricted to the 500 mb level. However, the composite cross section through the cyclonic cell, given in § 7, will throw some light on the influence of the baroclinity and vertical motion concurring with its displacement.

From an inspection of the 500 mb charts (fig. 3[1]) and the track diagrams (figs. 5 and 6) the principal changes over the area covered by the charts may be summarised as follows:

1. The flow pattern in *middle latitudes*, between 40° and 60° N approx., is featured by *almost complete absence of zonal motion*. There are two quasi-stationary depressions with cold cores, C_a and C_b, centred over the Northern Adriatic Sea and in the vicinity of the Azores resp. The longitudinal distance of these centres is about 50°, corresponding to the wave-length of a highly unstable planetary wave-train of whose growth the cells C_a and C_b are presumably a final product[2]. They are separated by a ridge R_a to the west of Spain, possessing a feeble anticyclonic cell A_a.

2. In *subpolar latitudes*, north of 60° N, there is on 3 Oct. (marking the beginning of the four-day period investigated) an intense quasi-zonal, strongly baroclinic current on which a series of short waves is superimposed (troughs t_1, t_2, t_3; ridge r_3). The first two of these disturbances propagate rapidly downstream without growth of amplitude. The third, situated southeast of Greenland and possessing an extremely short wave-length, undergoes rapid amplitude growth between 3 and 4 Oct., and small circulation cells are simultaneously formed in both the ridge r_3 and the trough t_3. These cells are indicated on the chart of 4 Oct., and the following, as A_3 and C_3. Subsequently C_3 breaks away from the main current at a point near Iceland and moves rapidly almost due south across Ireland, subsequently southwest, swinging in a semicircular, *anticyclonic path* to a point not far from its initial position (Fig. 5). The anticyclonic cell A_3 remains during its movement at an almost constant distance from the cyclonic cell C_3 so that these two cells constitute an anticyclonically rotating "vortex pair", if the translation between 4 and 5 Oct. is eliminated (see Fig. 6).

It is noted that the anticyclone grows in size rather rapidly and that its movement cannot be entirely divorced from that of the ridge belonging to the initial wave

[1] These charts have been drawn with the aid of all available data (D. W. R., Meteorological Office, London, 1945; Historical Weather Maps, H. Q., U. S. Army Air Forces, 1945; Swedish Meteorological and Hydrological Institute, Yearbook 1945). — Some of the data had not been taken into account in the U. S. charts for reasons unknown to the writer who, incidentally, came upon the situation whilst on duty at the Upper Air Section of the Meteorological Office, Dunstable.

[2] Compare the theory of long-wave instability a. o. CHARNEY (1947), BERSON (1950).

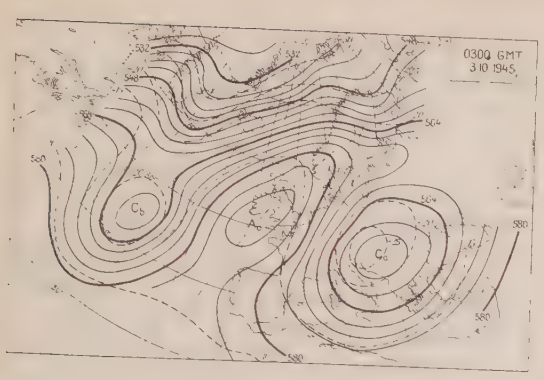

a

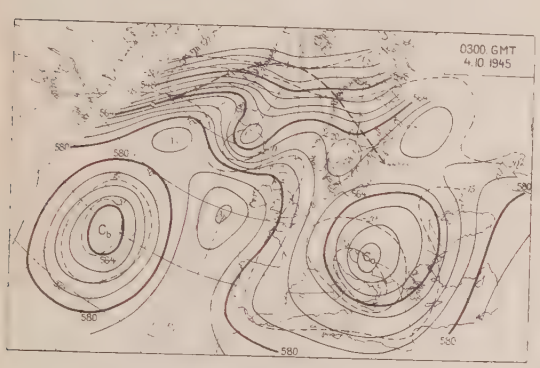

b

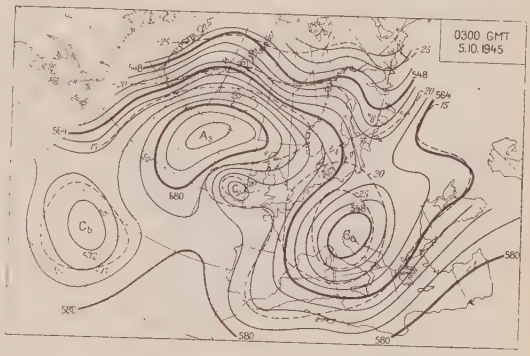

c

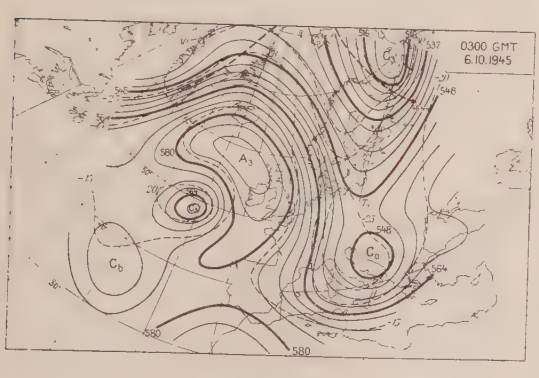

d

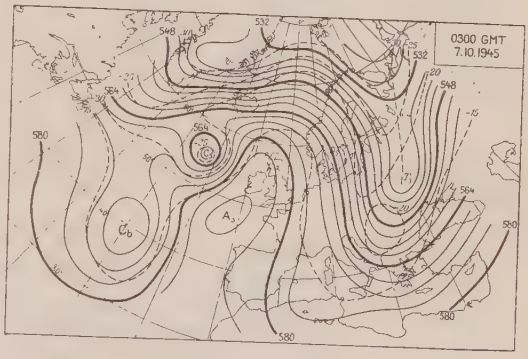

e

Fig. 3. Contours and isotherms of the 500 mb surface. The thick hatched line on the charts for 4 and 6 October is a constant absolute vorticity trajectory; the number at its endpoint denotes the time lapse (in hours) from the starting point.

disturbance r_3, t_3. The latter attains on 6 Oct. the dimensions of a *long wave* (R_3, T_3) which, as it grows considerably in amplitude, leads to the formation of a deep cyclone farther downstream in the White Sea area (C_3') and also to a strong connection of the northerly current in the rear of C_3' with the current in the rear of the quasi-stationary middle-latitude cyclone C_a. This in turn is finally, on 7 Oct., absorbed in the slowly progressive wave disturbance R_3, T_3 (The cell C_3' is no longer visible on the chart of 7 Oct. and the position of the northern portion of the trough T_3 is uncertain because of sparse observations.)

On the charts for 4 and 6 Oct. the dotted lines represent Constant Absolute Vorticity Trajectories originating on, or very close to, the south tip of Greenland at which the in-

flexion point in a periodically intensifying southwesterly current of jet-stream strength is situate. The trajectory of 4 Oct. gives a rather strikingly good verification for the movement and the marked amplification of the initial wave-disturbance r_3, t_3. Note that the southward bending portion of this trajectory predicts the formation of a northwesterly jet-stream after just under two days across Fennoscandia. The charts of 6 Oct. exhibits this current clearly, the central part, with maximum velocity, being only slightly shifted to the southwest, i.e. to Southern Norway and Denmark. This will be of importance in the detailed investigation into the behaviour of the system A_3, C_3; the verification of the *C. A. V* trajectory — originating at the upstream part of the circumpolar zonal current covered by the chart — suggests that in the middle troposphere the absolute vorticity vested in this current is largely conserved. The mass divergence which *is* however associated with the amplification of the wave disturbance, contributes to the growth of the anticyclonic cell A_3. To this extent one must *a priori* expect somewhat inexact results from an application of the relationships derived in the previous section; for these were deduced on the fundamental assumption that the absolute vorticity of each vortex filament be conserved. We shall now proceed to test the validity of these relationships.

5. Barrier, centre of inertia and equivalent vortex strength

It is evident from a closer study of the 500 mb charts that the system A_3, C_3 cannot be isolated from the environment in such a manner that the kinematic requirements of the theory are strictly satisfied. It is implied in these a.o. that the velocity field is a simply connected region which is true to the extent to which the atmosphere, as an infinitely thin envelope overlaying the earth, rotates with the angular velocity of the latter, whereby this imparts on all fluid filaments a spin, about vertical axes, equal to the Coriolis parameter. Because of the superimposed complex field of relative (horizontal) motion one cannot then any longer define a boundary enclosing the system A_3, C_3 such that this boundary would represent a "*diaphragm*" or a "*barrier*"[1] to the air masses external to the boundary; furthermore the motion at some distance from the cells is not everywhere irrotational.

Nevertheless, it is thought possible to overcome these difficulties arising from departures between the observed field and the model, by adopting the following subsidiary hypothesis. If the system A_3, C_3 were to lie wholly *within* a region of quasi-circular cross section at whose outer boundary the relative vorticity is small in comparison with the vorticity observed in the cells; and if this region were surrounded by an annular zone of some width in which the absolute vorticity is constant, then the (inner)boundary may be regarded as a diaphragm so that interaction between the fields internal and external to that boundary will be negligible.

The vorticity charts, Fig. 4,[2] show a thin dotted curve drawn in such a manner that it coincides as far as possible with an isoline of zero relative vorticity and at the same time encloses the vorticity fields pertaining to the cells A_3 and C_3. It is seen that this curve is semicircular and that the inequalities of vorticity in an annular zone surround-

[1] A diaphragm is a surface (or curve in the two dimensional case) drawn across the region and limited by the line (or points) in which it meets the boundary.

[2] The vertical component of relative vorticity has been approximated by a value obtained with grid methods from the geostrophic windfield, i.e. as a function of the two-dimensional Laplacian of contour height. It is noteworthy that the dependency on the geographical latitude is practically eliminated if a conical orthomorph chart projection (at 50° lat.) is used, since then the product of the square of the projection factor into the sine of the latitude is nearly constant, varying between 0.74 at 35° and 0.78 at 80°. — A closer approximation can be obtained from the gradient wind field. The effect of the curvature of the isobars (streamlines) and of the movement of the system on the value of the vorticity has been assessed applying the Bjerknes-Petterssen (1938, 1940) formula for the radius of a parcel trajectory, $1/\varrho = 1/\varrho_i\ (1 - c/G \cos\gamma)$, where c is the velocity of translation of the system, ϱ_i the curvature radius of the isobar and γ the angle between the translation direction and the wind direction. The percentage correction for isobar curvature, which is added in order to obtain the path curvature, can be directly read off a diagram (Fig. 7, p. 183). The method is one of successive approximation since in the above formula the "true wind" is approximated by the gradient wind (G). The values converge rapidly in most instances, after several successive approximations.

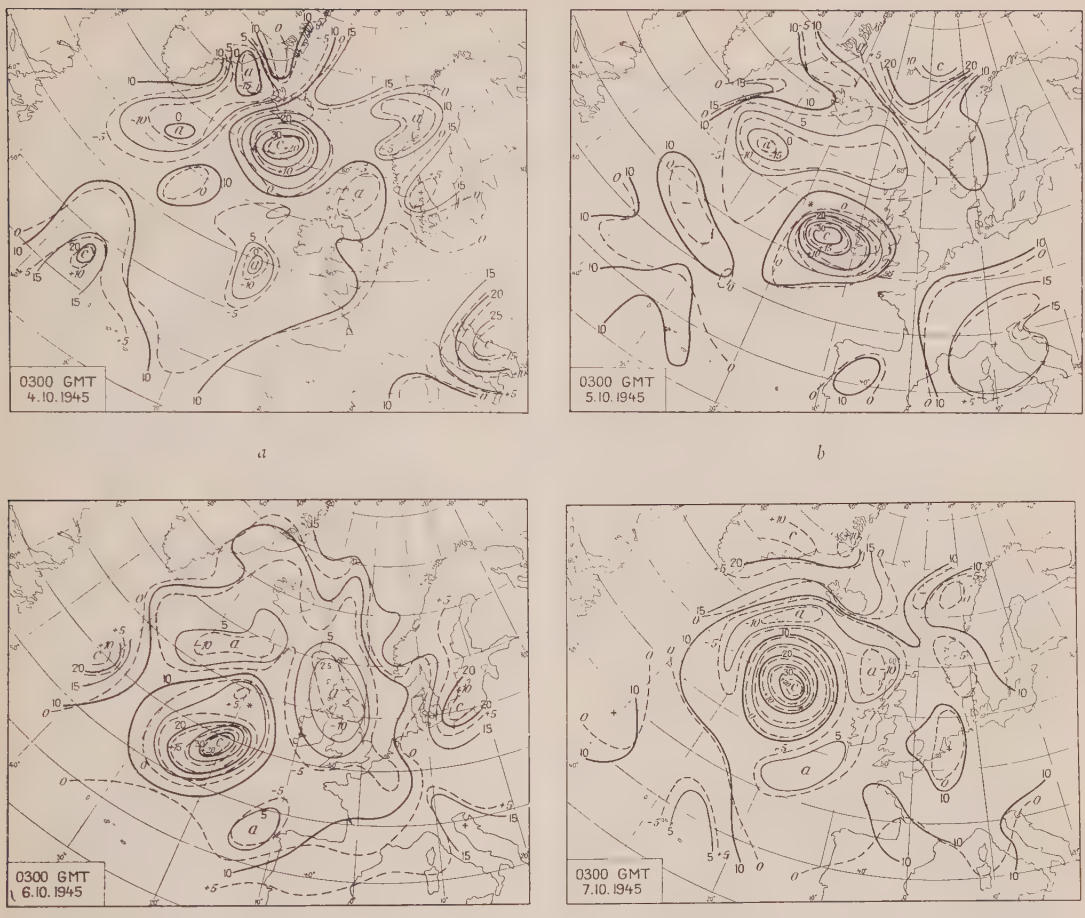

Fig. 4. Distribution of the vertical component of relative geostrophic vorticity (dashed curve) and of absolute vorticity (solid curve) in the 500 mb surface. The values of the isolines are in units of 10^{-5} sec^{-1}. The dotted semicircular curve is the "barrier" bounding the system A_3, C_3.

ing it are in some parts negligible and in other parts considerably less than the inequalities inside the curve. On the charts for 5 and 6 Oct. this condition is more closely fulfilled than on the charts for 4 and 7 Oct.

The flow pattern within the dotted curve may be described as follows: The cell C_3 resembles a *moon-shaped low pressure area*[1] denting, as it were, the cell A_3 at its convex part in which the strongest cyclonic vorticity is situate and at its concave part being separated from the environment by a col. Only on 6 Oct. the cell C_3 resembles a more perfect circular vortex, a larger number of closed semicircular contour lines being observed. The anticyclonic system has throughout an ellipsoidal cross section with at least two maxima of anticyclonic (relative) vorticity.

With a view to applying eq. (10) to these pattern, the vortical strengths $(I_a)_{A3}$ and $(I_a)_{C3}$ (henceforth I_{aA} and I_{aC}) are computed by taking for $\bar{R}_A$ and $\bar{R}_C$ the radii of circles whose surfaces are equal to the surfaces bounded by the isolines $\zeta = 0$. The centres of the *equivalent vortices* will, however, be identified with the highest and lowest pressure contour heights resp. In the case of the cyclonic cell this point is very

[1] See also p. 186.

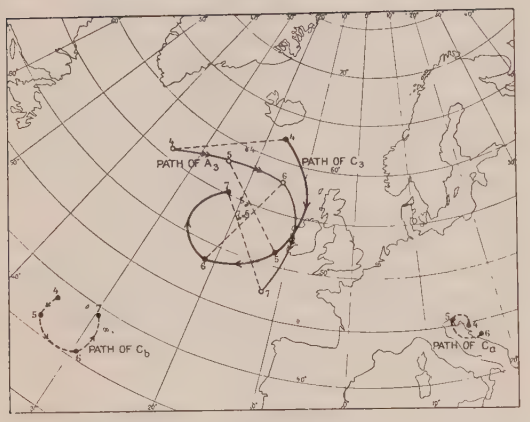

Fig. 5. The paths of cells A_3 and C_3 over the Northeastern Atlantic and the path of the (quasi-stationary) large-scale cold-core cyclones C_a and C_b between 4 and 7 October 1945. The asterisks give the position of the "centre of inertia" of the system A_3, C_3.

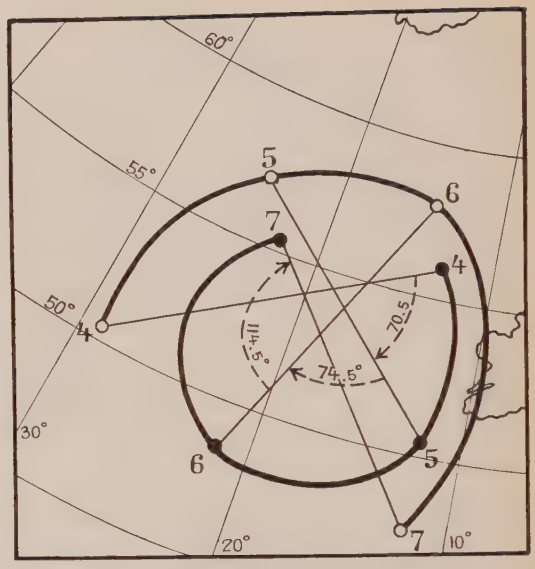

Fig. 6. The paths of cells A_3 and C_3 between 4 and 7 October 1945 that would result through the elimination of the translatory motion of the "centre of inertia". (Actually this motion is southward, whereas in this diagram the northward displacements in the negative time axis have been subtracted.)

close to the point at which the vorticity has a maximum, whereas in the case of the anticyclonic system this point ought to be found half way between the two principal minima of absoluted vorticity. It is seen, from the contour charts and the vorticity charts, that the latter condition is satisfied again on 5 and 6 Oct. only.

The coordinates of the inertia centre — this point being referred to the area within the "barrier" (dotted curve) — can be directly computed from equations (8). In Figs. 4 & 5 this point is marked by an asterisk. It is remarkable and gratifying to note that it lies very close to the line joining the centres of the low and high pressure areas.

6. Computed and observed displacements

The movement of the centre of inertia across the chart indicates the *drift* of the system A_3, C_3 as a whole. This drift is considerable between 4 and 5 Oct. only. During the following three days the centre of inertia is very nearly fixed relative to the earth's surface.

We may eliminate the *translation* of the system by shifting the inertia centre from the positions observed on 4, 5 and 6 Oct. onto the position observed on 7 Oct. and by shifting the centres of the cells A_3 and C_3 in parallel directions the corresponding distances. In this manner we obtain the paths of the cells about a fixed centre of inertia. These paths are shown in Fig. 6. It is seen that they are nearly concentric circles of unequal radii, as predicted by the theory for vortex filaments.

The quantities which enter the equations (8) and (10) are assembled in the first group of table I. The second group contains the absolute and relative angular velocities computed from eq. (10) and the corresponding periods of revolution $\tau^\star$ in pendulum days. The linear path velocities of the cells have been also computed, using the relations $V^\star = \omega^\star d$ where d is the distance from the center of inertia. The values of $\omega^\star$ and $\tau^\star$ have been computed either with the aid of geostrophically determined vortical strengths $\bar{I}$ (first row) or with vortical strengths obtained by applying an over-all correction for curvature of trajectory (second row; values in brackets). The method of correction is very briefly outlined in the footnote on p. 180.

The third group of table I contains the

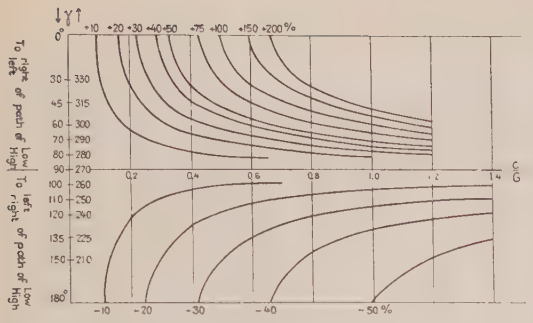

Fig. 7. Diagram for computing the trajectory curvature. The percentage correction of the isobar curvature (expressed through the radius of curvature ϱ_i) is given as function of the ratio between translation velocity, c, of the pressure system and the gradient wind velocity, G, and of the angle γ between the direction of translation and the direction of the (gradient) wind.

quantities signifying the observed rotary motion of the cells. The values in brackets denote the true linear path velocities of the cells resulting from both the rotary motion and the translation of the system as a whole.

The data in the table bring out the following noteworthy points:

i) the equivalent absolute vorticity $\bar{Z}$ pertaining to the cells is very nearly constant during the life of the system;

ii) the radii $\bar{R}$ increase from the first to the third day, i.e. during the southward displacement of the system, but undergo little change between the third and fourth day when the system shows no drift. The increase of the radii is responsible for the strong increase, proportional to their square, of the strengths $\bar{I}_a$;

iii) the relative vortex strength $\bar{I}_c$ increases during the southward displacement of the cyclone and decreases during its northward motion. This is partly a consequence of the corresponding variations mentioned in i) and ii). (The variation in vortex strength of a cyclone drifting across latitude circles may be analogous to the change of curvature, involving change if relative vorticity, along a *C. A. V.* trajectory drawn from a midpoint in a laterally uniform straight and broad current);

iv) the cell separation D is remarkably constant in the course of the last three days of the period during which the drift of the system as a whole is small or nil;

v) the order of magnitude of computed and observed average values of $\omega^\star$ agrees. Numerical agreement is significant only between the value computed on 5 Oct. and that assessed from the displacement between 5 and 6 Oct.; and

vi) in all instances with the exception of 4 Oct. the use of corrected vorticity improves the agreement between observed and computed quantities.

In view of the large standard deviation of the computed average value of $\omega^\star$ the numerical agreement recorded at a particular instance may be regarded as fortuitous. A closer study of the observational evidence given heretofore, as well as of additional data, is therefore indicated. It will be necessary to show that the fundamental and subsidiary assumptions leading to eq. (9 a) are more nearly fulfilled at that instance than at others. The practical value of such a test may be measured by setting it against the additional hypotheses we had made in the foregoing, i.e. the concept of equivalent vortex strength and the roughly sketched determination of a "barrier".

7. The deviation from non-divergent flow

We shall first deal with *subsidiary* assumptions. As to the centre of the vortices, it is seen from the 500 mb charts that on 4, 6 and 7 Oct. the identification of the anticyclonic centre with the centre of the cell A_3 is rather ambiguous. On the other hand, on the 5th the flow pattern over the whole area resembles more closely a "vortex pair" than on the other days (although on the 6th the cyclonic cell itself resembles more closely a circular vortex), since the vorticity chart of the 5th exhibits a more regular arrangement of the isolines of negative relative vorticity than on the other days. The centre of the high pressure area lies near the midpoint between the principle minima in the vorticity field on both the 5th and 6th, but on the latter day the existence of a third minimum detracts from the validity of the assumptions. On the 7th the cyclone is surrounded by an annular zone of anticyclonic vorticity, so that the distribution of vorticity is little suggestive of a "vortex pair". Because of some of these discrepancies the requirement that the separation of the centres

Table I

Group	Quantity	Symbol		4 Oct.	5 Oct.	6 Oct.	7 Oct.	Average 4—7 Oct.	Unit and Dimension
Computed equivalent vorticity, equivalent vortex strength and parameters of vortices	Absolute vorticity	$\overline{Z}$	A	6.7	6.4	6.4	7.0	6.7	10^{-5} sec^{-1}
			C	20.1	18.9	18.7	18.4	19.0	10^{-5} sec^{-1}
	Radius of cross section	$\overline{R}$	A	890	1,000	1,150	1,140	1,050	km
			C	450	490	600	510	510	km
	Separation of vortices	D		1,220	1,100	1,120	1,080	1,130	km
	Latitude of inertia centre	$\overline{\varphi}$		59.7	54.8	53.6	53.4	55.8	°N
	Absolute vortex strength	$\overline{I}_a$	A	16.8	21.6	27.9	28.5	23.7	10^7 m^{2}sec^{-1}
			C	12.6	14.2	21.1	15.1	15.7	10^7m^2 sec^{-1}
	Relative vorticity	$\overline{\zeta}$	C	7.9	7.5	7.7	6.4	7.4	10^{-5} sec^{-1}
	Relative vortex strength	$\overline{I}$	C	5.0	5.6	8.7	5.2	6.1	10^7m^2 sec^{-1}
Quantities determining motion of vortices, computed from theoretical relationships	Abs. ang. vel. of revolution	ω_a★		3.2	4.7	6.2	5.8	5.0	10^{-5} sec^{-1}
	Rel. ang. vel. of revolution	ω★		— 3.1 (— 3.4)	— 1.3 (— 1.6)	+ 0.4 (— 0.1)	0.0 (— 0.4)	— 1.0 — 1.4	10^{-5} sec^{-1} 10^{-5} sec^{-1}
	Period of revolution	τ★		2.0 (1.9)	4.6 (3.7)	14.7 (59)	— (14.6)		pendulum days
	Linear vel. of cells in reduced paths (see Fig. 6)	V★	A	24.8 (27.2)	6.6 (8.2)	(— 2.2) (0.5)	0.0 (3.2)		m sec^{-1} m sec^{-1}
			C	13.6 (15.0)	7.3 (9.0)	(— 2.5) (0.6)	0.0 (1.2)		m sec^{-1} m sec^{-1}
Quantities signifying observed motion of pressure cells A and C				4—5 Oct.	5—6 Oct.	6—7 Oct.			
	Rel. ang. vel. of revolution	ω★		— 1.9	— 1.5	— 2.3		— 1.9	10^{-5} sec^{-1}
	Period of revolution	τ★		3.2	3.9	3.0		3.4	pendulum days
	Linear vel. of cells in reduced (true)paths	V★	A	12.4 (7.5)	8.2 (7.9)	13.1 (13.3)		11.2 (9.6)	m sec^{-1} m sec^{-1}
			C	9.3 (15.6)	8.7 (9.4)	11.5 (11.7)		10.2 (12.2)	m sec^{-1} m sec^{-1}

of the vortices be constant is comparatively well established on the basis of the pressure centres between the 5th and the 6th only. Regarding the determination of the "barrier", it has been earlier mentioned that this is more realistic on the 5th and 6th than on the other two days, especially the 4th.

Concerning the *basic* assumption, viz. the conservation of absolute vorticity, it may be stated that the constancy of the equivalent vorticity $\overline{Z}$ points to the absence of any larger injections of momentum from without the area bounded by the "barrier". This conclusion is valid only to the extent to which that area remains fixed in size during the period in question. Actually it increases in size from the 4th to the 6th, whereafter it decreases markedly. Summarising these inferences regarding the preference given to the results obtained for 5 Oct., it is seen that on this date the subsidiary requirements of the theory are more nearly satisfied whereas no definite conclusions can be drawn with respect to the basic requirement.

It is however possible to obtain an idea of the presence of horizontal mass divergence from a consideration of the system's *baroclinity*. As far as the low-pressure area is concerned the available data suffice for a threedimensional treatment.

For each day two perpendicular cross sections have been drawn. These run very nearly through the centre of the cell C_3. They are simultaneously represented in the perspectively drawn cross section diagram, fig. 8 a, giving the position of the contours of the isentropes 293° and 313° K (potential temperature) in two perpendicular, vertical planes. Fig. 8 b gives the potential temperatures at standard isobaric surfaces used in the construction of the complex cross section. (Characteristic points provided by the radio soundings and weather flights have also been used.[1])

The slope of the isentropes with respect to the isobaric surfaces gives an indication of the vertical shear and thus of the change of the cyclonic field with height. The tangent of the slope of these two sets of surfaces, m_Θ and m_p are related to each other by the equation

$$m_\Theta = m_p + fA/S \qquad (11)$$

where, as before, f is the Coriolis parameter, S the static stability and A the vertical shear of the (geostrophic) wind. Since in the present case, as in most instances, m_Θ is of higher order of magnitude than m_p, the value of m_Θ is directly proportional to the shear. (The variations in f and S from one day to the next are in the present case sufficiently small so that we may simply write $A = m_\Theta \cdot \text{constant}$.)

The cross sections show that over the larger part and especially in the central portions of the depression, the isentropes are *descending* between the 4th and 5th, which indicates *subsiding* motion in the middle and upper troposphere whence, by virtue of the continuity equation, the horizontal divergence is there positive. The divergence concurs with a decrease in the (vertical) baroclinity as a result of which the contour gradient at the 500 mb level has decreased. A simultaneous weakening of the gradient in the cyclonic field at M. S. L. (not reproduced here) contributes also a little to that decrease. Between the 5th and 6th a *lifting* of the isentropic surfaces, associated with an increase of baroclinity, takes place. It is more marked in the middle troposphere as indicated by the changes of the 313° K isentrope. The strong local downward bulge of this isentrope in the section 44.7° N, 17.5° W to 54.9° N, 21.8° W is due to the high potential temperatures recorded at 58.3° N, 18.0° W — see Fig. 8 b. It could not be ascertained whether the data are faulty or whether the phenomenon is real. There is also a lowering of the 313° K isentropic surface in the right forward part of the cross section, but the ascent on 5 Oct. in this part (Penzance) falls actually outside the cyclonic system C_3. Over the central parts of the cross section both isentropes have anyhow ascended between the 5th and 6th. During the following 24 hours the height of the lower of these surfaces has hardly changed whilst the upper one continued its ascent, at an even increased rate. The baroclinity has also further increased, although this increase does not show up as an increase of the cyclonic circula-

[1] Fortunately, starting or terminal points of weather reconnaissance flights on 6 and 7 Oct. 1945 were situated very close to the cold core of the depression which could be ascertained from intermediate temperature data for 50 km distance apart, between start and terminal (ascent and descent of aircraft).

tion at the 500 mb level because by 7 Oct. the cyclonic circulation at M. S. L. has almost vanished.

It is seen that the interdiurnal height variations of the isentropic surfaces in the low and middle-troposheric layer of the depression change sign on the 5th, so that it may be assumed that during the hours preceeding and following 03:00 GMT on this day they undergo little height variation. Taking the corresponding variations of potential temperature (indicated by the observed height variation of the Θ-surfaces discussed above) to be chiefly produced by vertical motion, the following conclusions are permissible: *marked horizontal divergence* has ocurred in the middle troposphere during the first part of the 24 hours following 03:00 GMT, 4 Oct., coinciding with the most rapid *southward* displacement of the cell C_3 as well as of the "vortex pair" as a whole; *convergence* has set in some time after 03:00 GMT, 5 Oct. and has been rather strong between the 6th and 7th when the *northward* motion of the cyclone occurred; and the amounts of convergence or divergence have been very small at the 500 mb level at 03:00 GMT, 5 Oct. or near to this time.

The above results, obtained by a qualitative analysis of the temperature field of the cyclonic cell, have thus provided the additional evidence required for ascribing some measure of significance to the agreement between the observed and computed values of $\omega^\star$ for 5 October 1945.

In conclusion a few remarks on the genesis of the cyclonic cell C_3 are indicated. Certain structural and thermal properties of the "vortex pair", as observed on 4 Oct., suggest that the primary factor in the formation of the low-pressure area was the existence of an anticyclonically rotating cold core to the northwest of the trough t_3 on 3 Oct., since on the following day one can discern a shallow layer of cold air under the cyclone, indicated by the very low values of potential temperature at the 1,000 mb and 950 mb (750 m) levels in the ascent at Meeksfield on the 4 Oct. (see Fig. 8 b, left upper part of cross section). This sounding also gives extremely relative humidities (about 10%) between 950 and 750 mb suggesting that the air below an inversion at 750 mb, is part of a cold dome having undergone strong subsidence and spreading out.

Attention is drawn to two further points believed to be characteristic of the early stages in the life-history of the "vortex pair". The first point concerns the shape of the depression; as earlier mentioned, the low-pressure area has a moon-shaped configuration as the charts for 4 and 5 Oct. show clearly. The second point concerns the displacement of the system as a whole. The southward displacement is rapid between the 4th and 5th, but a closer study of the intermediate charts (M.S.L. and upper air) shows that between 3 and 4 Oct., 18:00 GMT this displacement is also accelerated.

The properties of the vortex pair in its early stages thus bear a distinct relation to the theoretical model of a *composite vortex* given by Rossby in the earlier cited paper (1949): the creation of a moonshaped low-pressure area to the east of the high pressure area is essentially the result of a deformation of the streamlines pertaining to an initially anticyclonic circular vortex with vertical axis, under the influence of an uniformly accelerated movement equatorward; this displacement in turn arising from the action of the force F_y which has been discussed briefly in § 2. The model of the composite vortex is reproduced in Fig. 9. It is to be noted that the theory for the creation of a complex vortex in this manner is based on the same fundamental assumptions as those used earlier in this paper and on the additional requirement that the total kinetic energy remains constant.

As to the aspects of the (two-dimensional) theory in application to a baroclinic anticyclone, Rossby has given an example which was analysed by C. C. Koo (see also Koo, 1950). This shows such a complex vortex over the Western United States, the depression at M.S.L. having the typical shape, a sinking of the cold core of the anticyclone and an increasing separation with time of the high-pressure center at the ground from the center of the cold core aloft. As to our system A_3, C_3 the data reveal that on 4 Oct. there is a considerable tilt westward of the axis of the cell C_3 between M.S.L. and the 500 mb level, although this tilt is not indicated by the distribution of temperature at the 500 mb level. In the later stages it is not possible to discern much resemblance with the composite vortex model, as the system $A_3\,C_3$ consists then

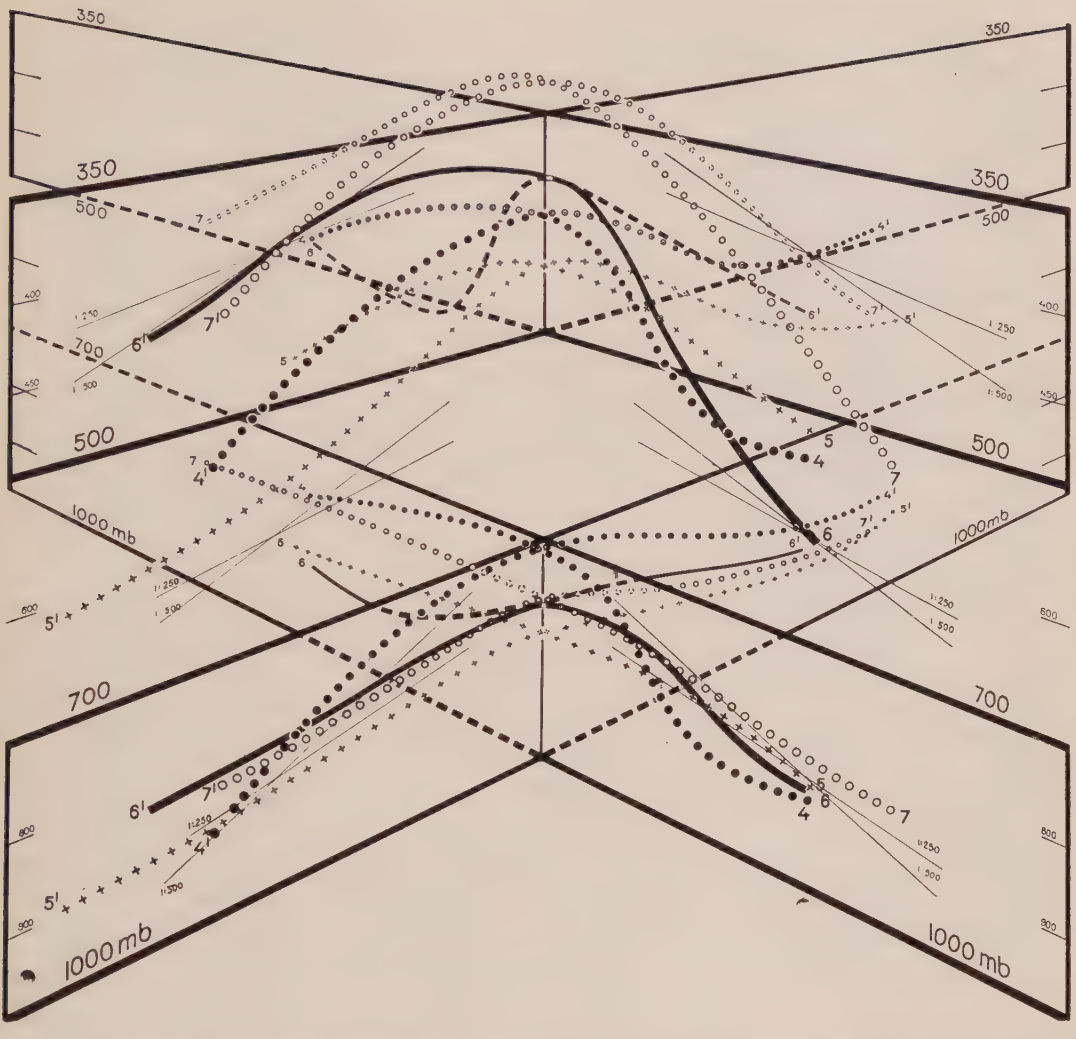

Fig. 8 a. Composite cross section showing the distribution of potential temperature through two selected isopleths, viz. the isentropes 293° K and 313° K, in the region of the cyclone C_3. Two perpendicular cross sections, intersecting in the vertical plane passing through the cold core of the depression, are shown in perspective. Numbers at the isentropes are calendar days. To facilitate in reading the diagram, the portions of the isentropes passing behind the vertical sheets 1,000—700 mbs and 500—350 mbs (which should be thought of as material walls) are indicated by primed numbers. The thin straight lines give the slopes of the isentropic with respect to the isobaric surfaces.

essentially of a cold cyclone and a warm anticyclone whose axes above some low level are quasi-vertical.

It is, however, indicated to draw attention to a further point bearing on the theory of composite vortices. Rossby points out that the continued deepening of the upper cyclone (verified in the present case by the high value of the vortex strength on the 6 Oct., see table I) would finally result in a vanishing of the Force F_y which drives the composite system southward. "*After surface friction had had a chance to reduce still further the anticyclonic circulation near the ground, the resultant force may ultimatively become positive, so that the composite vortex, or at least its upper cyclonic part, finally returns slowly to higher latitudes. It is difficult to analyse this*

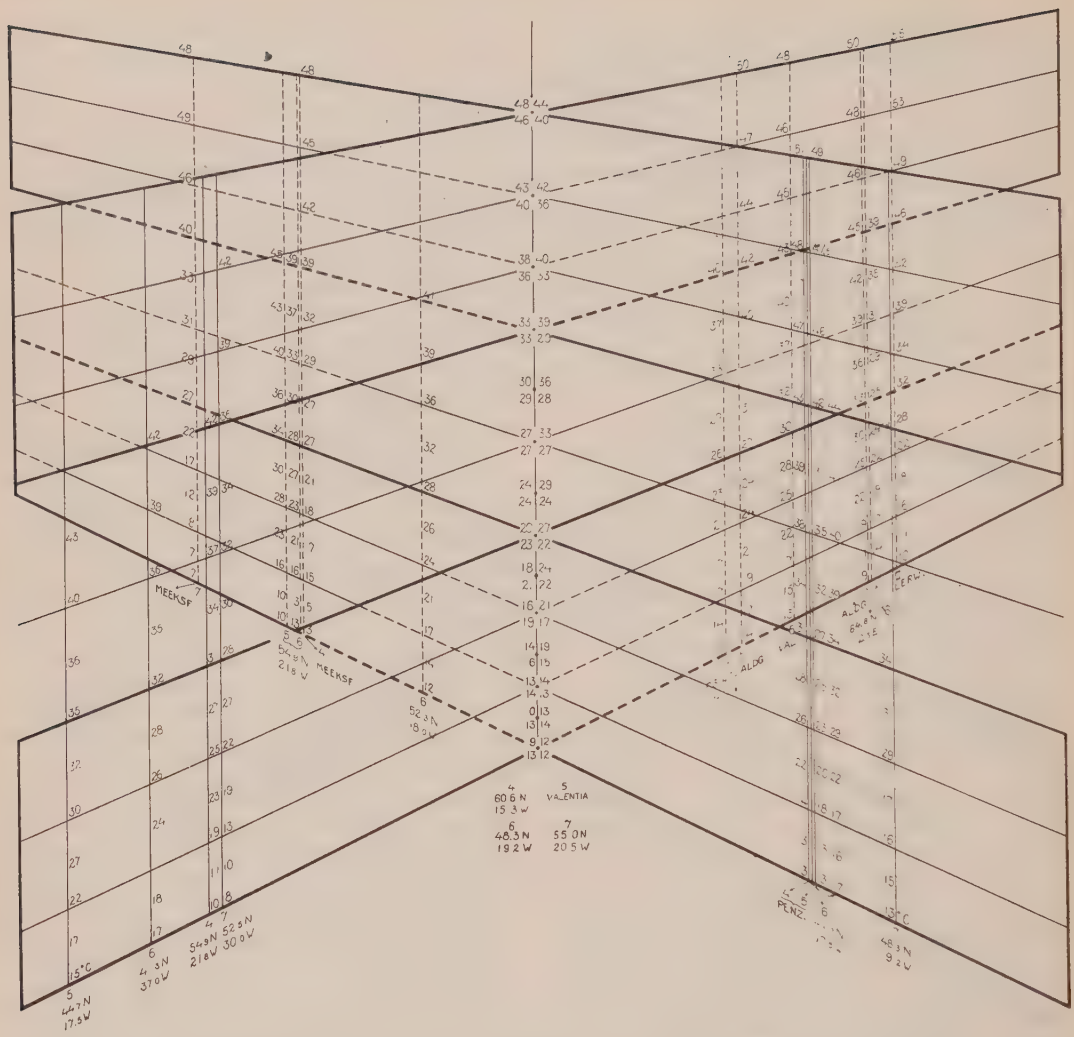

Fig. 8 b. Cross sections as in fig. 8 a. Vertical lines give the position of radiosonde or reconnaissance aircraft soundings, projected onto the corresponding cross section; numbers denote potential temperature at standard pressure.

behaviour of composite vortices quantitatively since it appears almost impossible to determine the extent to which the upper cyclonic vortex participates in the gradual displacement of the entire composite vortex, but it is evident that cold anticyclonic domes in their displacement southward must reach an equilibrium latitude at which the force F_y vanishes." Evidently, the model of a composite vortex makes no proviso for the genesis of a countercell to the upper cyclonic vortex, viz. an upper warm anticyclone. In the present case both these vortices had been generated almost simultaneously, as we have seen earlier, but it is the cyclonic circulation at the ground which was gradually reduced in the course of the rotary motion of the upper vortices; the anticyclonic base of the cold dome near Iceland collapsed almost at once during the first 24 hours. It appears from the study of this particular case that irrespective of the southward drift of the entire system (measured by the drift of the inertia centre, see Fig. 5), the motion of its cells and thus in particular the motion of the upper cyclone can only be

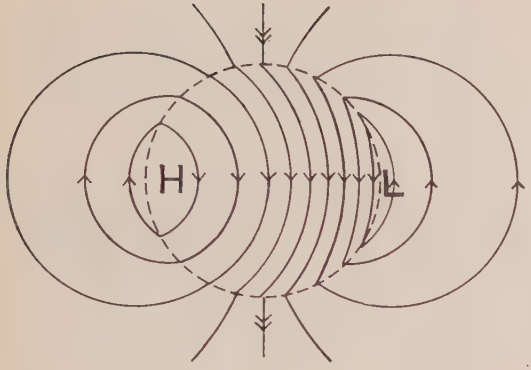

Fig. 9. Composite streamlines in the horizontal plane inside and outside an anticyclonically rotating, solid vertical vortex which is undergoing a uniformly accelerated motion southward. The ratio of the translational velocity to the peripheral tangential velocity of the vortex is assumed to be equal unity. (From C.-G. Rossby, 1949.)

understood as an *interaction between vortices possessing a circulation (cyclic irrotational motion) in their environment.* It must be assumed that this circulation has been communicated to the environment rather rapidly, but in a manner which cannot be easily explained. It is possible that lateral friction is largely responsible for this process.

In this study no mention has so far been made of the possible effects of heat transfer and of the transfer of momentum or vorticity in the vertical. In the particular case analyzed, they must be of a secondary nature because the circulation cells (vortices) are conserved in rather deep atmospheric layers for a number of days. If such transfers were of importance, the assumption of the quasi-constant absolute vorticity of individual vortex filaments underlying our theory would be entirely wrong, and the vorticity $\bar{Z}$ would show large variations. No such changes were observed. As to the vortex strength I_a, its variation may be associated partly with horizontal divergence, partly with a limited interaction between the masses inside and outside the "barrier" (dotted curve on Fig. 4). To support this conclusion it should be mentioned that between 7 and 8 Oct. the cyclonic cell has entirely disappeared from the 500 mb chart, suggesting that after the 7th heat and momentum transfer processes may have had a dominating effect. The cyclonic vortex still exists on the 8th in the uppermost troposphere, which can be ascertained from a detailed analysis of the 300 mb chart and other data; remnants of this vortex are found at this level to the north of Scotland. Simultaneously the anticyclone has moved considerably to the eastward; it seems that the entire system has undergone a translation eastward with the result that for the first time since the initial day (3 Oct.), a zonal flow is established over Northwestern Europe.

Postscript. It is frequently observed on the surface weather map that two cyclonic systems as e. g. a central low, usually in the stage of filling, and a secondary mostly in the stage of deepening, have a tendency to rotate around each other in cyclonic paths or just in an opposite manner to the motion observed in the October 1945 case. However, in such situations one of the vortices only, i. e. the central low extends at least to the upper part of the troposphere. The system as a whole is markedly baroclinic and interaction with cold and warm air currents in the environment can hardly be ruled out.

Acknowledgment

I am indebted to Prof. C.-G. Rossby for many helpful suggestions in formulating the theoretical parts of this paper. Thanks are also due to Mr D. Dutina for assisting in the preparation of the charts and cross sections.

REFERENCES

Berson, F. A., 1939: Über die Beziehung der ageostrophischen Windkomponente zum Isallobarenfeld. *Met. Z.*, **56**, 9, pp. 329—333.

— 1950: On the factors controlling the instability of long waves in zonal currents. *Arkiv f. Geof., K. Vetenskapsakad.*, **1**, 9 Stockholm. (See also Summary, 1949, *Tellus*, **1**, 4, pp. 44—52.)

Bjerknes, J. and Holmboe, J., 1944: On the Theory of Cyclones, *J. Met.* **1**, pp. 1—22.

Blaton, J., 1938: Zur Kinematik und Dynamik nicht-stationärer Luftströmungen. *Bull. Soc. Geophys.*, Varsovie.

Charney, J., 1947: The dynamics of long waves in a baroclinic westerly current. *J. Met.*, **4**, pp. 135—162.

Davies, T. V., 1948: Rotary flow on the surface of the

earth. — Part I. Cyclostrophic motion. *Phil. Mag.*, **39**, 6, pp. 482—492.

HELMHOLTZ, H., 1858: Über die Integrale der hydrodynamischen Gleichungen welche den Wirbelbewegungen entsprechen. *Ges. Abh.*, p. 101, Crelle.

JAMES, R. W., 1950: On the theory of large-scale vortex motion in the atmosphere. *Quart. J., R. Met. Soc.*, **76**, 7, pp. 255—276.

KELVIN, W, 1866: On vortex motion. *Edinb. Trans.*, **25**.

KOO, C. C., 1950: Some aspects of cut-off cyclonic vortices. *J. Chinese Geoph. Soc.*, **2**, 1. Academia Sinica.

KUO, H., 1950: The motion of atmospheric vortices and the general circulation. *J. Met.*, **4**, pp. 247—258.

LAMB, H., 1932: *Hydrodynamics*. 2nd ed. Univ. Press. Cambridge.

PALMÉN, E., 1949: On the origin and structure of high-level cyclones south of the maximum westerlies. *Tellus*, **1**, 1, pp. 22—32.

PETTERSSEN, SVERRE, 1940: *Weather Analysis and Forecasting*, 1st ed. New York and London, p. 225.

PRIESTLEY, C., 1947: Dynamic Control of atmospheric pressure. *Quart. J., R. Met. Soc.*, **73**, pp. 65—84.

ROSSBY, C.-G., 1948: On the displacements and intensity changes of atmospheric vortices. *J. Mar. Res.*, **7**, 175—187.

— 1949: On a mechanism for the release of potential energy in the atmosphere. *J. Met.*, **3**, pp. 163—180.

SCHERHAG, R., 1948: *Neue Methoden der Wetteranalyse und Wetterprognose*, pp. 227—234. Berlin-Göttingen.

Staff Members, Dept. Univ. Chicago, 1947: On the general circulation of the atmosphere in middle latitudes. *Bull. Americ. Met. Soc.*, **28**, pp. 255—280.

WILLIAMS, N. R., 1948: Development of dust whirls and similar small scale vortices. *Bull. Americ. Met. Soc.*, **29**, 3, pp. 95—105.

Some Remarks on the Climatology of Blocking Action

By H. BREZOWSKY, H. FLOHN and P. HESS,
Deutscher Wetterdienst in der US-Zone, Zentralamt Bad Kissingen

(Manuscript received 22 June 1951)

Abstract

Based on the revised Catalogue of European Large-Scale Weather Patterns (1881—1950) the annual course and the secular variations of the frequency of blocking highs in Europe are treated. Regions of blocking action and those of frequent cold-air centers mutually exclude one another, both corresponding to the orographically influenced asymmetry of the polar vortex.

In his recent paper on the effect of blocking action upon regional climate D. F. REX (1950) gives a significant contribution to the problem of dynamic climatology. The following remarks will furnish some supplements based on the Catalogue of European Large-Scale Weather Patterns ("Grosswetterlage") as developed by BAUR (1947) and later revised and extended by HESS and BREZOWSKY (1951). The term "Grosswetterlage" is understood as defining a tropospheric pressure and/or current pattern lasting unchanged in its essential features for a minimum of 3 days, especially in the location of steering centers and frontal zones.

While the mean duration of Atlantic blocking situations as used by REX, a summarization of several large-scale weather patterns in our sense, is 16.6 days, our large-scale weather patterns contain also blocking situations continuing for at least 3 days. The duration of each large-scale weather pattern averages 4.1 days. Thus, the number of cases increases substantially although some non-typical situations, such as quasistationary anticyclonic wedges instead of isolated high centers, are included. With our statistics extending over the 70-year period 1881—1950, we can study in a more comprehensive manner the annual course and the secular variations of the frequency of Atlantic blocking highs.

We group the large-scale weather patterns of our Catalogue as follows, determining the anticyclonic centers from surface charts:

1) *Anticyclonic axis over Northeastern Atlantic* (20° W—10° E): *A*

High Norwegian Sea	HN
High Norwegian Sea and Fennoscandia	HNF
High British Isles	HB
Northerly type	N

2) *Anticyclonic axis over Northern Europe* (10°—50° E): *E*

High Fennoscandia	HF
Northeasterly type	NE
Southeasterly type	SE
Southerly type	S

It is assumed that the mechanism of the blocking action, according to SEILKOPF (1949) and BREZOWSKY (1951), consists of a combined

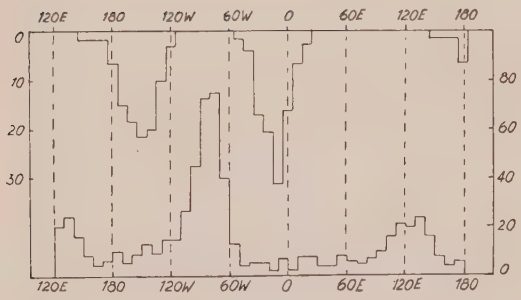

Fig. 1. Upper line; Frequency of blocking highs (according to Rex, 1950). Lower line; Frequency of intense cold-air centers, $\Delta t \geq 8°$ C (according to Flohn 1950 a).

effect, first of the ageostrophic components of a cyclogenesis on the western side of anticyclogenesis and secondly of the convergence between the warm-air current accompanying the cyclogenesis and the polar outbreak already in progress on the eastern side of anticyclogenesis. In typical cases the warm-air current is caused by a polar outbreak in the rear of the cyclogenesis, reaching so far south as to break through the subtropical high zone and to tap the subtropical warm air source.

The restriction of the onset of blocking action to relatively small sectors of the northern hemisphere (Rex 1950) corresponds to a similar restriction of intense tropospheric cold air centers on the intermediate sectors. By drawing a chart of all cold-air centers of 1949 and 1950 (Flohn 1950 a), which in the average for the layer between 500 and 1,000 mb are at least 8° C colder than their surroundings, we can show, their distribution by longitude in comparison with the distribution of blocking highs (see fig. 1). Regions of formation of warm, blocking anticyclones and of the occurrence of intense cold-air centers mutually exclude one another very nearly. If the investigation is restricted to the cold-air centers in latitudes 60° N or more, the mutual exclusion becomes even more distinct. This peculiar regional restriction corresponds closely to the asymmetry of the tropospheric polar vortex of the northern hemisphere. The regions of large upper troughs over eastern America and eastern Asia will encourage the formation of cold-air masses, while the regions of anticyclonic wedges near the western coasts of Europe and America are favoured by blocking highs. In our opinion (Flohn 1950 b) these climatological facts can be explained by theoretical investigations (Charney and Eliassen 1949, Bolin 1950) of the influence of high mountain chains upon the direction of the tropospheric westerlies, especially of the jet stream (planetary frontal zone).

The annual course of blocking action has been derived already by Rex (1950), with maxima in spring (April and May) and minima in late summer (August and September), in both the Atlantic and Pacific cases. Our catalogue permits a classification into two groups,

Fig. 2. Annual course of the frequency of blocking highs over northern Europe (E) and northeastern Atlantic (A), according to Hess and Brezowsky (1951), in percent (1881—1950).

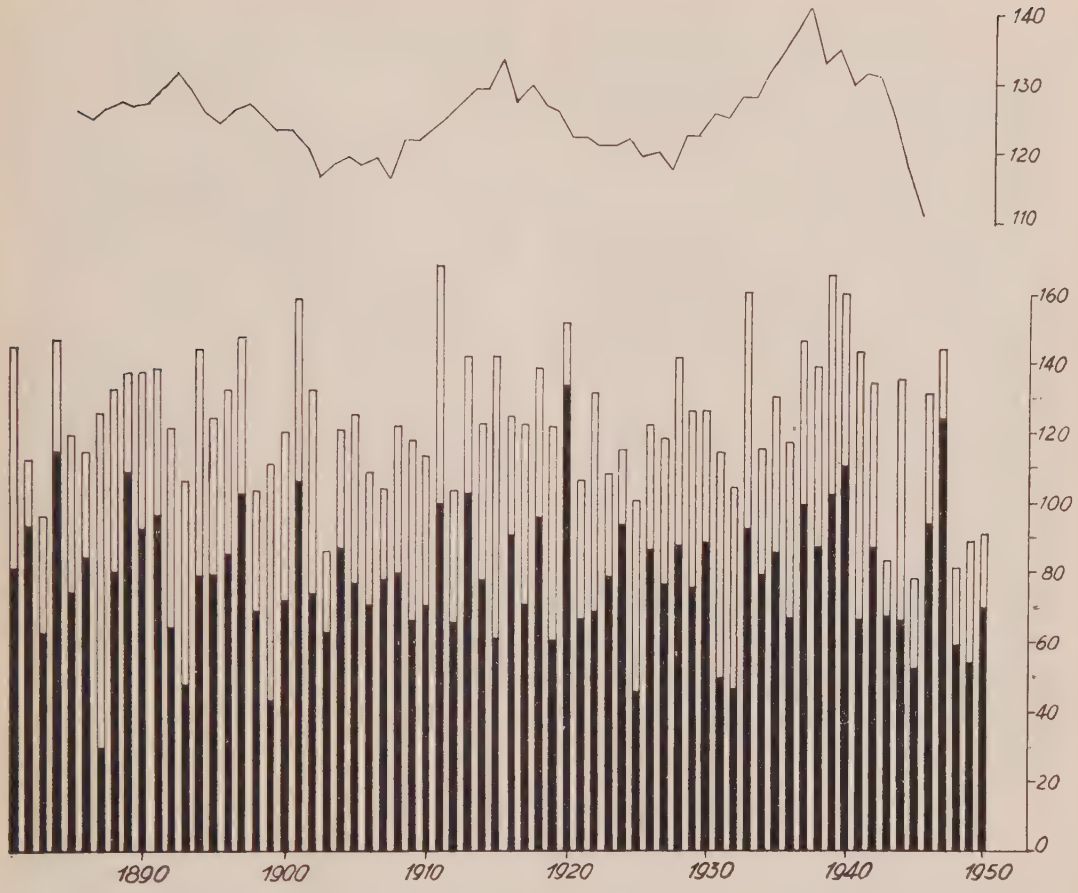

Fig. 3. Annual frequency of blocking highs (E-group black columns, A-group open columns) and overlapping 10-year means (upper line, A + E) in days (1881—1950).

A and E, and thereby an investigation of the influence of land and sea, and also the division of months into six pentades respectively, with the last pentade in February including 3, otherwise 5—6 days.

Fig. 2 shows that the E-group is most frequent from October to May, with weak maxima in the first half of March and in the second half of October, but is rather rare in summer. The anticyclones of the A-group, with centers at sea, are concentrated in the period, middle of April to middle of June, and rarely occur in summer and winter. The sum of both groups (A + E) confirms the annual course as estimated by Rex from the most typical cases during 13 years, with a frequency peak in the beginning of May (52 per cent of all days) and a clearly established minimum during July and August (only 18—26 per cent). A secondary peak is evident in fall, especially from October 21 to 25, and some minor minima from October to December.

The frequency distribution of high, zonal index situations (westerly types) shows a reverse two-fold annual course, with maxima in high summer and early winter, and minima in spring and (only weak) in fall. Obviously this two-fold annual course corresponds to the six-month pressure oscillation, a statistically verified climatological fact studied by Wahl (1941) and others. It has some amplitude maxima in sub-arctic latitudes which are difficult to explain. The remarkable difference

between the annual courses of our groups A and E requires a physical explanation. The spring anticyclones over the Norwegian Sea obviously are associated with the warm polar anticyclones which are most frequent from March to May, partly extending to early June, and also with the low index circulation associated with them.

The frequency of Atlantic blocking highs varies somewhat from year to year (see fig. 3). In the years 1911 (46 %) and 1939 they were most frequent, in 1945 (21 %) most rare. Confining our attention to each single group the relative frequency of A-anticyclones (over sea) varies between 4 % (1943) and 26 % (1887); that of E-anticyclones (over the continent) between 8 % (1887) and 36 % (1920). The high frequency of blocking highs in the three years 1939—41 (A + E 43 per cent in the average) is most remarkable, just as is the striking decrease during the last three years (1948—50, in the average 24 per cent), during which period zonal index situations were predominant. The repeated revision during the last ten years of the aforementioned Catalogue will serve as a guarantee of the reliability of these data.

If one arranges the annual frequencies of blocking highs in accordance with the sun-spot maxima or minima, we obtain at best a small peak coinciding with the sun-spot minima (such as in 1889, 1901, 1913, 1933 and 1944), which cannot be verified statistically. Any influence of solar activity is weak and uncertain, as is also confirmed by WEXLER (1950) in his investigation of hemispheric pressure charts 1899—1939.

Overlapping 10-year averages (see fig. 3, upper part) show no secular trend, but a remarkable periodicity with maxima in 1892, 1915 and 1937, and minima about 1902 (or 1907), 1927 and in the last years, apparently pointing to a 22—23 year oscillation. Whether we are dealing with an effect of the solar activity period, the length of which is really about 23 years due to the alternating magnetic polarization of sun-spots (HALE), can only be disclosed through further investigations. The maxima of the above mentioned 22—23 year oscillation are situated close to the sun-spot maxima of 1893, 1917 and 1937.

REFERENCES

BAUR, F., 1947: *Musterbeispiele europäischer Grosswetterlagen.* Wiesbaden, Dieterich, 35 pp.

BOLIN, B., 1950: On the influence of the earth's orography on the general character of the westerlies. *Tellus*, **2**, 3, 184—195.

BREZOWSKY, H., 1951: Synoptische Methoden zur Vorhersage von Umsteuerungen im europäisch-atlantischen Raum. *Ann. Meteor.*, **4** (in press).

CHARNEY, J. G., ELIASSEN, A., 1949: A numeral method for predicting the perturbations of the middle latitudes. *Tellus*, **1**, 2.38—54.

FLOHN, H., 1950 a: Kaltluftzentren und Höhentröge. "*Grosswetterlagen Mitteleuropas*", **3**, 102—104.

— 1950 b: Studien zur allgemeinen Zirkulation der Atmosphäre. *Ber. Dt. Wetterdienst US-Zone*, **18**.

HESS, P., and BREZOWSKY, H., 1951: Katalog der Grosswetterlagen Europas. *Ber. Dt. Wetterdienst US-Zone* (in press).

REX, D. F., 1950: Blocking action in the middle troposphere and its effect upon regional climate. II. The climatology of blocking action. *Tellus*, **2**, 4, 275—301.

SEILKOPF, H., 1948: Spezielle Grosszirkulation und Witterung. *Ann. Meteor.*, **1**, 312—326.

WAHL, E., 1941: Untersuchungen über den jährlichen Luftdruckgang. *Meteor. Z.*, **58**, 313—330, cf. loc. cit. p. 349—357.

WEXLER, H., 1950: Possible effects of ozonosphere heating on sealevel pressure. *J. Meteor.*, **7**, 370—381.

The Geostrophic Poleward Flux of Angular Momentum in the Month of January 1949[1]

By YALE MINTZ, University of California

(Manuscript received 7 August 1951)

Abstract

From sea level, 700, 500, 300 and 200 mb daily synoptic charts over the whole of the northern hemisphere and 100 mb charts over three fourths of the hemisphere, the mean geostrophic poleward flux of angular momentum is computed for January 1949. A northward total flux is found in all latitudes, with the maximum at latitude 32 1/2° N of 5.4×10^{16} t m² s^{-2}. Four fifths of this flux occurs between the 500 and 100 mb levels. From the meridional convergence of the flux, the mean zonal surface stress is computed. The sign of this derived stress is found to be in good agreement with the distribution of the surface zonal wind: its average magnitude, in the region of the surface westerlies, is 1.2 dynes cm^{-2}.

1. Introduction

The total poleward flux of angular momentum across the vertical surface σ_φ, at the latitude φ, can be expressed as the sum of terms, one of which is the mean geostrophic poleward flux of geostrophic angular momentum,

$$\bar{J} = \int_{\sigma_\varphi} r \overline{\varrho u_g v_g}\, \delta\sigma_\varphi \qquad (1)$$

where r is the distance from the earth's axis of rotation, ϱ density, u_g and v_g the zonal and meridional components of the geostrophic wind, $\delta\sigma_\varphi$ element of vertical surface in latitude φ, and the superior bar denotes the mean of $(\varrho u_g v_g)$ taken with respect to time. That this term is one of the most important, if not the most important, in the total poleward flux of angular momentum will be shown in section 4.

Utilizing the hydrostatic relation, to a close approximation equation (1) can be written

$$\bar{J} = -\int_{\tilde{p}_0}^{0} \delta p \frac{r^2}{g} \int_0^{2\pi} \overline{u_g v_g}\, \delta\lambda \qquad (2)$$

where g is the acceleration of gravity, $\delta\lambda$ element of longitude, δp element of pressure, and $\tilde{\bar{p}}_0$ is sea level pressure averaged with respect to time and longitude. In equation (2)

$$\frac{r^2}{g} \int_0^{2\pi} \overline{u_g v_g}\, \delta\lambda = \bar{j} \qquad (3)$$

is the mean geostrophic poleward flux of angular momentum per unit vertical pressure increment. $\bar{j}$ is easily evaluated, for any pressure p, from daily circumpolar synoptic charts.

2. Computation of the momentum flux and its convergence, per cb layer

For the month of January 1949, $\bar{j}$ was evaluated from daily charts of the 700, 500, 300

[1] U. C. L. A. Department of Meteorology, Papers in Meteorology, No. 13. The research resulting in this work has been sponsored in part by the Geophysical Research Directorate of the Air Force Cambridge Research Laboratories.

200 and 100 mb isobaric surfaces over the northern hemisphere. The sea level and 500 mb charts used were the Northern Hemisphere Historical Weather Maps, Sea Level and 500 Millibar, published by the Headquarters, Air Weather Service. The 700 mb charts used were the Northern Hemisphere 700 Millibar Charts, analyzed by the Extended Forecast Section of the U. S. Weather Bureau, and extended over India. For the 300, 200, and 100 mb levels, daily northern hemisphere charts were analyzed specifically for this investigation. The 300 and 200 mb level maps extended around the whole of the northern hemisphere, and the 100 mb maps covered all except the Asiatic quadrant from 30° E to 120° E. These high level circumpolar synoptic charts were made under the direction of Dr Jakob Bjerknes, with Dr Adam Kochanski as chief analyst. A detailed description of the construction of the maps has been given by KOCHANSKI (1950). In the construction of the maps emphasis was placed on systematically incorporating into the contour height analysis all available upper-air winds (pibals, rabals, and rawins) in accordance with the geostrophic wind relation.

From the upper level maps the contour heights to the nearest 25 feet (and from the sea level maps the pressures to the nearest millibar) were tabulated for every 5° latitude longitude intersection, from latitude 15° to 80° N, for each day of January 1949, and the data entered on IBM punch cards: 180,000 in number. Using the differences between the heights (or pressures) at the adjacent latitude longitude intersections to find u_g and v_g, $\overline{j}$ was computed from the cards by IBM machines. The IBM computations were done under the direction of Dr E. C. Yowell by the Institute for Numerical Analysis (National Bureau of Standards) on the U.C.L.A. campus. To find the geostrophic wind at sea level, mean densities for the latitude circles were used. To obtain the total flux at the 100 mb level, the flux in the missing Asiatic quadrant was estimated by graphical extrapolation of the flux at the lower levels of the same sector. For the pressure surfaces which are intersected by the ground, the integration of $(\overline{u_g v_g})$ in (3) should properly be taken only over those longitudes which lie between the continents and between the mountains. But examination of zonal cross-sections of $(\overline{u_g v_g})$ showed that the error in $\overline{J}$ introduced by computing $\overline{j}$ over all longitudes (through solid earth as well as through the air) is a small one, and the latter procedure, because it could be handled easily by the IBM machines, was therefore used.

The results of the computations of the mean geostrophic poleward flux of angular momentum, per centibar layer, are shown in Table 1 and in fig. 1. The greatest poleward flux of angular momentum takes place at 200 mb and 30° N. The level of maximum flux descends somewhat with increasing latitude, from above 200 mb at 20° N to about 300 mb at 70° N. The latitude of maximum flux decreases with increasing elevation, from 42° N at sea level to 28° N at 100 mb. Everywhere

Table 1

The mean geostrophic poleward flux of angular momentum, per centibar layer, in January 1949.

$$\frac{r^2}{g}\int_0^{2\pi} \overline{u_g v_g}\,\delta\lambda, \text{ in } 10^{14} \text{ t m}^2 \text{ s}^{-2} \text{ cb}^{-1}$$

	75° N	70°	65°	60°	55°	50°	45°	40°	35°	30°	25°	20° N
100 mb	— 0.1	0.0	0.4	1.1	1.6	2.5	3.5	4.5	5.5	7.0	7.0	6.0
200 mb	0.0	0.0	0.6	1.5	2.7	5.0	7.5	10.4	13.6	15.2	13.5	9.0
300 mb	0.0	0.1	0.7	1.9	3.6	6.2	8.8	10.8	13.1	13.7	10.3	4.8
500 mb	0.0	0.0	0.2	0.7	1.9	3.3	4.5	5.5	5.6	4.7	3.3	1.8
700 mb	0.1	0.1	0.0	0.2	0.6	1.0	1.4	1.9	2.4	2.0	1.5	1.1
Sea level	0.2	0.3	0.4	0.5	0.6	0.7	0.7	0.7	0.5	0.3	0.5	1.0

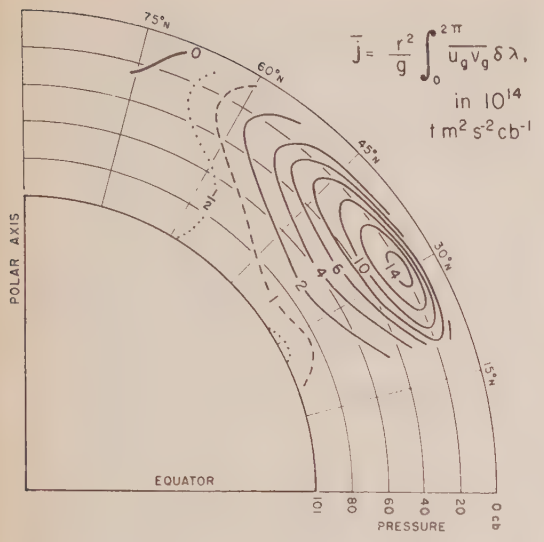

Fig. 1. The mean geostrophic poleward flux of angular momentum, per centibar layer, in January, 1949.

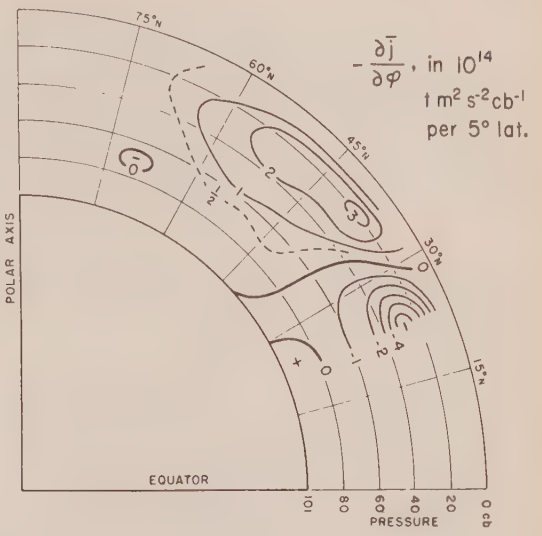

Fig. 2. Meridional convergence of the geostrophic poleward flux of angular momentum, per cb layer, in January, 1949.

within the region of the analysis the flux is toward the pole, except for very small negative transports in the highest levels at 75° N.

The meridional convergence of the geostrophic flux of angular momentum, per centibar layer, is shown in fig. 2. In the tropical and subtropical part of the atmosphere there is divergence of the flux, in the middle and higher latitudes convergence. The line of zero convergence, which is the axis of maximum flux, slopes equatorward with increasing elevation.

Fig. 3 shows the mean geostrophic zonal wind averaged over all longitudes, $\tilde{\bar{u}}$, in January 1949. From a comparison of figs. 2 and 3, it is seen that in the middle and higher latitudes there is convergence of $\bar{j}$ where the winds are westerly; but that in the sub-tropical latitudes there is strong divergence of $\bar{j}$ in a region of strong westerlies. Obviously, in this sub-tropical region the geostrophic poleward angular momentum flux is acting to diminish the westerly wind, $\tilde{u}$. Here, $\tilde{u}$ must be maintained by some other mechanism; either by convergence of the non-geostrophic terms in the total poleward angular momentum flux, or by convergence of the vertical momentum flux within the atmosphere, or by both. Which mechanism is the important one in this region cannot now be determined. In order to have convergence of the vertical momentum flux in this region, continuity considerations require that the flux itself be directed upward against the vertical gradient of $\tilde{u}$. Synoptic studies in

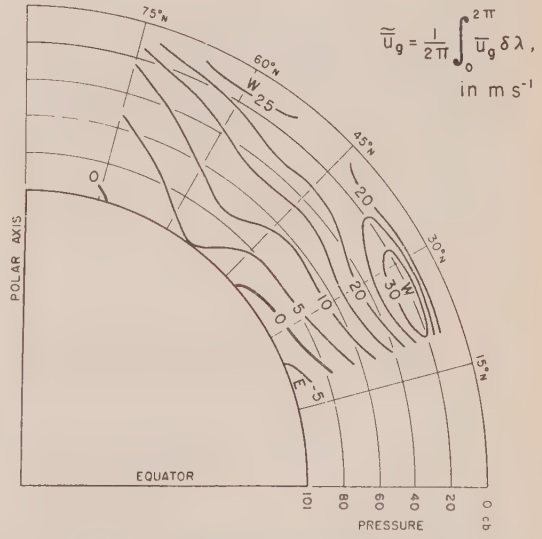

Fig. 3. The geostrophic zonal wind averaged for the month and for all longitudes, in January, 1949.

fact show[2] that the individual anticyclonic cells in this region have general ascending motion in their western parts, where u is large, and descending motion in their eastern parts, where u is small or negative, thereby producing an upward momentum flux opposite in direction to the gradient of $\bar{u}$. But the magnitude of this flux is still unknown.

3. The total momentum flux, and its convergence, from sea level to 10 cb

To find the total geostrophic angular momentum flux, $\bar{J}$, across the entire vertical surface at the latitude φ, the flux per unit isobaric layer must be integrated to the top of the atmosphere, where p approaches zero. The practical upper limit, however, was 10 cb, so that only the flux in the lowest 90 % of the mass of the atmosphere was computed. The total poleward flux in this layer, $\bar{J}_{(101-10\ cb)}$, was found from $\bar{j}$ by graphical integration with the results shown in fig. 4.

The total flux, $\bar{J}_{(101-10\ cb)}$, is positive at all latitudes. The maximum flux is at latitude 32 1/2° N and equal to 5.4×10^{16} t m² s⁻². As may be seen in fig. 1, 80 % of this maximum flux occurs between the 50 and 10 cb levels.

From $\tilde{\bar{u}}$ we find that, in the mean for January 1949, the total relative angular momentum in the atmosphere north of latitude 32 1/2°, from 101 to 10 cb, was 5.1×10^{22} t m² s⁻¹. A constant poleward angular momentum flux across latitude 32 1/2° of 5.4×10^{16} t m² s⁻² would therefore suffice to bring the atmosphere

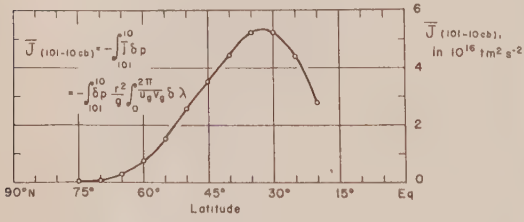

Fig. 4. The total geostrophic poleward flux of angular momentum, from 101 to 10 cb, in January, 1949.

[2] From work in progress on the three-dimensional structure of the North Pacific Anticyclone, Sub-tropical Meteorology Project, Department of Meteorology, University of California, Los Angeles.

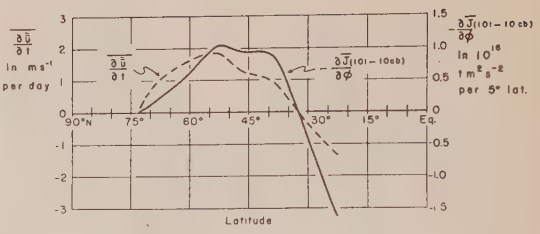

Fig. 5. Convergence of the total geostrophic poleward flux of angular momentum, in t m² s⁻² per 5° latitude, and in m s⁻¹ per day change of zonal wind speed between 101 and 10 cb, in January, 1949.

from a state of rest to the state of zonal flow shown in fig. 3 in 9.4×10^5 seconds, or 11 days.

Integration of $-\frac{\partial \bar{j}}{\partial \varphi}$ from 101 to 10 cb, or differentiation of $\bar{J}_{(101-10\ cb)}$ with respect to latitude, yields $-\frac{\partial \bar{J}_{(101-10\ cb)}}{\partial \varphi}$, the meridional convergence of the total flux, as shown by the solid curve in fig. 5. The maximum total flux convergence is at latitude 52° N and is equal to 1.0×10^{16} t m² s⁻² per 5° latitude. The total flux convergence is zero at 32 1/2° N and approaches zero near 75° N. South of 32 1/2° N there is flux divergence.

Dividing $-\frac{\partial \bar{J}_{(101-10\ cb)}}{\partial \varphi}$ by the mass of air in each latitude ring from 101 to 10 cb and by the moment, r, enables one to express the flux convergence in terms of its influence on the zonal wind speed. This is shown by the broken curve in fig. 5, where $\tilde{u}$ is the instantaneous zonal wind averaged over all longitudes and over pressure from 101 to 10 cb (the 101—10 cb weighted zonal index). The maximum convergence of the geostrophic angular momentum flux, thus expressed in terms of its effect on $\tilde{u}$, is 1.9 m s⁻¹ per day, at 53° N. It should be emphasized that fig. 5 shows the flux convergence averaged for an entire month. At any given time there may be large deviations from the monthly average. The day to day variation of the flux convergence, and its correlation with the observed day to day change of weighted zonal index, is being investigated and will be reported upon at a later time.

4. Computation of the mean surface stress from the geostrophic angular momentum flux

Neglecting the non-geostrophic terms in the total poleward flux of angular momentum, the zonal stress of the atmosphere on the earth, averaged with time and over all longitudes, is

$$\bar{\tilde{\tau}}_{x,s} = -\frac{1}{2\pi r^2 \delta}\left(\frac{\partial \bar{J}}{\partial \varphi} + \frac{\overline{\partial M}}{\partial t}\right) \qquad (4)$$

where M is the angular momentum per unit latitude ring, and δ is length of unit latitude. Taking $\frac{\partial \bar{J}_{(101-10\ cb)}}{\partial \varphi}$ from section 3 above, and $\frac{\overline{\partial M}_{(101-10\ cb)}}{\partial t}$ from the change of $\bar{\tilde{u}}_g$ between the first and last day of the month, $\bar{\tilde{\tau}}_{x,s}$ was computed for January 1949. (The change of both relative and absolute angular momentum due to net change of mass was very small and was neglected). The results of the computation are shown by the broken curve in fig. 6.

The fact that in this particular month, January 1949, $\frac{\overline{\partial M}_{(101-10\ cb)}}{\partial t}$ was negative between latitudes 35° and 52° N and positive south of 35° N was fortuitous. At 40° N, for example, $\tilde{u}$ was 5 1/2 m s^{-1} smaller on January 31 than on January 1, 1949. But if this calendar month had begun a few days earlier or later, $\frac{\overline{\partial M}_{(101-10\ cb)}}{\partial t}$ might have been reduced to zero or changed in sign. In any event, $\frac{\overline{\partial M}}{\partial t}$ will approach zero as the time over which the mean is taken increases continuously without limit.

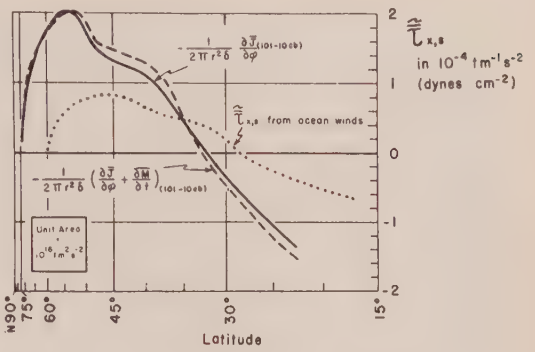

Fig. 6. The mean zonal stress of the atmosphere on the earth.

The solid and broken curves are computed from the convergence of the geostrophic poleward angular momentum flux and the momentum change of the atmosphere in January 1949.

The dotted curve is the mean stress estimated directly from the surface winds over the Atlantic and Pacific Oceans, January Normal (Priestley, 1951).

Arna in the figure is proportional to total torque on earth. Unit area equals 10^{16} t m^2 s^{-2} when $\bar{\tilde{\tau}}_{x,s}$ is the mean stress over all longitudes.

The mean surface stress in January 1949, from (4), if we assume $\frac{\overline{\partial M}}{\partial t} = 0$ and $\bar{J} = \bar{J}_{(101-10\ cb)}$, is shown in Table 2 and by the solid curve in fig. 6. (In fig. 6, $\bar{\tilde{\tau}}_{x,s}$ is plotted against $\int_0^{\varphi} \cos^2\varphi\, \delta\varphi$, so that between any two latitudes the area under the curve is proportional to the torque of the atmosphere on the earth. By construction, then, the area under the solid curve from 32 1/2° to 90° N equals the value of $\bar{J}_{(101-10\ cb)}$ at 32 1/2° N, or a torque of 5.4×10^{16} t m^2 s^{-2}).

Between 32 1/2° N and 75° N $\bar{\tilde{\tau}}_{x,s}$ was positive, with the average value of the westerly

Table 2

The mean zonal stress of the atmosphere on the earth, computed from the geostrophic poleward flux of angular momentum, in January 1949

$$-\frac{1}{2\pi r^2 \delta}\frac{\partial \bar{J}_{(101-10\ cb)}}{\partial \varphi}, \text{ in } 10^{-4} \text{ t m}^{-1} \text{ s}^{-2} \text{ (or dynes cm}^{-2}\text{)}$$

Latitude	72 1/2°	67 1/2°	62 1/2°	57 1/2°	52 1/2°	47 1/2°	42 1/2°	37 1/2°	32 1/2°	27 1/2°	22 1/2° N
Stress	0.1	1.1	1.6	1.9	2.0	1.5	1.2	0.9	0.0	— 0.7	— 1.4

stress of atmosphere on earth equal to 1.2×10^{-4} t m^{-1} s^{-2} (1.2 dynes cm^{-2}). The maximum $\bar{\tilde{\tau}}_{x,s}$ 2.0×10^{-1} t m^{-1} s^{-2}, was at 53° N; which was unexpectedly far to the north as the mean sea level and lower level tropospheric winds for all Januaries have their westerly maxima between latitudes 35° and 40° N (MINTZ and DEAN, 1951, fig. 47). But subsequent examination of the zonal winds of January 1949 showed that this was in fact an unusual month. Fig. 3 shows that the sea level and lower tropospheric zonal winds, in this particular month, did indeed have their maxima near latitude 53°. The fact that in January 1949 $\bar{\tilde{\tau}}_{x,s}$ was zero near 32 1/2° N, whereas the sea level zonal wind was zero near 43° N, is also not inconsistant; as between 32 1/2° and 43° N, where the sea level winds are easterly, many mountains and plateaus extend up as high as 700 and 500 mb into strong westerlies.

The above computed values of $\bar{\tilde{\tau}}_{x,s}$ are about twice as great as the January normal zonal wind stress over the Atlantic and Pacific Oceans as estimated directly from the surface winds by PRIESTLEY (1951), and about one and a half times as great as the normal wind stress on the oceans as estimated by PRITCHARD and SAUR (1948) and COCHRANE and OSBORN (1950). Priestley's values of the normal January zonal wind stress, averaged for the Atlantic and Pacific Oceans, are shown in figure 6 by the dotted curve. The fact that the latitudes of zero and of maximum zonal stress, computed from the momentum flux convergence of January 1949, are displaced some seven to eight degrees to the north of the corresponding features of the normal wind stress on the oceans probably has its explanation, in part, in the unusual character of this particular month, as shown by fig. 3.

Fig. 6 indicates that the geostrophic angular momentum flux convergence is of the same order of magnitude as the torque due to the surface wind stress. For a number of reasons it is not profitable, at this point, to press for a closer comparison than order of magnitude. First, the geostrophic flux in January 1949 may differ from the January normal geostrophic flux. Secondly, in relative magnitude the mean wind stress on the oceans is almost certainly smaller than the mean stress over the whole earth: although over the oceans the zonal surface winds are much stronger than over the continents, over the continents the influence of the large mountain barriers must be taken into account.[1] Thirdly, all direct estimates of the absolute surface stress over land and sea are subject to considerable error. Indeed, one might with equal if not greater reliability assume the geostrophic wind from the outset and from the geostrophic poleward flux of angular momentum deduce what the mean surface stress, and the mean coefficient of surface resistance, must be. But the computed order of magnitude of $\frac{\partial \bar{J}}{\partial \varphi}$, and its relative distribution with latitude, leave no doubt that of the total poleward flux of angular momentum — which maintains the zonal motion of the atmosphere against the torques of surface friction — the geostrophic flux is an important, perhaps the most important, part.

[1] The cumulative zonal pressure drop across the very large scale topographic features of North America is being computed from surface (station level) pressure observations and will be described in a subsequent report.

REFERENCES

COCHRANE, J. D., and OSBORN, P., 1950: The mean wind stress over the Atlantic Ocean. *Oceanographic Report No. 21, Scripps Institution of Oceanography (mimeographed).*

KOCHANSKI, A., 1950: The construction of 300, 200, and 100 mb maps of the northern hemisphere. *Appendix to Report No. 4, Investigation of the general circulation of the atmosphere (mimeographed).*

MINTZ, Y. and DEAN, G., 1951: The observed mean field of motion of the atmosphere. *Part II, Report No. 7, Investigation of the general circulation of the atmosphere.*

PRIESTLEY, C. H. B., 1951: A survey of the stress between the ocean and the atmosphere. *Australian Journ. Sci. Res., Ser. A.* **4**. 3 (in press).

PRITCHARD, D. W. and SAUR, J. F. T., 1948: The field of mean wind stress over the North Pacific Ocean. *Oceanographic Report No. 14, Scripps Institution of Oceanography (mimeographed).*

SHORTER CONTRIBUTIONS

Note on the Numerical Integration of the Equations of Meteorological Dynamics

By J. S. SAWYER and F. H. BUSHBY, Meteorological Office, Dunstable

(Manuscript received 16 August 1951)

The work of CHARNEY (1949 a, 1949 b and 1950) and his collaborators on the numerical integration of the equations of meteorological dynamics is of considerable theoretical interest and of potential practical importance. In view of the promising nature of Charney's earlier results an independent examination has been carried out in the Forecasting Research Division of the Meteorological Office at Dunstable. The purpose of the present note is to report the results of some calculations performed along the lines of those of CHARNEY (1949 a, 1949 b) and also to indicate the results of experience which we have gained from some small-scale computational experiments with a baroclinic model used by SUTCLIFFE (1947) and now being studied by CHARNEY (1950).

The one-dimensional method of computing the change in the 500 mb height profile given by CHARNEY (1949 a) has been applied to various latitudes on a total of about 60 charts. Significant success was achieved; the correlation coefficient between predicted and observed height changes was + 0.54 along latitude 50° N and + 0.35 along latitude 40° N in a summer series; it was + 0.34 along latitude 45° N on a winter series. However the success was definitely less than that achieved by conventional forecasting methods on the same charts. On the other hand our results showed that better results were obtained from the computations than would have been achieved if it had merely been assumed that features of the pressure profile moved eastward with the zonal current. This fact gives one confidence that the one-dimensional barotropic model, despite its manifest limitations, does contain some essential features which are important in large-scale atmospheric motions, although it does not yet provide a basis for practical use in forecasting.

It appeared also from the cases studied that the failures of the predicted changes were most serious when the basic assumptions underlying the one dimensional model were not satisfied; for example, when the 500 mb contours included a closed centre, a flat area with practically no zonal flow, or a trough or ridge of large amplitude and distorted shape, and also when isotherms and contours crossed at a considerable angle. As CHARNEY himself has pointed out (1950) the assumption that isotherms and contours are parallel is probably a serious shortcoming of his earlier models. We therefore considered a model used by SUTCLIFFE (1947) and also more recently by CHARNEY (1950), in which the thermal wind has the same direction in all layers but is not necessarily parallel to the wind direction. In this latter model the equation for the motion at the equivalent barotropic level contains an additional term (see CHARNEY (1950) equation (32) which is proportional to

$$V_T \cdot \nabla \zeta_T$$

where V_T and ζ_T are the thermal wind and the vorticity of the thermal wind through a layer of the troposphere. Evaluation of this term at points along a parallel of latitude showed that its inclusion in the equation for the equivalent barotropic motion would have involved corrections to the 24-hr height changes predicted by Charney's one-dimensional method which were substantially greater than the changes actually occurring. It would probably be more appropriate to evaluate the corrections from values of $V_T \cdot \nabla \zeta_T$ averaged over a latitude band of

some 20 degrees, but even so the corrections remain substantial.

We were also led to consider that the barotropic model had serious short-comings from the results of two calculations of the theoretical height tendency $\frac{\partial z}{\partial t}$ along the lines suggested by CHARNEY (1949 b). The numerical solution of his equation (45) was carried out on the assumption that the 500 mb level corresponded to the equivalent barotropic level. Although some correspondence between the predicted and actual areas of 500 mb height change was apparent the correlation between the two was very low, about + 0.4 in one example and less than + 0.1 in the other. Also root mean square errors of the forecast at a selection of points were greater than those obtained from a forecast of 'no change'. An examination of the charts showed that the absolute vorticity was not conserved in the motion at 500 mb, and although some of the discrepancies might be accounted for by errors of analysis and errors associated with computations on a finite difference grid, we were also led to regard the effect of baroclinic development as important.

Numerical calculations have also been made by us on Sutcliffe's baroclinic model of the atmosphere from a slightly different point of view, our purpose being primarily to evaluate the vertical velocities in baroclinic development. SUTCLIFFE (1947) uses the relative divergence between two levels in the troposphere as a measure of the cyclonic development. In cases where the changes of thickness of atmospheric layers are due solely to horizontal advection (i. e. adiabatic motion and neutral vertical stability) he obtains an expression for the relative divergence between two levels as follows: —

$$f(\text{div } V - \text{div } V_0) = -V_T \cdot \nabla (f + \zeta + \zeta_0) \quad (1)$$

where V and V_0 are the velocities at the upper and lower levels, ζ and ζ_0 are the corresponding vorticities and V_T is the thermal wind through the layer, f is the coriolis parameter, and divergences are evaluated in isobaric surfaces.

Fields of vertical velocity computed from equation (1) show very plausible agreement with areas which the synoptician generally regards as areas of upward motion and subsidence. The areas of substantial upward velocity as computed agree well with observed rain areas, but comparison with the amounts of rainfall suggests that the computed vertical velocity is too great.

SUMNER (1950) had modified Sutcliffe's equation slightly to take account of the effect on the thickness pattern of vertical motion in a stably strafied atmosphere. Summer gives an equation corresponding to (1) of the form

$$f(\text{div } V - \text{div } V_0) = -V_T \cdot \nabla (f + \zeta + \zeta_0) + \\ + \frac{R}{f} \int_{p_1}^{p_0} \left\{ \Delta \left(\Gamma_p \frac{dp}{dt} \right) \right\} d(\log p) \quad (2)$$

where R is the gas constant and Γ_p is the rate of change of temperature with regard to pressure, $\partial T/\partial p$, in the air column minus its value in an atmosphere with a dry (or saturated) adiabatic lapse rate. Evaluations of mean vertical velocity based on the numerical solution of equation (2) give values of the vertical motion from ¼ to ½ those based on equation (1) and values of the corresponding rate of change of thickness of the 1,000—500 mb-layer accord fairly closely with the changes observed.

The success of these experiments in deriving values of the thickness tendency suggests that the tbaroclinic model of the atmosphere with the h ermal wind direction the same at all levels may prove a useful basis for numerical integration. Equation (2) can be used in conjunction with an equation for the thickness change given by SUTCLIFFE and FORSDYKE (1950) to give a method of computing $\partial z'/\partial t$, the rate of change of thickness of a selected isobaric layer (conveniently chosen to include most of the troposphere), in terms of the existing distribution of z' and $\bar{z}$, the height of a selected isobaric level (conveniently chosen as Charney's equivalent barotropic level). Charney's equation for the motion at the equivalent barotropic level modified by the inclusion of the term $V_T \cdot \nabla \zeta_T$ gives $\frac{\partial \bar{z}}{\partial t}$ in terms of z' and $\bar{z}$, so that we have a closed system of equations which might possibly be adapted to numerical integration, provided suitable assumptions can be made about the lapse rate and the effect of condensation on it.

Quite clearly, from the experience of CHARNEY (1950), the work of numerical integration will be very heavy and may tax the capacity of even modern electronic methods. However it does appear to us that the baroclinic model chosen, including the effect of vertical stability is the simplest which we can hope will provide a basis for useful numerical forecasting, and it is most desirable that its potentialities should be explored.

REFERENCES

CHARNEY, J. G. and A. ELIASSEN, 1949 a: A Numerical method for predicting the perturbations of the middle latitude westerlies. *Tellus*, **1**. 2. pp. 38—54.

CHARNEY, J. G., 1949 b: On a physical basis for numerical prediction of large-scale motions in the atmosphere. *Journal of Met.* **6**. pp. 371—385.

CHARNEY, J. G., R. FJÖRTOFT and J. VON NEUMANN, 1950: Numerical Integration of the barotropic vorticity equation. *Tellus*, **2**. 4. pp. 237—254.

SUMNER, E. J., 1950: The significance of vertical stability in synoptic development. *Quart. J. R. Met. Soc.* **76**, pp. 384—392.

SUTCLIFFE, R. C. 1947: A contribution to the problem of development. *Quart. J. R. Met. Soc.* **73**, pp. 370—383.

SUTCLIFFE, R. C. and A. G. FORSDYKE, 1950: The theory and use of upper air thickness patterns in forecasting. *Quart. J. R. Met. Soc.* **76**, pp. 189—217.

Photographs of the "Complete Precipitation" of a Cumulus Cloud

By L. SHERMAN, Institute of Geophysics, University of California[1]

(Manuscript received 28 December 1950)

It is well known that in higher latitudes the lower parts of cumulonimbus may precipitate completely leaving only the anvil. It is also well known (KOTSCH, 1947) that in tropical latitudes precipitation occurs from clouds which have not reached the freezing level. Finally, it is known, at least to most tropical meteorologists, that quite commonly in the tropics a cumulus cloud will precipitate completely.

PALMER and ELLSAESSER (1949) describe this last phenomenon as follows: "In low latitudes the entire cloud may precipitate and disappear, and in the last stages you observe precipitation falling from a clear sky. ... the cloud begins to show evidence of shear, and precipitation usually begins. The top part then breaks away and the bottom dissolves. In the final stage the falling precipitation from the top portion of the cloud is white and fibrous and is sometimes mistaken for cirrus (Figure 3)." I have reproduced this figure 3 as my figure 1. In a recent article CRADDOCK (1949) has presented several photographs of this phenomenon. In addition the reader may find other published examples in DEPPERMANN's (1937) collection of cloud photographs, although Depperman does not specifically call attention to them. Both these sources, however, have portrayed clouds dissipating inland over a coastal area. In this note we present photographs of this occurring over the sea, with its horizontally uniform properties as a source of heating and of moisture.

During the summer of 1950 there occurred Operation MIDPAC—a geophysical research cruise jointly sponsored by the U.S. Navy, through its Office of Naval Research, and the University of California, through the Scripps Institute of Oceanography and the Institute of Geophysics of the University of California. The author was a member of the meteorological group aboard the Scripps' vessel *Horizon*. This group, headed by D.S. Johnson of the Department of Meteorology, UCLA, was the meteorological component of MIDPAC. It was during this cruise that the photographs, which are the reason for this note, were taken.

On 20 August 1950 at approximately 0800 local time the color photographs of figure 3, reproduced

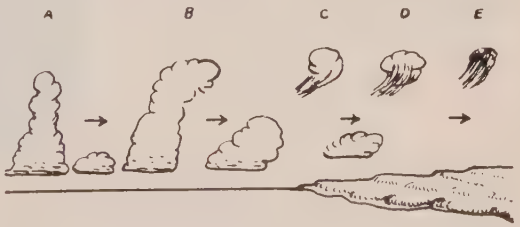

Fig. 1. The complete precipitation of cumulus (after Palmer and Ellsaesser).

[1] Publication No. 9 of the Institute of Geophysics of the University of California.

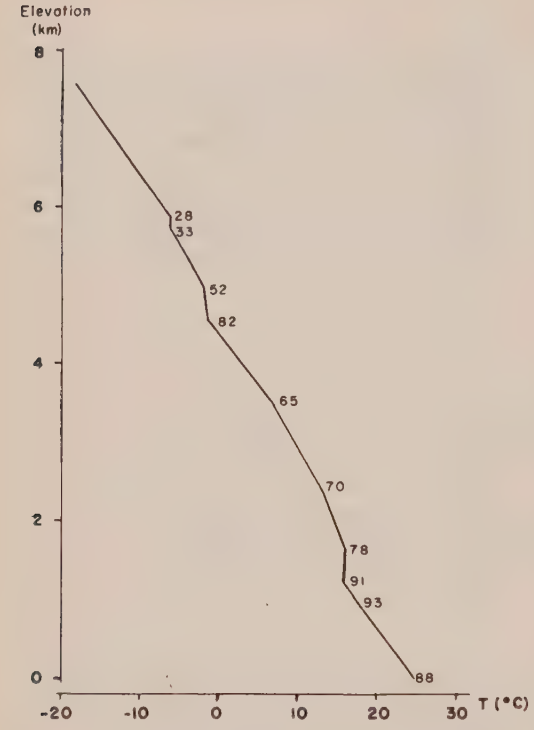

Fig. 2. A sounding released from the ship *Horizon* two hours and forty minutes prior to the time at which the photographs of figure 3 were taken. The temperature is plotted against elevation; relative humidities are entered to the right of the temperature curve. Note that the freezing level is well above 6,000 feet, which is the height just reached by the topmost tower of the clouds pictured in figure 3.

in black and white, were taken at intervals of less than a minute. At that time the approximate position of the *Horizon* was 16.2N, 152.8W. Earlier that morning, at 0520 local time, a radiosonde had been released; this sounding is shown in figure 2. From the surface weather log of the expedition we find that the 0800 surface observation included: 1/10 cumulus humilis, bases 2,000 feet; 1/10 swelling cumulus, bases 2,000 feet; 2/10 stratocumulus, bases 4,000 feet; light showers in sight (from the swelling cumulus), surface wind 050 degress 20 knots. The cloud heights were estimates.

In the three photographs we see almost exactly the sequence shown in figure 1, save that the lower portion of the original cumulus does not disappear. Initially a cumulus cloud, with base about 2000 feet and capped by a narrow tower reaching to 6000 feet or less was observed to the southwest of the ship. The tower showed evidence of shearing, and a rainbow was observed between two and four thousand feet. At this juncture a mad dash to obtain the camera ensued. Then the pictures of figure 3 (a, b, and c), which show the tower shearing and breaking away from the cloud, were taken. During all the time that the tower was tilting and drifting away, it was also precipitating. Ultimately it disappeared entirely. The last photograph is taken obliquely through the rain falling from a clear sky (not evident in the photo) with the remaining lower portion of the original cumulus in the background. It strikingly bears out the statement of Palmer and Ellsaesser that this precipitation might be mistaken for cirrus. Were it not for the evidence of its low elevation given by the cumulus cloud in the background, the photograph of this rain could easily be identified as a photograph of cirrus.

REFERENCES

Craddock, J. M., 1949: The Development of Cumulus Cloud; Results of Observations Made in Malaya. *Q. Jour. Roy. Met. Soc.*, **75**, 324, pp. 147—153.

Depperman, C. E., 1937: *The Weather and Clouds of Manila.* Manila Bureau of Printing.

Kotsch, W. S., 1947: An Example of Colloidal Instability of Clouds in Tropical Latitudes. *Bull. A.M.S.*, **28**, 2, pp. 87—89.

Palmer, C. E. and Ellsaesser, H. W., 1949: Notes on Tropical Meteorology. *Tech. Bull. of 2143d Air Weather Wing*, **1**, 2, pp. 1—49.

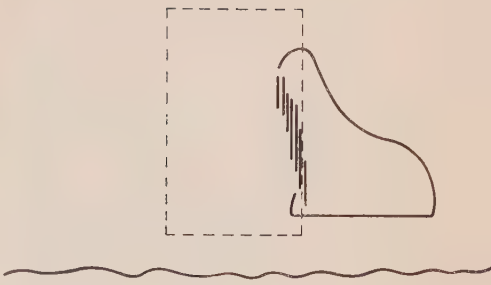

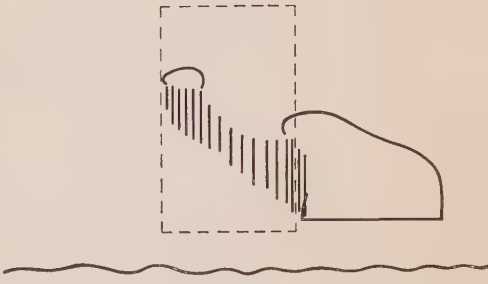

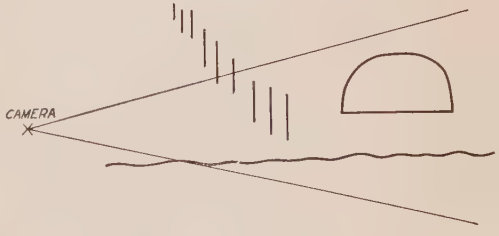

Fig. 3. A sequence of 3 photographs of the "complete precipitation" of cumulus. Taken 0800 local time on 20 August 1950 at 16° N, 153° W. The camera was pointed approximately toward 245° (SW). To the right of each picture is given a diagrammatic sketch of what was occurring together with an indication of the extent of the photograph.

A Note on the Kinetic Energy Balance of the Zonal Wind Systems

By H. L. KUO, Massachusetts Institute of Technology

(Manuscript received 25 July 1951)

Broadly speaking, there are two processes that may produce the needed transport of angular momentum from the zones of surface easterlies to those of surface westerlies. One is a large-scale mean convective process, with ascending motions in lower latitudes and descending motions in higher latitudes. The other is the large-scale eddy motions. Although some types of mean meridional circulations might be able to account for the necessary transport, the existence of such circulations is hard to establish observationally. On the other hand, the investigations conducted at the Massachusetts Institute of Technology and at the University of California have demonstrated that the eddy process not only produces enough angular momentum transfer but also produces sufficient transfer of energy to maintain the atmosphere in radiational equilibrium. This suggests that the general circulation is maintained mainly by the large-scale eddy process.

However, before any definite conclusion is drawn, one must also investigate the relative efficiency of the two processes as regards the kinetic energy balance of the mean zonal flow. For this purpose each velocity component may be decomposed into a mean value, defined as the average along a latitude circle, and a deviation from this mean so that $u = \bar{u} + u'$, $v = \bar{v} + v'$, $w = \bar{w} + w'$, where u, v, w are respectively the eastward, northward and upward components, and u', v', w' are the eddy components. In spherical coordinates the zonal momentum equation may be written

$$\frac{\partial \varrho u}{\partial t} = -\frac{\partial (\varrho u v \cos^2 \Phi)}{a \cos^2 \Phi \, \partial \Phi} - \frac{\partial (\varrho u w)}{\partial z} + f \varrho v - \frac{\partial (p + \varrho u^2)}{a \cos \Phi \, \partial \lambda}$$

where Φ is latitude, λ longitude, z elevation, f the coriolis parameter, a earth's radius, ϱ density, p pressure and t time. The effect of the vertical component of the deflecting force is small and is neglected. This equation may be multiplied by the mean zonal velocity $\bar{u}$ and integrated over the volume V bounded by two complete latitude circles and over the entire column of air in the vertical. For this particular problem the effect of the variation of density along latitude circles and with time is small so that $\int \bar{u} \frac{\partial \varrho u}{\partial t} \, d\lambda = \pi \partial \overline{\varrho u^2} / \partial t$. It follows that

$$\frac{\partial E_x}{\partial t} = -2\pi a^2 \iint \left[\bar{\dot{\lambda}} \frac{\partial (\overline{\varrho u v} \cos^2 \Phi)}{\partial \Phi} + \right.$$

$$\left. + \bar{u} \cos \Phi \frac{\partial (\overline{\varrho u w})}{\partial z} - f \bar{u} \overline{\varrho v} \cos \Phi \right] d\Phi \, dz =$$

$$= \int \left[\overline{\varrho u' v'} \cos \Phi \frac{\partial \bar{\dot{\lambda}}}{\partial \Phi} + \overline{\varrho u' w'} \frac{\partial \bar{u}}{\partial z} \right] dV +$$

$$+ \int \left[\overline{\varrho w} \, \bar{u} \frac{\partial \bar{u}}{\partial z} + \left(f + \cos \Phi \frac{\partial \bar{\dot{\lambda}}}{\partial \Phi} \right) \overline{\varrho v} \, \bar{u} \right] dV +$$

$$+ \int \overline{\varrho u v_n} \cdot \bar{u} \, ds_1 + \int (\overline{\varrho u w})_0 \, \bar{u}_0 \, ds_0$$

where $E_x = \frac{1}{2}\int \overline{\varrho}\overline{u}^2 dV$ is the total kinetic energy of the mean zonal motion, $\overline{\dot{\lambda}}$ is the mean zonal current in angular measure ds_1 and ds_0 are the area elements of the lateral walls and bottom respectively, v_n is inward meridional velocity and the limits of integration are as stated. This equation is of basic importance for the study of the general circulation. It is the writer's desire to call attention to the integral requirement which it expresses. It may be noted that this equation is similar to the Reynold's energy equation for the mean motion, except for the term involving f due to earth's rotation. However, it is derived without the assumptions of incompressible motion and the vanishing of the velocities along the boundaries. The pressure force does not appear in this equation. According to this equation, the kinetic energy of the mean zonal flow can change not only by the presence of mean meridional circulations, as represented by the terms containing $\overline{\varrho v}$, $\overline{\varrho w}$, but also by a *conversion of the eddy kinetic energy into that of mean zonal flow*. This rate of conversion is given by the products of the eddy stresses $\overline{\varrho u'v'}$ and $\overline{\varrho u'w'}$ into the horizontal and vertical shears of the mean zonal wind. Because the vertical velocity w generally differs from zero at the level where surface wind is measured, we also retained the last term, where the subscript zero denotes surface values. This term may be interpreted as representing the dissipation of the kinetic energy of mean zonal flow through ground friction. The dissipation of mean zonal kinetic energy directly through molecular viscosity in the free atmosphere is too small and is neglected. The equation obtained may also be looked upon as a continuity equation expressing the balance of mean zonal kinetic energy for the atmosphere. Thus the volume integrals can be looked upon as sources (or sinks) and the surface integrals as net inward transports of this energy across the boundaries.

To the extent that data are available it is possible to examine whether the eddy process can provide sufficient kinetic energy to account for the frictional loss. This is given by the first two terms containing $\overline{\varrho u'v'}$ and $\overline{\varrho u'w'}$ in the last member of the equation. These terms as they stand include the effects of small scale eddies as well as of large scale. It is probable that the small scale eddies lead to dissipation so that only large eddies need be considered.

To estimate the order of magnitude of the first term arising from the large eddies, we may make use of the values of $\overline{\varrho u'v'}$ obtained by STARR (1951) over the American continent. Although these values may not be very representative for the hemisphere, the order of magnitude and the trend of the meridional distribution are probably correct. In Starr's data, the meridional shear of the zonal wind, $\partial\overline{\dot{\lambda}}/\partial\Phi$ varies very little with height above 700 mb, therefore one may compute this rate of conversion by using the integrated values of the angular momentum transfer $\tau = 2\pi a^2 \cos^2\Phi \int \overline{\varrho u'v'}\, dz$ (actually up to 100 mb level), and take the meridional wind shear at the 500 mb level as the mean wind shear. Such values are given in table 1.

Integrating from 25° N to 70° N, the result is that $\int \tau\, \partial\overline{\dot{\lambda}}/\partial\Phi\, d\Phi \sim 125 \times 10^{19}$ gm cm² sec^{-3}. There is also a net influx of about 100×10^{19} units through the latitude walls. A zero value of τ at around 10° N is suggested by an as yet unfinished study. Integration from 10° N to 70° N gives a total of about 200×10^{19} gm cm² sec^{-3}. Each of these computations gives an average rate of conversion of about 10^{-4} watts per cm².

As for the second term, we still lack any reliable determinations. However, since almost all the large disturbances in middle latitudes have their axes inclined toward west with increasing elevation (one reason for this inclination is the thermal asymmetry), the correlation $\overline{u'w'}$ is mostly negative in middle latitudes. This conclusion has been confirmed by a few indirect computations by WHITE (1950). In low latitudes the correlation $\overline{u'w'}$ is probably positive. Since $\partial\overline{u}/\partial z$ is either negative or small there, the total contribution of the second term from the large eddies is probably negative. Thus this

Table 1

Values of τ in units of 10^{25} gm cm² sec^{-2} and of $\partial\overline{\dot{\lambda}}/\partial\Phi$ in 10^{-5} sec^{-1}

Lat. (deg. N)	10°	25°	35°	45°	55°	63°	76°
τ	(0)	+ 56.0	+ 41.5	+ 8.40	— 6.20	— 2.00	+ 0.60
$\partial\overline{\dot{\lambda}}/\partial\Phi$	+ 0.63	+ 1.2	+ 0.57	+ 0.17	— 0.23	— 2.10	— 2.80

term may be combined with the last term and the parts of the first term arising from small eddies and looked upon as constituting the total dissipation through skin and turbulent friction.

According to BRUNT (1941) and others, the rate of dissipation of the total kinetic energy in the surface layer and in the free atmosphere is about 5×10^{-4} watts per cm^2. Since less than one-third of this total dissipation can be attributed to the loss of the kinetic energy of the mean zonal flow, and since the use of long period averages of $\overline{u'v'}$ and $\partial\overline{\dot{\lambda}}/\partial\Phi$ gives an underestimation, it seems that the rate of conversion obtained is of the right order of magnitude and is sufficient to account for the frictional loss.

This seems to suggest that the eddy process in the atmosphere is a self consistent and self sufficient mechanism in maintaining the zonal wind systems. One or two consequences of the energy equation may be noted. Although this equation itself does not depend upon the scale of the motion, as already mentioned, the properties of the eddy stresses may be quite different for the small scale turbulent motions and for the large-scale disturbances. In the ordinary turbulence regime, the momentum flux is generally in the direction of the gradient of the mean velocity so that a virtual coefficient of viscosity K can be defined such that $\overline{\varrho u'v'} = -K\varrho\,\partial\bar{u}/\partial\gamma$, where γ is in the direction of increasing $\bar{u}$. However, this is not necessarily true for large-scale eddies. When the flow is stable and the disturbances are sustained by some other processes, the reverse may happen and the disturbances may add their momentum and energy to the main flow. The values of $\overline{\varrho u'v'}$ and $\partial\overline{\dot{\lambda}}/\partial\Phi$ cited above show that this is really the case for the large-scale disturbances in the atmosphere. This is not only true for momentum, but also true for other properties. Thus even when the absolute vorticity of an element of air is nearly conserved during its motion, it does not necessarily follow that vorticity will be transported in the direction of the gradient; rather the reverse is what should be expected when the flow is relatively stable for horizontal disturbances. Only when the flow is quite unstable so that disturbances develop at the expense of the mean flow and a thorough mixing is produced, the momentum and vorticity will be transported along the gradient. One must not therefore use the concept of virtual viscosity in discussing the effect of the large-scale eddy motions in the atmosphere (unless the possibility of a negative viscosity coefficient is admitted).

REFERENCES

BRUNT, D., 1941: Physical and Dynamical Meteorology, London, Cambridge University Press 1941.

STARR, V. P., 1951: A note on the eddy transport of angular momentum. *Quart. Journ. R. Met. Soc.*, **77**, 44—50.

WHITE, R. M., 1950: A mechanism for the vertical transport of angular momentum in the atmosphere. *J. Meteor.* **7**, 349—350.

Possible Heavy Turbulent Exchange between the Extratropical Tropospheric Air and the Polar Stratospheric Air

By H. ARAKAWA, Meteorological Research Institute, Tokyo

(Manuscript received 27 July, 1951)

Abstract

In 1941 the present author pointed out that there exists a criterion for the development of heavy (horizontal) turbulence in zonal motion which deviates widely from th ewellknown criterion of dynamic stability. If the anticyclonic wind shear is greater than the critical anticyclonic shear given by the condition of zero absolute vorticity, the zonal motion is dynamically unstable; and if the wind shear is greater than a proper critical cyclonic shear, heavy dynamic turbulence results. The wind shear reaches this critical cyclonic value in a narrow zone just north of the latitude of the jet stream. Then, there must be a zone of heavy turbulent exchange of air masses between the extratropical tropospheric air and the stratospheric air through the slit between the extratropical and polar tropopauses.

Through investigations by SOLBERG (1939,) KLEINSCHMIDT (1941), VAN MIEGHEM (1946 a, b, 1948) and others, the question of the stability of zonal motion has been introduced in meteorology. In the case of stability the absolute angular momentum of the zonal flow must decrease with increasing latitude, and in the case of instability the absolute angular momentum must increase with increasing latitude. In the case of transition to instability the absolute vorticity vanishes. According this criterion the critical value of shear is given by

$$\frac{\partial u}{\partial y} = f + \frac{u}{R} \tan \Phi, \qquad (1)$$

where y is the meridional coordinate (positive to the north), u is the zonal (gradient) wind, Φ the latitude, $f = 2\,\omega \sin \Phi$ the Coriolis parameter, ω the angular velocity of the earth's rotation and R the radius of the earth. If the anticyclonic shear is greater than the value given by the formula (1), dynamic instability results; if the shear is smaller, the motion is dynamically stable (fig. 1).

As early as in 1941, the present author published three papers (1941 a, b, c) containing the same criterion as the one given by SOLBERG, KLEINSCHMIDT, VAN MIEGHEM and others. Moreover he also pointed out the existence of another criterion for turbulent motion in zonal flow which deviates widely from the dynamic instability criterion well known in recent meteorological literature.

According to this theory, the critical cyclonic shear is given by

$$-\frac{\partial u}{\partial y} = \omega \sin \Phi + \frac{2\,u}{R} \tan \Phi, \qquad (2)$$

where the symbols have the same meaning as in Eq. (1). If the shear is cyclonic $\left(-\frac{\partial u}{\partial y} > 0\right)$ and greater than the value given by (2), heavy dynamic turbulence results. Formula (1) gives the critical anticyclonic shear, and if the wind shear is greater than the value given by (1), the motion is dynamically unstable. Formula (2) gives the critical cyclonic shear, and if the wind shear is less than the value

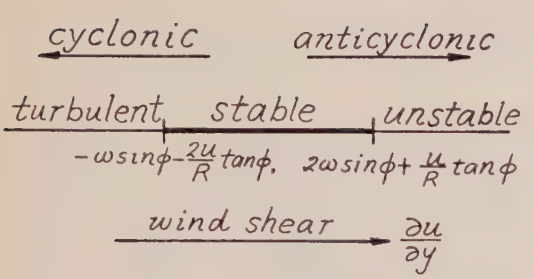

Fig. 1. Graphical representation of the turbulent, stable and unstable zones as function of wind shear.

given by (2), dynamical heavy turbulent motion results (fig. 1). Assuming a west wind of 80 m sec^{-1} at latitude 45° N, the critical value given by (1) is $(10+1)\times 10^{-5}$ sec^{-1} corresponding to a shear of 11 m sec^{-1} (100 km)$^{-1}$; while the critical value given by (2) is $(5+2.5)\times 10^{-5}$ sec^{-1} corresponding to a shear of 7.5 m sec^{-1} (100 km)$^{-1}$. According to PALMÉN (1948) and PALMÉN, NAGLER (1948) the anticyclonic wind shear reaches the critical value determined by formula (1) in a rather narrow zone (of a width not in excess of 300 km) just south of the latitude of the "jet stream". Furthermore, the cyclonic shear reaches the critical value determined by formula (2) in a rather narrow zone just north of the latitude of the "jet stream".

Assuming the flow to be zonal, the absolute angular momentum of the westerlies, Ω, is composed of the angular momentum of the earth at a given latitude, Ω_e, and the relative angular momentum Ω_u of the westerly flow. Thus

$$\Omega = \Omega_e + \Omega_u, \tag{3}$$

where

$$\Omega_e = \omega R^2 \cos^2 \Phi, \quad \Omega_u = R u \cos \Phi. \tag{4}$$

The present author has discussed the turbulent motion of zonal flow under the assumption that the absolute angular momentum of an individual parcel is conserved while it travels cross-stream. This absolute angular momentum Ω may be a function of the Φ-direction normal to the mean zonal flow. Assuming as a working hypothesis that the parcel, as a result of the turbulent motion, is displaced in the Φ-direction a certain distance $l = R\,d\Phi$ before it loses its individuality through mixing with its new environment. The distance l is called the mixing length after PRANDTL. When a parcel of air is displaced from a position $\Phi - d\Phi$ to Φ, the wind speed $u^\star$ of the moving element in its new position Φ is then given by

$$\omega R^2 \cos^2 \Phi + R u^\star(\Phi) \cos \Phi =$$
$$= \omega R^2 \cos^2 (\Phi - d\Phi) +$$
$$+ R u(\Phi - d\Phi) \cos (\Phi - d\Phi),$$

or approximately,

$$u^\star(\Phi) - u(\Phi) =$$
$$= \left(2\,\omega R \sin \Phi + u \tan \Phi - \frac{\partial u}{\partial \Phi}\right) d\Phi.$$

The wind speed of the surroundings is $u(\Phi)$. The difference between the wind speed of the displaced air parcel and the wind speed of the surroundings is given by

$$u' = l\left(-\frac{\partial u}{R\,\partial \Phi} + \frac{u}{R}\tan\Phi + 2\omega \sin \Phi\right), \tag{5}$$

or

$$u' = -l\,\frac{\partial \Omega}{R^2 \cos \Phi\, \partial \Phi}. \tag{6}$$

This value is at least an approximation to the turbulent velocity component u'. Thus, whenever the angular momentum decreases with increasing latitude the relative west wind increases in a poleward moving air parcel but decreases in a parcel moving equatorward.

The centrifugal force acting on the displaced parcel per unit volume is

$$\varrho\,(u + R\omega \cos \Phi + u')^2 / R \cos \Phi,$$

approximately, while the centrifugal force on the surrounding air per unit volume is given by

$$\varrho\,(u + R\omega \cos \Phi)^2 / R \cos \Phi.$$

Stability prevails when the centrifugal force on the surrounding air is smaller than that on the displaced parcel, i.e., stability demands that for the displacement $l > 0$. If $u' > 0$ for $l > 0$, then the displaced parcel will be pushed back to its original position since the centrifugal force acting on it is larger than the centrifugal force on the surrounding air. While being forced back, the parcel of air acquires kinetic energy and therefore tends to overshoot its equilibrium position. In this manner a stable oscillation around the equilibrium position is brought about. This type of stability is called dynamic stability.

If the centrifugal force acting on the parcel were smaller than the centrifugal force acting on the environment, the particle would move further from

its original position. This distribution of the zonal motion would tend to create instability. If finally the centrifugal force on the parcel were equal to that on the surrounding air, no force would be acting on a displaced air parcel; it would everywhere be in indifferent equilibrium.

The stability condition $u' > 0$ for the displacement $l > 0$ can also be written in the form

$$\frac{\partial \Omega}{\partial \Phi} < 0, \text{ or } \frac{\partial u}{R \partial \Phi} < 2\omega \sin \Phi + \frac{u}{R} \tan \Phi, \quad (7)$$

which states that stability with respect to small perturbations exist if the absolute angular momentum decreases with increasing latitude in the atmosphere. If the absolute angular momentum is constant, we have indifferent equilibrium; if the angular momentum increases with increasing latitude, instability prevails. Those results have been obtained by SOLBERG and others, as given by Eq. (1).

RICHARDSON (1920) has given a criterion to determine whether turbulence will increase or decrease. The principle on which his criterion is based is that the flow will remain turbulent if the rate of supply of energy by the eddy stresses is at least as great as the work which has to be done to maintain the turbulence against gravity or other stabilizing forces.

The mean excess of centrifugal force per unit volume which drives a displaced parcel back to its original position is half of its extreme value, or

$$\frac{\varrho}{2} \left\{ (u + R\omega \cos \Phi + u')^2 - \right.$$

$$\left. - (u + R\omega \cos \Phi)^2 \right\} / R \cos \Phi \approx$$

$$\approx \varrho \left(\omega + \frac{u}{R \cos \Phi} \right) u'.$$

When a parcel of air is displaced from a position $\Phi - d\Phi$ to Φ ($R d\Phi = l$), the work done against this excess centrifugal force is $\varrho l \left(\omega + \frac{u}{R \cos \Phi} \right) u' \sin \Phi$. If v' is the instantaneous normal velocity to an element of the vertical area F standing on a latitude circle, then the volume of air flowing across an element of this area per unit time is $v' dF$. The time rate of the work done on the air flowing across the vertical area F is, therefore, $\int \varrho l \left(\omega + \frac{u}{R \cos \Phi} \right) \times \sin \Phi \; u' v' \, dF$. From the stability condition (7), the product $u' v'$ is always positive. The amount of

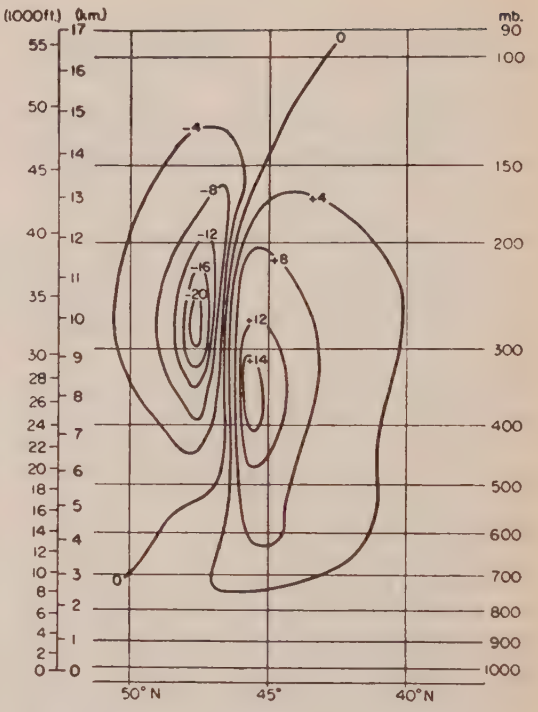

Fig. 2. Increase of the geostrophic wind computed along isentrophic surfaces. (Acc. PALMÉN and NAGLER 1948).

the work required to maintain the turbulence under stable conditions is always positive. Determining the sign in appropriate ways, the time rate of the work to be done on the air flowing across the vertical area F in order to maintain the turbulence against the centrifugal force is, therefore,

$$F \varrho \, |l| \left(\omega + \frac{u}{R \cos \Phi} \right) \sin \Phi \cdot \overline{u' v'}, \quad (8)$$

where the bar indicates that the mean value of the product is to be taken.

The time rate of work done by the eddy stresses per unit volume is $-\varrho \overline{u' v'} \left(\frac{\partial u}{R \partial \Phi} + \frac{\tan \Phi}{R} u \right)$, where $-\varrho \overline{u' v'}$ stands for the Reynolds or eddy stress. Now consider a parallelepiped with horizontal edges $|l|$ and bounded by one pair of parallel vertical planes F. Then the time rate of work done on the air whose volume is $F \cdot |l|$ by the eddy stresses becomes

$$-\varrho F \cdot |l| \cdot \overline{u' v'} \left(\frac{\partial u}{R \partial \Phi} + \frac{\tan \Phi}{R} u \right). \quad (9)$$

From Eqs. (8) and (9), the condition that turbulence should increase may therefore be written,

$$-\left(\frac{\partial u}{R\partial \Phi}+\frac{\tan \Phi}{R}u\right)>\left(\omega+\frac{u}{R\cos \Phi}\right)\sin \Phi.$$

This inequality may be written in another form,

$$-\frac{\partial u}{R\partial \Phi}>\omega \sin \Phi+\frac{2u}{R}\tan \Phi, \qquad (10)$$

or

$$\frac{\partial}{\partial \Phi}\left(\frac{u+R\omega \cos \Phi}{\cos^2 \Phi}\right)<0,$$

which is the relation expressed as Eq. (2). The criterion seems to be valid in this form, with reservations for a numerical factor which appears on the right-hand side of the inequality (10). It is readily seen that the quantity $\overline{u'v'}$ in Eq. (8) need not of necessity be equal to the quantity $\overline{u'v'}$ in Eq. (9), and this circumstance may give rise to a different factor on the right hand side of the above inequality.

Palmén (1948) and Palmén, Nagler (1948) showed that the strongest wind or jet stream can regularly be observed just south the latitude where the tropopause is split in two, i.e., the extratropical tropopause and the polar tropopause (fig. 2). The wind shear reaches the critical value determined by formula (2) in a rather narrow zone just north of the latitude of the jet stream. Then there must be a zone of heavy turbulent exchange of air masses between the extratropical tropospheric air and the polar stratospheric air. It might be emphasized that the turbulent exchange between the extratropical tropospheric air and the polar stratospheric air through the slit of two tropopauses will be an important problem in the general circulation of the atmosphere.

REFERENCES

Arakawa, H., (1941 a): Stabilitätskriterien der atmosph. horizont. Turbulenz, *Gerlands Beitr. z. Geophys.*, **58**, 1/2.

— (1941 b): Der Grenzwert für die Turbulenz in der Atmosphäre, (in Japanese), *Journal of Met. Soc. of Japan, 2nd Ser.*, **19**, 171—175.

— (1941 c): Stabilitäts- und Böigkeitsbedingungen der allgemeinen Zirkulation der Atmosphäre (in Japanese), *Journal of Met. Soc. of Japan, 2nd Ser.*, **19**, 205—208.

Kleinschmidt, E., (1941): Stabilitätstheorie des geostrophischen Windfeldes, *Ann. d. Hydr. u. Mar. Meteorol.*, **49**, 305—325.

Mieghem, J. van, (1946 a): Sur la stabilité du courant géostrophique, *La Météorologie*, 9—33.

— (1946 b): Contribution à l'étude de la Cyclogénese, *Inst. Roy. Météor. de Belgique, Mém.*, **23**, 1—24.

— (1948): L'instabilité hydrodynamique et les perturbations du courant zonal d'Ouest, *Arch. für Meteorol., Geophys. und Bioklimatologie*, Ser. A, **1**, 143—148.

Palmén, E., (1948): On the distribution of temperature and wind in the upper westerlies. *Journal of Meteorology*, **5**, 20—27.

Palmén, E. and K. M. Nagler, (1948): An analysis of the wind and temperature distribution in the free atmosphere over North America in a case of approximately westerly flow. *Journal of Meteorology*, **5**, 58—64.

Richardson, L. F., (1920): The Supply of Energy from and to Atmospheric Eddies, *Proc. Roy. Soc.*, **97**, 354—373.

Solberg, H., (1939): Le mouvement d'inertie de l'atmosphere stable et son role dans la théorie des cyclones. *Procès-Verbaux de l'Assoc. de Météorologie, UGGI, Edinburgh (1936), II.* Mémoires et discussions, 66—82.

NOTE

Note on Cooperative Research Projects

During the last few years, while the writer has served as professor of meteorology at the University of Stockholm, attempts have been made in Sweden to develop an informal type of international cooperation in meteorological research, similar to that which flourished in Europe before the outbreak of the Second World War, but at the same time adapted to meet the needs of the vastly enlarged scope and responsibilities of the meteorology of today.

In these efforts the writer has been able to enlist the administrative and financial support of the Swedish Institute for Cultural Exchange with Foreign Countries and of the University of Chicago; through the latter institution liberal additional financial contributions have been obtained. It is the purpose of this note to comment on some problems which have to be solved before a suitable permanent pattern of cooperative research efforts can be established, and to review briefly the Stockholm program.

It is a truism, repeated almost *ad nauseam*, that the winds blow and the storms move without regard for political boundaries. It is somewhat less self-evident but equally important from the point of view of applied meteorology that different portions of the earth's atmosphere may influence each other, over such long distances and with such a speed that even the rapid transport of atmospheric properties by the strong winds aloft must be considered inadequate as an explanation for the observed interactions. For these reasons it is now fairly generally admitted that it is impossible to isolate certain portions of the atmosphere and to analyze them as if they were mechanically or thermally closed systems. This indivisibility of the atmosphere and its problems makes meteorology a particularly interesting field in which to experiment with the organization of cooperative research projects on an international basis.

It is probable that meteorologists would have been slow in recognizing the indivisibility of the atmosphere if they had not had at their disposal a worldwide grid of daily observations from the upper atmosphere where obscuring local influences are much less marked than at the ground. It is certain that these data would not yet have been available if the operational service demands of commercial and military aviation had not made it possible to obtain the funds with which to organize an observational program on a nearly global scale.

Under the circumstances stated above it has been a relatively easy task, even in these politically troubled times, not only to maintain observation posts in all parts of the world, but also to build up an efficient and truly international scheme for the exchange of weather observations and forecasts on a global basis. Any one-sided interference with this free flow of information would lead to reprisals and might thus be to the disadvantage of everybody and to the gain of no one.

This principle appears to be quite clearly recognized even by the many non-professional managers who now gradually are taking over the mounting administrative burdens of the applied meteorological service organizations. This is demonstrated by the fact that a financially extremely well-supported International Bureau now is being set up, under the World Meteorological Association, to facilitate the flow of daily weather observations.

While thus the managerial aspects of applied meteorology seem to be taken care of in a satisfactory manner, very little has been done to provide adequate and reasonably well-distributed facilities for the organization of cooperative research teams in basic meteorology, in spite of the fact that with-

out such organized cooperation the central area of our science easily might degenerate into a hollow weather reporting and collecting system.

Most of those scientific problems which arise out of our recognition of the indivisibility of the earth's atmosphere are of such a complex nature and of such a broad scope that they cannot be studied successfully except through the efforts of well-integrated research teams in which various branches of meteorology are adequately represented and for which adequate facilities have been made available. In the United States there are several examples of basic problems studied successfully by such well-equipped teams, for instance the physical structure of thunderstorms, and the nature of the prevailing circulation of the atmosphere; in the adjacent field of oceanography one might refer to the recent, beautifully organized and executed synoptic survey of the Gulf Stream. It should not be denied that just in the United States, where this technique of cooperative research seems to have reached its fullest development, teams sometimes have been organized around meaningless problems or have outlined their usefulness. However, eqvivalent amounts of waste motion may be found also in countries adhering to more traditional forms of research organization. Furthermore, research teams are readily dissolved or regrouped to meet changing requirements; in this way the entire scientific body acquires a highly desirable flexibility to which there is no counterpart in the older forms of research organization.

In spite of the demands for cooperative research effort and team work which spring from the nature of the world-wide meteorological problems themselves one finds, with few exceptions that the pattern of European meteorology of today is the same as the pattern of a few decades ago. At those universities where meteorology is represented at all, a lone professor, with one or two assistants, is supposed to keep up with, and contribute to, the advance of the whole broad front of the science. His nearest colleagues, in the official national meteorological office are most likely overburdened with administrative and service problems and have to concentrate on day-by-day tasks. Thus even the few opportunities which do exist for the development of a stimulating milieu and a cooperative research program in fundamental meteorology are not always utilized, to the serious disadvantage of both the academic and the applied meteorologist.

There are of course exceptions to this state of affairs. The brilliant achievements of the meteorologists assembled in Bergen, Norway, shortly after the end of the first World War were the result of effective collaboration within a team of high-spirited young men working under the protection and guidance of V. Bjerknes. Even today, there are a few countries in Europe which appear to have solved quite successfully the problem of creating a milieu in which team work and bold joint attacks on basic problems may be undertaken. Nevertheless, these cases are exceptions; most European research meteorologists still work in an isolation which is highly detrimental to the advance of the science.

Under these circumstances the individual research worker is likely to select some special problem which can be isolated to such an extent that it may be investigated by a single person. In the past this policy has often resulted in contributions of a fundamental nature, but may just a likely lead the investigator onto a side track well removed from the central problems of world-wide meteorology. It hardly needs to be stressed that no one can assert in advance the ultimate significance of the heroic tasks which isolated investigators may set for themselves. What can be asserted, however, is that in the absence of organized group activity certain central fields in our science necessarily must remain uncultivated.

In many cases the isolated academic worker seeks to affiliate himself with some institution abroad where the opportunity exists to work in a larger milieu and where he has the opportunity to receive and give stimulation through contact with a large number of colleagues in his own and adjacent fields. This latter process has already led to an irreversible drain of highly competent research workers from some of the smaller countries of Europe into the insatiable research laboratories of a few of the larger and scientifically more well-situated countries.

The emphasis that has been placed above on the importance of group activity in research does not imply any underestimate of the fundamental role of the individual. On the contrary it has been demonstrated over and over again that the talented research worker normally contributes most effectively when he is in the position to test his ideas in daily contact with a group of interested colleagues. We are frequently concerned with questions of interpretation of the processes we observe in the atmosphere. In such studies it is hardly possible to establish the ultimate value of a view point or method of description except by demonstrating its fertility when applied over a broad range of phenomena. For indirect testing of this type group discussions are nearly indispensable.

On top of the particular difficulties which are associated with the "normal" isolation of most academic meteorologists in the smaller European countries, meteorology on our continent still suffers from the consequences of the last war and from the curtains that then were lowered between the fighting countries. No one who has glanced through and compared a few issues of the resurrected journals of Central Europe with, for instance, the corresponding British or American publications can fail to get the impression that they represent entirely different worlds, in spite of the indivisibility of the atmosphere with which they deal.

There are good physical geographical reasons why American, Central and North European meteorologists to a very considerable extent should occupy themselves with different manifestations of atmospheric behaviour, though one might deplore the fact that theories based on the study of phenomena of a distinctly regional character not infrequently have been presented with claims of universal validity. It is more disturbing, however, when one finds identical phenomena described in completely different terms, and without reference to work done on the same problem by groups in other countries.

Restrictions on travel and on the exchange of publications, as well as language barriers, have contributed to the present state of affairs, but one can hardly escape the impression that national prides, as a result of the last war, have been stimulated to a pitch probably seldom reached before among scientific workers. A distinct improvement is now noticeable but at times it has seemed as if our science were cultivated by a number of national olympic teams pitted against each other in rather furious competition.

In our science, as in all other intellectual activities, diversity is essential to progress. No one in his right senses would wish to see meteorology become an All-American or an All-European affair. To derive the maximum benefit and enjoyment from this diversity it is of course necessary to develop a healthy appetite for a varied intellectual diet. Once this attitude has been established, tact and mutual respect in our international scientific relations will follow by themselves and one of the greatest obstacles to interaction and free flow of information between the different national groups is removed. Certainly there is no reason for responsible research workers in our field to let pride, or other causes such as differences in language, drive them to help the many eager hands who are attempting to lower war time curtains right in our midst.

It has been customary to look upon language as a means of communications. In later years it has acquired another and more sinister role, that of a shield behind which to hide one's own contributions or, in other cases, one's unwillingness to look into the achievements of other language groups. Even within the relatively small and culturally fairly homogeneous area of Central and Western Europe much harm is being done by this viewpoint on language. Some of the damage might be overcome if one recognizes the simple fact that by adopting as an auxiliary the language of the other fellow you deprive him of exclusive control of his language and change it from a shield to its rightful role of a means of (international) communication.

There are of course basic language difficulties which can not be solved by such a simple adaptation on the part of the European groups. There is for instance every reason to expect, during the next few years, an extremely vigorous development of Chinese meteorology and, as a result, many significant realistic contributions from that part of the world. Fortunately, the new generation of Chinese meteorologists has already shown its willingness to adopt English as an auxiliary language, to the benefit of us all.

From what has been said above it is clear that many difficult questions have to be tackled before we can hope to solve even the regional problem of establishing a permanent workable pattern for European cooperation in basic meteorological research. Nevertheless, the attempt must be made. Many of the more significant contributions to meteorology during the last decade have been made by Europeans who have been given the opportunity, for instance in the United States or in other parts of the world, to operate in and on groups capable of responding to stimuli, and equipped with the necessary physical resources. Our task must be to attempt to organize such groups on our continent, to help us tap the talent which now to a large extent is wasted because it is scattered ineffectively over the continent.

After more than twenty years of work with such research groups in the United States the author of this note feels a deep gratitude for the escape from pomposity and for the opportunities to intellectual development that work with an imaginative and intellectually courageous American team brings with it. However, during such a long stay on the other side of the Atlantic, one gradually begins to think of Europe as somewhat of a cultural unit and one learns to look at this continent with a perspective

which would be hard to acquire from our side of the water. It is not unreasonable to demand that persons who have had the privilege of working on both continents must take over a heavy share of the responsibility for a satisfactory solution of the problems here discussed. This does not mean that European science, with its long and valuable traditions, should be blindly americanized. The European chinashop is a delicate one and must be handled with a great deal of care if we want to avoid serious damage to its antiques.

The European scientist frequently occupies an enviable position *sine cura* as far as his responsibilities to society are concerned. His cares and worries, of which there are many, have to do with an entirely different problem, the inadequacy of the resources at his command. On both sides of us basic science has been organized much more completely into service for the community. Fortunately the applied research problems in which society is vitally interested, and the central problems of world-wide meteorology, are largely identical or at least overlapping. Hence it would seem wise to organize our research in such a manner that we are capable of tackling these problems before they are rammed down our throats.

The very modest meteorological "seminar" activities that have been conducted in Stockholm since the autumn of 1947 to meet the needs reviewed above, had as their initial goal the reestablishment of normal working relations between scientists in some of the war-scarred countries of Central Europe and their colleagues in Sweden. This activity was in fact a small part of a much larger program with similar aims set up by the Swedish Institute for Cultural Exchange with Foreign Countries, and supported by grants from the Swedish Government. It soon became apparent that much could be gained by a considerable broadening of the objectives of this program. Thus the important basic contributions to meteorology made in Great Britain and the United States during the last war were inadequately known on the Continent, and the civilian meteorological community in America and Western Europe was certainly only vaguely conscious of the interesting lines of research followed in Central Europe. Even the contact between individual countries on the Continent suffered from antagonisms and barriers erected during the war. It was therefore decided to combine the invitations to our central European guests with similar invitations to scientists from other parts of Europe and North America, to permit an informal exchange of information in a friendly setting of absolute equality which would foster mutual respect for the intellectual activities of the different groups thus brought together.

In 1950 additional funds were obtained through an agreement with the University of Chicago and it was then possible to continue and to expand the program initiated by the Swedish Institute. In this manner meteorologists from fourteen different countries have been brought together in Stockholm. It has been our desire to keep the groups small and the discussions informal, to permit a maximum amount of personal contact. It is nevertheless our hope to add in a significant manner to the number of countries successively drawn into these group discussions, but in order to avoid complications resulting from language difficulties it will be necessary to proceed quite slowly with this expansion.

Three conferences with a fairly well-defined program were organized during the last few years. In May 1949, in cooperation with the Geographic Institute of the University of Stockholm, then under the direction of professor Hans W:son Ahlmann, and with the Swedish Geophysical Society, a conference on the structure of the general circulation of the atmosphere and on the problem of postglacial climatic fluctuations was arranged, in which not only meteorologists but also botanists, glaciologists, geologists and geographers took part. A somewhat smaller group met again in May 1950 to continue the discussions of these problems. Finally, in June 1951 a last conference was arranged during which problems of cyclone and jet stream structure were considered as well as certain aspects of the general circulation, particularly in low latitudes.

The relations between meteorologists in the south and in the far north of Europe are not nearly as intimate as one might wish. A first small step towards the establishment of real cooperation with Italian meteorologists was taken when it was arranged to have a Scandinavian representative take part in the First International Congress on Alpine Meteorology arranged by prof. M. Bossolasco in Milano during the autumn of 1950. We expect to develop much more fully the contacts then established.

It is quite evident that meetings of the type discussed above are of great value in bringing about diffusion of information, but they do not eliminate the need for the organization of facilities where meteorologists from different countries would have the opportunity to work together, over longer periods of time, on projects of a joint nature.

The organization of one or several large institutes with permanent staff positions open to foreigners would not be an adequate answer to this problem. Such a solution would again contribute to the drain of talent away from some of the smaller European countries which deserve a better fate since they in the past have contributed so much to the evolution of modern meteorology.

It seems more desirable to set up one or several regional institutions with rotating, overlapping staffs, to which scientific workers from different countries may be sent or invited for participation, over limited periods of time, in certain broad scientific projects. With the help of the institutions from which the collaborating scientists are sent, such a system of rotating assignments would reduce the cost of operations and would furthermore eliminate the otherwise very real danger that the institution be looked upon as a comfortable place of retreat.

Basic research institutions of the kind envisioned above must be built around individuals, not set up as paper schemes. Studies are now being conducted by UNESCO to determine the advisability of organizing international scientific laboratories, and in a few cases these explorations have advanced quite far: thus the organization of an International Computing Center appears to have been accepted in principle. However, it is important to bear in mind that such a center to a very large extent must function as a technical service organization. In our case we are faced with the necessity of creating, not only facilities but also leadership for joint research tasks which under the changing conditions of our science no longer can be undertaken on a purely national basis. This demands an institution of a far more personal character than one would find in a scientific organization charged primarily with house keeping or service functions. Thus there are no precedents to guide us and we must experiment until a satisfactory solution has been found.

A modest experiment of this type will be conducted in Stockholm during the coming academic year (1951-1952). Eight or ten young scientists, representing half a dozen different countries, will be brought together to work as a team on a few basic problems which now occupy the foreground in meteorology. Thus the aerological and theoretical description of the large-scale flow patterns in the atmosphere will receive much attention. If possible, a small experimental weather service will be set up to serve as a "clinic" and as a testing ground for theoretical atmospheric models developed by the members of our group.

It should be quite evident from what has been said earlier that the organization of similar experiments elsewhere on our continent and dealing with other aspects of meteorology would be highly desirable. Taken together these experiments should help us to arrive at a reliable answer to the pressing problem of how to provide the best setting for European meteorological research. It is at any rate certain that conclusions drawn from experiences gained with such teams will be far more dependable than any set of abstract recommendations as to how our research work should be organized.

It is also fairly evident that the limited objectives of the Stockholm research team are distinctly different from those important responsibilities which the World Meteorological Organization would wish to assign to any technical bureau which might be set up under its auspices. Experience has shown that the various national weather services represented in the latter organization are likely to profit more from properly staffed and equipped independent research teams organized and operated in academic settings outside the regular government services than from any attempt to conduct the required research within the rigid framework of the official government meteorological bureaus. In a similar way one might reasonably conclude that the World Meteorological Organization is likely to profit more by fostering the organization of independent units or teams to conduct its research than by attempting to enter directly into research operations.

Stockholm in July 1951

C.-G. Rossby